Characterization of intra-litter variation on myogenic development and myogenic progenitor cell response to growth promoting stimuli

by

Mathew Alan Vaughn

B.S., Iowa State University, 2010
M.S., Texas Tech University, 2012

AN ABSTRACT OF A DISSERTATION

submitted in partial fulfillment of the requirements for the degree

DOCTOR OF PHILOSOPHY

Department of Animal Sciences and Industry
College of Agriculture

KANSAS STATE UNIVERSITY
Manhattan, Kansas

2017

Abstract

This series of studies focuses on the impact of intra-litter variation on fetal myogenesis, and the ability of porcine progenitor cells to respond to growth promoting stimuli. In study 1, the smallest (**SM**), median (**ME**), and largest (**LG**) male fetuses from each litter were selected for muscle morphometric analysis from gilts at d-60 ± 2 and 95 ± 2 of gestation. On d-60 and 95 of gestation LG fetuses had greater whole muscle cross-sectional area (**CSA**) than ME and SM fetuses, and ME fetuses had greater whole muscle CSA than SM fetuses. Indicating that SM and ME fetuses are on a delayed trajectory for myogenesis compared to LG fetuses. At d-60 the advanced trajectory of LG compared to ME fetuses was due to increased development of secondary muscle fibers; whereas, the advanced myogenic development of LG and ME fetuses compared to SM fetuses was due to the presence of fewer primary and secondary muscle fibers. At d-95 of gestation the advanced myogenic development of LG and ME was due to increased hypertrophy of secondary muscle fibers. For study 2, porcine fetal myoblasts (**PFM**) were isolated from SM, ME, and LG fetuses from d-60 ± 2 of gestation fetuses and for study 3, porcine satellite cells (**PSC**) were isolated from the piglet nearest the average body weight of the litter. Both myogenic cell types were utilized to evaluate effects of porcine plasma on proliferation, differentiation, and indications of protein synthesis. For the proliferation assay, cells were exposed to one of three treatments: high serum which consisted high-glucose Dulbecco's Modified Eagle Medium supplemented with 10% (vol/vol) fetal bovine serum, 2% (vol/vol) porcine serum, 100 U penicillan/mL, 100 μg of strepmycin/mL, and 20 μg of gentamicin/mL (**HS**), low serum which consisted of HS without 10% FBS (**LS**), and LS supplemented with 10% (wt/vol) porcine plasma (**PP**). Treatments for the differentiation and protein synthesis assays consisted of either HS or LS media that either contained porcine plasma

at 10% (wt/vol; **PPP**) or 0% (wt/vol; **PPN**). The HS-PFM had a greater proliferation rate compared to the LS and PP-PFM, and PP-PFM had a greater proliferation rate compared to LS-PFM. The LG fetuses' PFM had a reduced proliferation rate compared to SM and ME fetuses' PFM, which were similar. The PPP-PFM had a decreased myotube diameter compared to PPN-PFM. Small fetuses' PFM had a greater myotube diameter compared to ME and LG fetuses' PFM, and ME fetuses' PFM had a greater myotube diameter compared to LG fetuses' PFM. The proliferation rate of PP-PSC was decreased compared to the HS- and LS-PSC, and HS-PSC had a greater proliferation rate compared to LS-PSC. The PPP-PSC had greater differentiation capacity and myotube diameter than PPN-PSC. In conjunction these results indicate divergent myogenic development among different fetal sizes within a litter and suggest that porcine plasma supplementation stimulates myogenic progenitor cell activity in an age specific manner.

Characterization of intra-litter variation on myogenic development and myogenic progenitor cell response to growth promoting stimuli

by

Mathew Alan Vaughn

B.S., Kansas State University, 2010
M.S., University of Kansas, 2012

A DISSERTATION

submitted in partial fulfillment of the requirements for the degree

DOCTOR OF PHILOSOPHY

Department of Animal Sciences and Industry
College of Agriculture

KANSAS STATE UNIVERSITY
Manhattan, Kansas

2016

Approved by:

Major Professor
John M. Gonzalez

Copyright

Abstract

This series of studies focuses on the impact of intra-litter variation on fetal myogenesis, and the ability of porcine progenitor cells to respond to growth promoting stimuli. In study 1, the smallest (**SM**), median (**ME**), and largest (**LG**) male fetuses from each litter were selected for muscle morphometric analysis from gilts at d-60 ± 2 and 95 ± 2 of gestation. On d-60 and 95 of gestation LG fetuses had greater whole muscle cross-sectional area (**CSA**) than ME and SM fetuses, and ME fetuses had greater whole muscle CSA than SM fetuses. Indicating that SM and ME fetuses are on a delayed trajectory for myogenesis compared to LG fetuses. At d-60 the advanced trajectory of LG compared to ME fetuses was due to increased development of secondary muscle fibers; whereas, the advanced myogenic development of LG and ME fetuses compared to SM fetuses was due to the presence of fewer primary and secondary muscle fibers. At d-95 of gestation the advanced myogenic development of LG and ME was due to increased hypertrophy of secondary muscle fibers. For study 2, porcine fetal myoblasts (**PFM**) were isolated from SM, ME, and LG fetuses from d-60 ± 2 of gestation fetuses and for study 3, porcine satellite cells (**PSC**) were isolated from the piglet nearest the average body weight of the litter. Both myogenic cell types were utilized to evaluate effects of porcine plasma on proliferation, differentiation, and indications of protein synthesis. For the proliferation assay, cells were exposed to one of three treatments: high serum which consisted high-glucose Dulbecco's Modified Eagle Medium supplemented with 10% (vol/vol) fetal bovine serum, 2% (vol/vol) porcine serum, 100 U penicillan/mL, 100 μg of strepmycin/mL, and 20 μg of gentamicin/mL (**HS**), low serum which consisted of HS without 10% FBS (**LS**), and LS supplemented with 10% (wt/vol) porcine plasma (**PP**). Treatments for the differentiation and protein synthesis assays consisted of either HS or LS media that either contained porcine plasma

at 10% (wt/vol; **PPP**) or 0% (wt/vol; **PPN**). The HS-PFM had a greater proliferation rate compared to the LS and PP-PFM, and PP-PFM had a greater proliferation rate compared to LS-PFM. The LG fetuses' PFM had a reduced proliferation rate compared to SM and ME fetuses' PFM, which were similar. The PPP-PFM had a decreased myotube diameter compared to PPN-PFM. Small fetuses' PFM had a greater myotube diameter compared to ME and LG fetuses' PFM, and ME fetuses' PFM had a greater myotube diameter compared to LG fetuses' PFM. The proliferation rate of PP-PSC was decreased compared to the HS- and LS-PSC, and HS-PSC had a greater proliferation rate compared to LS-PSC. The PPP-PSC had greater differentiation capacity and myotube diameter than PPN-PSC. In conjunction these results indicate divergent myogenic development among different fetal sizes within a litter and suggest that porcine plasma supplementation stimulates myogenic progenitor cell activity in an age specific manner.

Table of Contents

List of Figures

List of Tables

Acknowledgements

I would like to thank Dr. John Gonzalez for providing me a great opportunity to develop my professional and scientific skills. I appreciate the profound investment and faith that he has placed in me over to course of my doctoral program. Thank you to all of my committee members, Dr. James Drouillard, Dr. Barry Bradford, and Dr. Deryl Troyer, for your support and thorough evaluation of my professional development. Thank you to Dr. Jeroen Roelofs for serving as the outside chair on my doctoral committee.

I am appreciative for the collaborative relationship and assistance of the swine nutrition and physiology groups. Specifically, I would like to thank Dr. Jim Nelssen, Dr. Duane Davis, Dr. Jason Woodworth, Jodi Morton, Julie Feldpausch, and Dr. Chad Paulk for support in completing my doctoral research. Thank you to all of the undergraduate students for their assistance performing laboratory analysis and for providing me the opportunity to develop my mentorship skills. A special thanks to, Tyler Pohlenz, Keegan Johnson, Anna Williamson, Stephanie Davis, and Abby Olberding for their substantial efforts that made data collection possible. I would like to thank the Meat Science faculty and graduate students for all of your comradery and support throughout my doctoral program. It goes without saying that I would not of made it through my program without “the core Gonzalez Lab”, which consisted of Kelsey Phelps, Derris Burnett, Sara Ebarb, and Jere Noel. They were helpful in many more aspects of my doctoral program than would likely be apparent from the outside looking in and I am forever grateful for each of you!

Most important I need to thank my family for being incredibly supportive of my professional and personal ambitions. The support of my mother, father, sister, grandparents, and extended family has been un-wavering every day for the last 29 years of my life. During my time here at Kansas State University I was blessed to be able to marry my best friend Jalane Vaughn.

Jalane and our two children, Adalynn (3 yrs) and Alden (4 mo), are the constant inspiration I needed every day to continue to push forward in the pursuit of my doctoral degree.

Chapter 1 - Review of Literature

Swine Production Efficiency

Improving efficiency of pork production is a multi-faceted task that includes digestive function, immunity, and tissue deposition. A sow's overall efficiency encompasses a variety of different traits, such as litter size, litter weight, and the length of time that the sow is capable of remaining in the herd (Rodriguez-Zas et al., 2003). Aggressive genetic selection for hyperprolific sows increased average litter size within the top 25% of U.S. sow farms from 12.3 in 2008 to 13.6 in 2013 pigs per sow (Stalder, 2014). Increasing litter size has decreased piglet survivability and individual greater variability among piglets with respect to size, percent of lean mass, and visceral adiposity (Fix et al., 2010). Increased piglet variability results in a greater number of piglets with low birth weights (Milligan et al., 2002). It has been previously reported that piglets weighing less than 1.27 kg had greater probability of pre-weaning mortality compared to heavier littermates (Panzardi et al., 2013; Tanghe et al., 2014). The population of piglets with a birth-weight lower than 1.27 kg accounted for 55% of total mortality within the first three days following parturition (Panzardi et al., 2013). Low birth weight piglets have greater adiposity and decreased muscle mass at birth and the growing period (Rehfeldt and Kuhn, 2006). Of the low birth weight piglets that survive, their developmental detriments may affect growth during the remainder of the post-natal period.

Current efforts in genetic selection have focused on increasing piglets that survive until d-5 post-parturition. This measure serves as a better metric of sow productivity, as it takes in account the large proportion of piglets that fail to survive the first few days of life. (Su et al., 2007). This review will avoid extensive discussion of genetic selection, rather will focus on

nutritional and phamocological interventions that may improve physiology of the low birth weight piglets. thus improving their chances for survival.

Skeletal Muscle Structure and Muscle Growth

Muscle is a heterogeneous tissue composed of myofibers, fibroblasts, and adipocytes which, respectively, give rise to the lean, connective tissue, and fat. The lean component is skeletal muscle is organized into structural hierarchies where individual muscles are surrounded by epimysial connective tissue and within that, muscle bundles are surrounded by a layer of perimysial connective tissue. These bundles are in turn composed of individual muscle fibers that are surrounded by endomysial connective tissue. Individual muscle fibers are considered the cellular unit of skeletal muscle and have numerous myofibrils that impart the contractile functions on the muscle. Muscle mass is determined primarily by the number and size of the individual muscle fibers (Oksbjerg et al., 2004). Muscle tissue grows through hyperplasia and hypertrophy of muscle fibers. The development of the all-important fiber begins in utero and in fact the total number of muscle fibers is established prior to the birth of the animal. Once the animal is born, muscle hypertrophy is the predominant force driving muscle accretion in livestock species. This occurs via radial and longitudinal growth of muscle fibers as a result of increased net protein accretion. Both pre and postnatal muscle development require a favorable environment replete with nutrients and growth factors to support optimal muscle growth. Muscle accretion occurs when protein synthesis outweighs protein degradation. The following sections will describe how each of the components of the net growth equation contribute to overall muscle growth and how these components are influenced by regulatory growth factors.

Muscle is a dynamic and demanding tissue that accounts for approximately 40% of body mass (Yates et al., 2012) and 65% of fetal glucose disposal (Hay, 2008), therefore muscle growth

is dependent on nutrient availability, endocrine status, and the presence or absence of regulatory growth factors. While the majority of management practices are tailored towards maximizing postnatal muscle growth and production efficiency, skeletal muscle development actually begins in-utero. The time spent in-utero represents approximately 35- 40% of the entire production cycle from "conception to consumption" in a typical livestock operation and total fiber number is established by day 90 pigs (Wigmore and Stickland, 1983). Muscle growth potential is positively correlated to muscle fiber number (Dwyer et al., 1993), and because hyperplasia does not occur postnatally (Oksbjerg et al., 2004), effective approaches to maximize muscle growth must target or at least consider the in-utero window. This phase of development determines the potential for postnatal muscle growth and thus represents an opportune, yet often overlooked window to manipulate muscle growth potential and maximize postnatal performance. Nutritional or hormonal events occurring during these critical time points are likely to have lasting consequences on postnatal growth potential. Favorable changes in the hormonal and metabolic environment in-utero can improve the foundation upon which postnatal management strategies have to build. Conversely, if these foundations are compromised by unfavorable conditions, the impact may not be immediately observed in fetuses or neonates, but the potential growth trajectory and performance may be permanently altered.

Fetal myogenesis

Skeletal muscle development begins early in gestation through the development of somites in the paraxial mesoderm (Tajbakhsh and Buckingham, 2000; Bajard et al., 2006). The genes Pax3 and Pax7 are hallmarks for the onset of myogenesis, and play a role in the survival of myogenic cells in the dermomyotome (Relaix et al., 2005). For determination of a cell of the dermomyotome to the myogenic fate Pax3 expression is required; however, when Pax3 is absent,

Pax7 is capable of compensating its function and committing cells to myogenesis (Relaix et al., 2006).

Muscle fiber formation occurs in two distinct waves that develop both primary and secondary muscle fibers. Primary muscle fibers begin to develop around day 30 of gestation, and exhibit centrally located nuclei (Wigmore and Stickland, 1983; Handel and Stickland, 1987). Wigmore and Stickland (1983), evaluated the semimebranosus muscle of the smallest and largest fetus of each litter over the course of gestation. Histological examination revealed that in the early stages of myogenesis the primary muscle fibers are arranged closely together, and primary muscle fibers begin to spread apart to allow for secondary muscle fibers to develop. Secondary fibers had begun to develop on the surface of the muscle fibers at d-54 of gestation.

Myogenesis is the term that encompasses the commitment, proliferation, and differentiation of muscle precursor cells into mature muscle cells (Tajbakhsh, 2009; Bentzinger et al., 2012). Multipotent mesenchymal stem cells commit to the myogenic lineage becoming immature myoblasts. These myoblasts then proliferate and differentiate into myotubes and ultimately into myofibers which then undergo maturation to acquire the metabolic machinery necessary for muscle function (Sabourin and Rudnicki, 2000; Bentzinger et al., 2012). These mature muscle fibers then grow via hypertrophy. The myogenic process is tightly regulated and requires the coordinated activity of regulatory growth and transcription factors that govern lineage determination, proliferation, differentiation and growth (Bentzinger et al., 2012). The progression of progenitor cells through the myogenic lineage can be readily monitored because expression of the regulatory factors is temporally and spatially restricted to specific phases of the lineage. Some of these factors have redundant functions in order to ensure robustness in the regulatory system (Rudnicki et al., 1993), but generally speaking their expression is transient and

reflect a cell in a specific phase of commitment, proliferation or differentiation. As such, this also makes these regulatory factors and checkpoints potentially valuable therapeutic targets to enhance the myogenic process. Additionally, the relative gene and protein expression levels for these factors can be used to monitor the extent to which myogenesis is occurring in response to various treatment or management strategies.

Muscle development begins during the embryonic stage of development and occurs in two waves. Primary and secondary fibers arise from a pool of multipotent mesenchymal stem cells that commit to the myogenic lineage (Bailey et al., 2001). Primary muscle fibers develop during the first wave of myogenesis, which occurs between d 25 and 50 of gestation in pigs (Bailey et al., 2001; Oksbjerg et al., 2013). These myofibers then serve as the scaffold for secondary myogenesis, with 16 to 24 secondary fibers developing per primary muscle fiber (Wigmore and Stickland, 1983; Handel and Stickland, 1987). These secondary fibers form the bulk of muscle fibers and thus the fetal stage in which secondary myogenesis occurs represents a critical phase of muscle development (Du et al., 2011). As mentioned before, myogenesis is sensitive to nutrient and energy availability therefore nutritional or hormonal insults during this phase are particularly detrimental to muscle growth and development. Once secondary myogenesis is completed, between day 80 and 90 of gestation in pigs, muscle fiber number is set and can no longer be altered (Stickland et al., 2004; Oksbjerg et al., 2013)

Myogenic Progenitor Cell Dynamics

Myoblasts are derived from the somite pool of the dermomyotome (Tajbakhsh and Buckingham, 2000), and give rise to mesenchymal stem cells that will ultimately diverge to give rise to chondroblasts, adipoblasts, and myoblasts (Caplan, 1991; Du et al., 2011). The commitment of mesenchymal stem cells to the myogenic fate is associated with the upregulation

of the paired homeobox transcription factors (Pax) -3 and -7. Upregulation of the Pax genes in mesenchymal stem cells during embryogenesis promotes their survival and commitment towards the myogenic lineage. The majority of the cells in the dermomyotome co-express Pax3 and Pax7 and the ones that do not will undergo programmed cell death or adopt a non-myogenic lineage (Relaix et al., 2005). The majority of fetal myoblasts the contain expression of the Pax genes proliferate rapidly to create a pool of myoblasts to needed for the formation of both primary and secondary muscle fibers. As in adult myogenesis the commitment of fetal myoblasts to differentiation is cued through the down regulation of the Pax genes and the upregulation of the myogenic regulatory factors (Relaix et al., 2005; Zammit et al., 2006; Zammit et al., 2008). This occurs as a gradual process that involves the co-expression of the Pax genes with the myogenic regulatory factors. The first myogenic regulatory factor present in the dermomyotome is myogenic factor-5 (Myf-5) and when co-localized with the Pax genes there is a marked decline in the percentage of proliferative cells. Additionally, cells of the dermomyotome do not co-express Pax7 and myogenic determination factor (MyoD), which marks the cells commitment to terminal differentiation (Relaix et al., 2005; Zammit et al., 2006). The fetal myoblasts that proceed through the expression of myogenic regulatory factors will contribute to muscle fiber development as described in the previous section and the cells that retain the expression of the Pax genes will constitute the postnatal satellite cell pool (Bentzinger et al., 2012).

Satellite cells are the muscle progenitor cell that is present in adult skeletal muscle and was first identified in the hind limb of a frog through electron microscopy as an unknown cell type lying between the basal lamina and the sarcolemma of the muscle fiber (Mauro, 1961). It was later determined that this cell type is solely responsible for the addition of new nuclei to

existing muscle fibers to allow for postnatal muscle growth (Moss and Leblond, 1971). The role of satellite cells in postnatal muscle hypertrophy will be elaborated on in the subsequent sections.

Intrauterine Growth Restriction and Muscle Growth

Intrauterine growth restriction is a phenomenon that occurs as a result of compromised physical or chemical environment in the uterus, resulting in impaired growth of the developing fetus. Skeletal muscle is particularly vulnerable to the consequences of IUGR as it is relatively low on the list of metabolic priorities compared to other tissues such as the brain and liver. Low birthweight is generally associated with a reduced number of secondary muscle fibers (Handel and Stickland, 1987; Dwyer et al., 1994) and has a detrimental impact on the long term growth potential of these offspring. This results in a delayed trajectory of muscle growth and development in IUGR fetuses (Yates et al., 2012). In addition to the absolute number of fibers, the metabolic machinery and disposition of skeletal muscle are also affected by in-utero programming. For example, mitochondrial energetics are compromised in low birthweight offspring in mice and this results in reduced oxidative capacity in skeletal muscle and increased adiposity in the postnatal period (Beauchamp et al., 2015).

The classical definitions of IUGR which classify offspring based on their birthweight relative to a pre-determined threshold or a normally distributed population may not fully appreciate or account for the lasting impacts of suboptimal uterine environments on muscle growth and development (Handel and Stickland, 1987). This is because even fetuses that fall in the normal birth weight category may have been prevented from reaching their full potential in terms of muscle fiber number or metabolic machinery and may also suffer from the phenotypic and metabolic consequences of the suboptimal environment (Gluckman and Pinal, 2003). In

contrast, an enhanced or enriched growth factor/nutritional environment may have also lasting, but not immediately apparent impacts on postnatal growth potential.

Studies focusing on reducing within litter variation in birthweight via nutritional or hormonal strategies in pigs, the greatest impact has been observed with the small fetuses and piglets. Such manipulations influence the variety of growth factors and nutrients available for fetal growth. This indicates that the compromised uterine environment has a more severe impact on birthweight and postnatal performance in the lighter animals (Dwyer et al., 1994; Rehfeldt et al., 2000). Therefore, focusing on maternal nutrition and therapeutic interventions during in-utero development is likely to enhance the effectiveness of postnatal strategies to improve the efficiency and profitability of meat production.

Specifically, Rehfeldt and Kuhn (2006) observed that lowest birth weight litter mate is born with an increased percentage of percentage of adipose tissue, and fewer muscle fibers compared to the heaviest and middle weight fetuses within the litter. Additionally, at 182 d of age the lowest birth weight piglet maintained a lower body weight and carcass weight compared to the heaviest littermates (Rehfeldt and Kuhn, 2006). Addtionally, Gondret et al. (2005) evaluated growth and carcass characteristic of the low and heavy birth weight piglets of the litter and observed that the low birth weight piglets had lower average daily gain during the suckling and post-weaning period. In this study pigs were fed to a constant weight, which took the low birth group an average of 12 d longer than the heavy birth weight group. However, at slaughter there was not a difference in carcass weight or fat percentage when the low birth weight piglets were finished to the same weight as the heavy birth weight group. The increased lean content that the low birth weight group deposited was due to increased muscle fiber hypertrophy in the longissimus, rhomboideus, and semitendinosus muscles (Gondret et al., 2005).

Promoting Fetal Myogenesis

As outlined in previous sections, embryonic and fetal myogenesis are highly sensitive processes where the results have lasting impacts on postnatal growth and overall systemic metabolism (Sarr et al., 2012). Management strategies that promote early stages of myogenesis have potential to improve growth and metabolism. Early efforts to improve in utero development in pigs included administration of somatotropin, genetic selection, and increasing nutrient intake (Rehfeldt et al., 2011), with porcine somatotropin administration proving to one of the most successful.

Early in the development of porcine somatotropin there was significant improvements in average daily gain, feed conversion, and percentage of lean mass (Machlin, 1972). Soon after there were was interest in porcine somatotropin administration during gestation, in an attempt to increase piglet birth weight and fetal myogenesis. Sterle et al. (1995) observed that administration of recombinant porcine somatotropin from d-30 to 43 of gestation resulted in an greater fetal and placental weights. With skeletal muscle constituting approximately 40% of the piglets mass it is likely that the mode of increase in fetal weight is through improvements in myogenesis. Rehfeldt et al. (2004) observed that there tended to be an interaction of administration of porcine somatotropin and birth weight group. The low weight fetuses reared from sows that were administered porcine somatotropin had a greater total muscle fiber number than piglets from sows administered the placebo. Somatotropin elicits its biological response through stimulation of the somototropic axis, and produces elevated levels of IGF-1 and IGF-2 (Renaville et al., 2002). As expected administration of recombinant porcine somatotropin to gestating gilts did result in evlevated levels of IGF-1 and IGF-2; however, there was no change in the concentration of the IGFs from their fetuses (Sterle et al., 1995). Therefore, the data from

Sterle et al. (1995) indicates that increased fetal weight observed following maternal administration of recombinant porcine somatotropin was not due to stimulation of the somatotropic axis of the fetus, but rather improvements in placental transfer of nutrients. With an estimated half-life of somatotropin of 15.7 min providing logistical complications related to dosing prevelance (Lanzi et al., 1995), and the ever looming activist push driving consumer desire for hormone free meat products makes it unlikely that porcine somatotropin administration can be a long term solution to stimulating fetal growth and myogenesis.

The data previously discussed indicate that stimulation of the somatotropic axis can improve fetal development through improvements in placental efficiency to stimulate myogenesis. With particular impracticalities of administering porcine somatotropin research efforts set forth to characterize and mimic the mechanism of porcine somatotropin administration. Gatford et al. (2003) administered two doses of porcine somatotropin to gilts on two different plains of nutrition from d-25 to 50 of gestation and evaluated muscle morphometrics of the semitendinosus of fetuses at birth. Their results indicated that porcine somatotropin administration increased muscle fiber cross-sectional area, regardless of feed intake level. However, maternal feed intake of 3.0 kg/d resulted in fetuses that had a greater number of muscle fibers compared to when maternal feed intake was 2.2 kg/d. Interestingly, Gatford et al. (2003) did not observe an increase in maternal IGF-1 status when gilts were on a greater plane of nutrition. Nissen et al. (2005) observed that ad libitum feeding during mid-gestation resulted in increased circulating maternal IGF-1 concentrations. This data illustrates that the quantity of a diet can influence fetal development, but does not address the influences of diet composition.

Protein content and amino acids play an integral role in cellular signaling events and deficiency in these components has potential to have long term consequences on offspring. The

protein requirement changes over the course of gestation but recent research indicates that the average protein requirement is 14-18% of total intake (Elango and Ball, 2016). In addition to indicating that the protein requirement during gestation is higher than the current recommendation, Elango and Ball (2016) indicate that the requirements of key amino acids are elevated during late gestation due to elevated fetal and mammary protein deposition. The average fetus deposits 17.5 g of protein from d-0 to 70 of gestation and 203.7 g of protein from d-70 to 114 of gestation, which increases the protein requirement of the sow in late gestation (McPherson et al., 2004; Kim et al., 2009). Oster et al. (2012) fed sows isoenergetic diets that contained 6.5% and 12.5% protein and evaluated the short and long term effects on skeletal muscle gene expression in offspring. Even though it is not likely for a commercial sow to receive a diet that consists of 6.5% crude protein the data from this study is valuable in obtaining mechanistic information of IUGR. The genes participating in the G1/S checkpoint regulation, somatropin signaling mammalian target of rapamycin (mTOR) pathway signaling, and IGF-1 signaling were down regulated in offspring of mothers that received a 6.5% protein diet during gestation (Oster et al., 2012). The tissue deposition responses to protein availability are likely due to the intracellular signaling mechanisms of amino acids which will be discussed in more detail in the following section (Fox et al., 1998; Kimball and Jefferson, 2002).

Protein Synthesis Signaling

Skeletal muscle protein synthesis is mediated largely through changes in growth factor profiles, and amino acid availability. A major protein synthesis pathway that interacts with growth factors and amino acids is mTOR pathway signaling. The phosphorylation of protein kinase B (AKT) serves as a critical branch point in mTOR pathway signaling, simultaneously promoting protein synthesis through the actions of mTOR, and inhibits cellular apoptosis by

down regulating Forkhead Box O (FOXO). Full activation of AKT depends on the phosphorylation of Thr308 in the activation loop, and Ser473 in the hydrophobic C-terminal regulatory domain (Hill et al., 2001); however, the contribution by each phosphorylation site is not equal. The Thr308 phosphorylation is capable of stimulating AKT activity, but Ser473 is not (Alessi et al., 1996). Phosphorylation of mTOR stimulates protein synthesis through the phosphorylation of both p70 S6 kinase (S6) and eukaryotic translation initiation factor 4E-binding protein (4E-BP). Additionally, AKT stimulates FOXO phosphorylation, consequently inhibiting the production of two muscle-specific E3 ubiquitin ligases muscle atrophy F-Box (MAFbx) and muscle RING Finger-1 (MURF-1; Schiaffino and Mammucari, 2011).

Amino acids are have been implicated in partial or complete stimulation of mTOR pathway signaling. Fox et al. (1998) indicated that a mixture of complete amino acids promoted the phosphorylation of 4E-BP, thus relieving the negative regulation of the eukaryotic initiation factor eIF-4E. Further evaluation of individual amino acids that leucine was responsible for the majority of phosphorylation of the translational repressor 4E-BP (Fox et al., 1998). Additionally, Kimball et al. (1999) found that in addition to 4E-BP phosphorylation leucine stimulated the activity of elongation initiation factor eIF-4E through the hyperphosphorylation of S6 Kinase in L6 myoblasts. The introduction of rapamycin, an inhibitor of mTOR activity, inhibited all stimulatory effects of leucine, suggesting that the translational stimulation of leucine is mTOR mediated. Sikalidis et al. (2013) evaluated the abundance of total 4E-BP and phosphorylation ratio of 4E-BP in response to varying levels of methionine and cysteine concentrations supplementation to rats. Authors observed that the total 4E-BP was elevated when cysteine was not present and the increase was independent of methionine level and that ratio of

phosphorylation of γ4E-BP was not affect by methionine dose or cysteine presence (Sikalidis et al., 2013).

Insulin-like growth factor-1 (IGF-1) plays a central role in activating mTOR pathway signaling through binding of the IGF-1 receptor, activating its intrinsic tyrosine kinase activity, and a phosphorylation cascade. Supplementation of IGF-1 to porcine satellite cells isolated from 6 week old pigs resulted in increases in the abundance of the protein synthesis proteins involved in mTOR pathway signaling, AKT, mTOR, S6 kinase, and 4E-BP, which resulted in increased protein synthesis (Han et al., 2008). Insulin-like growth factor-1 can also promote overall protein accumulation in satellite cells by stimulating the phosphorylation of FOXO, which will in turn reduce the production of the ubiquitin ligases, MURF-1 and MAFbx, decreasing the rate of protein degradation (Stitt et al., 2004). The actions of IGF-1 described here are dependent on IGF-1 binding to its receptor, which is mediated by a variety of

Insulin-Like Growth Factors

The next section describes the regulation of muscle growth by the growth factors, namely, the insulin like growth factors (IGF). The IGF proteins are structurally and functionally similar to insulin and play a central role in pre- and postnatal growth. Species ranging from yeasts to worms to humans have some form the evolutionarily conserved IGF pathway and the 70 amino acid IGF-I peptide is highly conserved across species with pigs, cattle, and humans sharing an identical amino acid sequence (Tavakkol et al., 1988) indicating the importance of this pathway to growth and survival.

The IGFs were initially known as sulfation factors because in studies using hypophesectomized rats, the incorporation of sulfate into chondroitin sulfate was severely impaired (Murphy et al., 1956). When these rodents were treated with exogenous somatotropin

sulfate incorporation was restored; however, when somatotropin was added on in-vitro cultures the improvement was minimal. This led the researchers to believe that there was an intermediary factor that mediated the effects of the somatotropin in-vivo. These factors came to be known as "sulfation factors" based on their apparent ability to restore sulfate incorporation into cartilage. Subsequent studies further isolated and purified these factors, and, based on their structural and functional homology to the proinsulin peptide, identified as IGF-I and IGF-II.

Our understanding of how somatic growth is accomplished via the members of the somatotropic axis has evolved over decades of research in the area. Le Roith et al. (2001) reviewed the evolution of the somatomedin hypothesis over the past 50 years. In their summary, the original somatomedin hypothesis (Murphy et al., 1956) suggested that somatic growth was accomplished via stimulation of hepatic IGF-I production form pituitary derived growth hormone. Next came the dual effector hypothesis (Green et al., 1985) which indicated that there were both direct somatotropin stimulates actions on peripheral tissues as well as those indirect actions mediated by hepatic IGF-I. The current hypothesis merges the somatomedin and dual effector hypotheses recognizing that there are both somatotropin dependent and somatotropin independent effects of IGF-I on postnatal growth. All of these hypotheses recognize the importance of IGF-I in normal growth and development which is supported by various lines of evidence across species.

Various tissues express IGF-I including liver, muscle, adipose, and bone adding to the complexity of the IGF system in regulating cellular proliferation and growth. In cases of IGF deficiency, severe retardation of growth occurs. Liu and LeRoith, (1999) reported that roughly 1/3 of birthweight and 2/3 of mature weight is attributable to IGF-I function. In these studies, IGF-I null mice had birthweights that were only 65% of that of their normal counterparts. By 8

weeks, their body weight was only 1/3 that of their wild-type littermates. These data suggests that while IGF-I signaling is important to the pre and postnatal growth, the negative impacts become more profound as the animal matures. Again this must be considered cautiously because despite a worsening disparity in the postnatal period, prenatal programming is also a likely contributor to the severity of the undesirable postnatal phenotypes.

IGF action can occur via endocrine, paracrine, or autocrine signaling depending on the source and target of the IGF-I. Stimulation of the anterior pituitary by hypothalamic growth hormone releasing hormone results in the production of growth hormone which then enters into circulation and targets the liver to cause production of IGF-I. Hepatic IGF-I is released into the bloodstream to exert endocrine effects on target tissues. The majority of circulating IGF-I is of hepatic origin with liver production exceeding other tissues by about 10 fold (Stewart and Pell, 2010). In addition, peripheral tissues also produce IGF-I locally which acts in an autocrine/paracrine fashion via the IGF-I signaling pathway. The exact contribution of endocrine vs. autocrine/paracrine signaling to overall IGF action remains debatable.

In circulation IGFs are largely complexed to a family of IGF binding proteins (IGFBP) which modulate the delivery and availability of IGF-I and IGF-II to target tissues (Baxter, 2000). There are six homologous members of the IGFBP family (IGFBP1-6) which share a high binding affinity for the IGFs (Clemmons, 2001). The expression patterns for the IGFBPs are tissue specific and varies with the stage of growth and development (Schneider et al., 2000). The activity of these binding proteins is regulated by nutritional and endocrine factors including insulin and growth hormone. Much like myogenic regulatory factors the roles of the IGFBPs are redundant to ensure robust regulation of IGF actions. The majority (80-90%) of circulating IGF-I is complexed with IGFBP3 which serves to prolong its half-life. Non-complexed IGF-I

represents only about 1% of the total circulating IGF-I (Frystyk, 2004) and has a half-life of about 10 minutes in circulation whilst when complexed to IGFBP-3 the half-life is extended to about 12 hrs (Guler et al., 1989). Muscle expresses high levels of IGFBP-5 which complexes with the IGFs to regulate binding to the IGF1R (Schiaffino and Mammucari, 2011). In mice overexpression or under expression of IGFBP5, results in impaired muscle growth along with reduced survivability and reproductive performance. These examples demonstrate how the IGFBPs allow the body to control when and where IGF-I action is exerted in response to nutrient and energy status.

Regardless of the source, the actions of IGF-I and IGF-II are mediated through the IGF-I receptor (IGF1R) which shares structural homology to the insulin receptor (Varewijck and Janssen, 2012). Once bound the receptor the IGFs initiate signaling cascades that regulate a myriad of cellular functions including cell proliferation, hypertrophy, and migration via activation of the mitogen-activated protein (MAP) kinase and phosphatidylinositol 3 kinase (PI3K)/Akt pathways (Perez-Perez et al., 2010). As previously discussed skeletal muscle pathways are responsive to cellular energy and nutrient status and is particularly sensitive to amino acid levels which are the building blocks for muscle protein synthesis (Maiter et al., 1989). Activation of mTOR pathway signaling in the presence of adequate nutrient and energy reserves results in activation of translational machinery to accomplish protein synthesis. The insulin receptor can also bind IGF-I but with much lower affinity than it binds insulin (Varewijck and Janssen, 2012). This leads to some crossover of their functions but insulin is generally considered to regulate metabolic functions while IGF-I regulates cellular proliferation and differentiation. Of the primary insulin sensitive tissues (liver, adipose, and muscle), only the muscle expresses appreciable quantities of the IGF1R which indicates that the primary metabolic

target of IGF-I is skeletal muscle to promote nutrient uptake and support growth (Yakar et al., 1999).

Regulation of muscle growth by IGF-I

The IGF system is critical to embryonic growth with IGF-II being the major component during this phase (Florini et al., 1996). The actions of IGF-II are mediated primarily through the IGF1R while interaction with the IGF2R mainly serves to clear IGF-II from circulation (Haig and Graham, 1991). This is important because loss of a functional IGF2R results in embryonic overgrowth due to a lack of regulatory clearance of circulating IGF-II (Gluckman and Pinal, 2003). During later phases of gestation IGF-I has an increasing role in fetal growth (Gluckman and Pinal, 2003) and circulating levels are tied to maternal nutrition, placental blood flow, and nutrient transfer capacity (Bassett et al., 1990). Even though IGF-II is the major IGF involved in fetal muscle development marked increases in circulating maternal IGF-1 may improve placental and fetal nutrient availability and IGF expression (Rehfeldt et al., 2004; Sterle et al, 1995).

The absolute requirement for the IGFs in skeletal muscle growth remains controversial. Mice lacking the IGF-I gene exhibit severe growth retardation (Baker et al., 1993) and lack of a functional IGF-I receptor is usually lethal at birth due to impaired development of the diaphragm and intercostal muscles to support respiration (Liu et al., 1993). When production of only hepatic IGF-I is ablated circulating concentrations of IGF-I are reduced by 75%; however, postnatal body growth still occurs (Yakar et al., 1999) indicating that local production may be sufficient to support growth. Spangenburg et al. (2008), reported that in mice incapable of responding to insulin or IGF-I, mechanical load was capable of stimulating the mTOR pathway and increasing muscle growth similar to wild-type animals. These findings question the necessity for IGF-I in at least load induced muscle growth, but moreover highlight redundancies which ensure tissue

development. Highlighting the fact that the IGFs are pertinent for optimal myogenesis, these animals still had smaller muscles compared to their wild-type counterparts.

Porcine Plasma Supplementation

Previous sections of this review have indicated the importance of the growth factor IGF-1 and amino acids in protein synthesis. Spray dried porcine plasma is a commercially available product that is commonly fed in the nursery phase that contains elevated levels of both amino acids and IGF-1 (de Rodas et al., 1995). Coffey and Cromwell (1995) completed a series of experiments to first determine the appropriate level to supplement porcine plasma for nursery pigs, and compared feed ADG, G:F, and feed intake to pigs being supplemented with spray dried porcine plasma, dried skim milk, and a soybean meal. Authors observed that pigs that were supplemented with spray dried porcine plasma experienced greater ADG compared to pigs supplemented with soybean meal and dried skim milk. Additionally, pigs supplemented with spray dried porcine plasma had increased daily feed intake compared to pigs supplemented with soybean meal or dried skim milk. In one of their experiments pigs were fed in an experimental nursery that had fewer pigs and improved climate control compared to a conventional nursery. It is interesting that the impact of spray dried porcine plasma on ADG and feed intake was greater for pigs in a conventional nursery compared to the experimental nursery. This study illustrates that supplementation of spray dried plasma to nursery pigs effectively stimulates ADG through and increase in feed intake, but provides little insight into its impact on growth metabolites.

A study conducted by de Rodas et al. (1995) was aimed at determining the mode of action in which spray-dried porcine plasma improves ADG and feed intake in nursery pigs. Similar to the previous study discussed ADG and feed intake was increased for the first 14 days in the nursery. The plasma concentrations of insulin, IGF-1, growth hormone, and glucose were

also evaluated. The plasma concentrations of IGF-1 and glucose were not affected by spray dried porcine plasma supplementation. Pigs that were supplemented with spray dried porcine plasma tended to have elevated levels of plasma growth hormone and decreased levels of insulin compared to pigs supplemented with soybean meal. In conjunction, these two studies indicate that spray dried porcine plasma can effectively improve growth performance nursery pigs through an increase in daily feed intake and partial stimulation of the somatotropic axis.

Crenshaw et al. (2007) supplemented lactating sows with spray-dried porcine plasma to evaluate parameters involved in sow productivity and litter characteristics. Young sows (parity 1 and 2) that were supplemented with spray-dried porcine plasma had increased feed intake and decreased weight loss during lactation. In contrast mature sows (parity > 3) had decreased feed intake when they were supplemented with spray-dried porcine plasma. Interestingly, the weaning to estrus interval was improved in both young and mature sows. Litters from mature sows that were supplemented with spray-dried porcine plasma had an increased number of marketable pigs weaned and a greater average litter weights compared to sows that were not supplemented with spray dried porcine plasma.

The current literature has evaluated the effects of porcine plasma on young pigs; however, there has been little research conducted regarding the effects of porcine plasma on fetal development of pigs. Campbell et al., (2006) conducted a statistical process control analysis on supplementation of spray-dried plasma on gestating sows from a herd with a history of porcine reproductive and respiratory syndrome virus with porcine plasma at a rate of 0.5% of the diet and observed an increased farrowing rate, more pigs born alive, and increased number of pigs weaned. This report provides evidence that supplementation of porcine plasma can positively

benefit swine production when supplemented during gestation, but does not define the mode of action in which porcine plasma elicits its response.

Tran et al. (2014) supplemented intestinal epithelial cells with varying levels of porcine plasma to evaluate their proliferative response. This model can serve as a model for enterocyte growth, which is related to improved gut health. Supplementation of porcine plasma to intestinal epithelial cells resulted in a greater proliferation rate compared to all control treatments (Tran et al., 2014). Additionally, in vivo supplementation of spray dried plasma to nursery pigs resulted in a greater villus height in the duodenum compared to non-supplemented pigs. It is interesting that porcine plasma supplementation at a dose of 5% spray dried porcine plasma results in improvements in villus height of the duodenum but not the ileum (Tran et al., 2014).

Postnatal Muscle Growth

Because hyperplasia only occurs prenatally, postnatal muscle accretion is dependent on hypertrophy and net protein accretion in existing muscle fibers established in the prenatal period. This occurs through increasing the cross-sectional area (CSA) and length of muscle fibers. Postnatal growth and ultimate protein deposition is mediated by transcriptional signals of myonuclei (Moss, 1968). Myonuclear domain can be defined as the volume of cytoplasm that can be supported by one copy of DNA (Van der Meer et al., 2011). Therefore, as muscle fibers grow in size, more DNA must be added to maintain the myonuclear domain and support protein synthesis. Myonuclei are post mitotic, meaning they can no longer undergo replication to increase the DNA content within muscle fibers. In skeletal muscle 50-99% of the total nuclear content is accumulated postnatally (Allen et al., 1979). As described previously satellite cells are progenitor cells that reside within adult skeletal muscle. Satellite cells retain the ability to proliferate and undergo asymmetric division to produce daughter cells that can both replenish the

satellite cell pool and terminally differentiate into myonuclei (Kuang et al., 2007). Terminal differentiation of satellite cells contribute the DNA template needed for postnatal muscle hypertrophy (Moss and Leblond, 1971). These cells must be activated to proliferate before eventually fusing and contributing their nuclei to the growing muscle fiber. Activation of satellite cells in response to injury or growth stimuli occurs via a regulated signaling cascade that serves to induce muscle growth.

CONCLUSION

Prenatal myogenesis plays a critical role in nutrient metabolism of the developing fetus, and has lasting effects on the long term growth of the animal. In litter bearing species such as the pig there is spontaneous intrauterine growth restriction that occurs as a result of placental insufficiency. Research efforts to improve fetal myogenesis include maternal administration of porcine somatotropin, increasing maternal feed intake, and augmentations of dietary protein content. In many cases successful interventions were accompanied by elevated circulating levels of maternal IGF-1. The metabolite IGF-1 is capable of promoting both cell proliferation and protein synthesis. However, protein synthesis mediated through mTOR pathway signaling can also be mediated by specific amino acids, where the presence or absence can either stimulate or inhibit the translational processes downstream from mTOR. Therefore, protein synthesis *in utero* through maternal interventions proves to be highly complex. Ultimately, the impact of placental insufficiency on fetal myogenesis has permanent implications on skeletal muscle development and postnatal growth.

REFERENCES

Alessi, D. R., M. Andjelkovic, B. Caudwell, P. Cron, N. Morrice, P. Cohen, and B. A. Hemmings. 1996. Mechanism of activation of protein kinase B by insulin and IGF-1. EMBO. J. 15:6541-6551.

Allen, R. E., R. A. Merkel, and R. B. Young. 1979. Cellular aspects of muscle growth: myogenic cell proliferation. J. Anim. Sci. 49:115-127.

Bailey, P., T. Holowacz, and A. B. Lassar. 2001. The origin of skeletal muscle stem cells in the embryo and the adult. Curr. Opin. Cell Biol. 13:679-689.

Bajard, L., F. Relaix, M. Lagha, D. Rocancourt, P. Daubas, and M. E. Buckingham. 2006. A novel genetic hierarchy functions during hypaxial myogenesis: Pax3 directly activates Myf5 in muscle progenitor cells in the limb. Genes Dev. 20:2450-2464.

Baker, J., J. P. Liu, E. J. Robertson, and A. Efstratiadis. 1993. Role of insulin-like growth factors in embryonic and postnatal growth. Cell. 75:73-82.

Bassett, N. S., B. H. Breier, S. C. Hodgkinson, S. R. Davis, H. V. Henderson, and P. D. Gluckman. 1990. Plasma clearance of radiolabelled IGF-1 in the late gestation ovine fetus. J. Dev. Physiol. 14:73-79.

Baxter, R. C. 2000. Insulin-like growth factor (IGF)-binding proteins: interactions with IGFs and intrinsic bioactivities. Am. J. Physiol. Endocrinol. Metab. 278:E967-976.

Beauchamp, B., S. Ghosh, M. W. Dysart, G. N. Kanaan, A. Chu, A. Blais, K. Rajamanickam, E. C. Tsai, M. E. Patti, and M. E. Harper. 2015. Low birth weight is associated with adiposity, impaired skeletal muscle energetics and weight loss resistance in mice. Int. J. Obes. 39:702-711. doi:10.1038/ijo.2014.120

Bentzinger, C. F., Y. X. Wang, and M. A. Rudnicki. 2012. Building muscle: molecular regulation of myogenesis. Cold Spring Harb. Perspect. Biol. 4. doi:10.1101/cshperspect.a008342

Caplan, A. I. 1991. Mesenchymal stem cells. J. Orthop. Res. 9:641-650. doi:10.1002/jor.1100090504

Clemmons, D. R. 2001. Use of mutagenesis to probe IGF-binding protein structure/function relationships. Endocr. Rev. 22:800-817. doi:Doi 10.1210/Er.22.6.800

Coffey, R. D., and G. L. Cromwell. 1995. The impact of environment and antimicrobial agents on the growth response of early-weaned pigs to spray-dried porcine plasma. J. Anim. Sci. 73:2532-2539.

Crenshaw, J. D., R. D. Boyd, J. M. Campbell, L. E. Russell, R. L. Moser, and M. E. Wilson. 2007. Lactation feed disappearance and weaning to estrus interval for sows fed spray-dried plasma. J. Anim. Sci. 85:3442-3453. doi:10.2527/jas.2007-0220

de Rodas, B. Z., K. S. Sohn, C. V. Maxwell, and L. J. Spicer. 1995. Plasma protein for pigs weaned at 19 to 24 days of age: effect on performance and plasma insulin-like growth factor I, growth hormone, insulin, and glucose concentrations. J. Anim. Sci. 73:3657-3665.

Du, M., J. X. Zhao, X. Yan, Y. Huang, L. V. Nicodemus, W. Yue, R. J. McCormick, and M. J. Zhu. 2011. Fetal muscle development, mesenchymal multipotent cell differentiation, and associated signaling pathways. J. Anim. Sci. 89:583-590. doi:10.2527/jas.2010-3386

Dwyer, C. M., J. M. Fletcher, and N. C. Stickland. 1993. Muscle cellularity and postnatal growth in the pig. J. Anim. Sci. 71:3339-3343.

Dwyer, C. M., N. C. Stickland, and J. M. Fletcher. 1994. The influence of maternal nutrition on muscle fiber number development in the porcine fetus and on subsequent postnatal growth. J. Anim. Sci. 72:911-917.

Elango, R., and R. O. Ball. 2016. Protein and Amino Acid Requirements during Pregnancy. Adv. Nutr. 7:839S-844S. doi:10.3945/an.115.011817

Fix, J. S., J. P. Cassady, J. W. Holl, W. O. Herring, M. S. Culbertson, and M. T. See. 2010. Effect of piglet birth weight on survival and quality of commercial market swine. Livest. Sci. 132:98-106. doi:DOI 10.1016/j.livsci.2010.05.007

Florini, J. R., D. Z. Ewton, and S. A. Coolican. 1996. Growth hormone and the insulin-like growth factor system in myogenesis. Endocr. Rev. 17:481-517.

Fox, H. L., P. T. Pham, S. R. Kimball, L. S. Jefferson, and C. J. Lynch. 1998. Amino acid effects on translational repressor 4E-BP1 are mediated primarily by L-leucine in isolated adipocytes. Am. J. Physiol. 275:C1232-1238.

Frystyk, J. 2004. Free insulin-like growth factors -- measurements and relationships to growth hormone secretion and glucose homeostasis. Growth Horm. IGF. Res. 14:337-375. doi:10.1016/j.ghir.2004.06.001

Gatford, K. L., J. E. Ekert, K. Blackmore, M. J. De Blasio, J. M. Boyce, J. A. Owens, R. G. Campbell, and P. C. Owens. 2003. Variable maternal nutrition and growth hormone treatment in the second quarter of pregnancy in pigs alter semitendinosus muscle in adolescent progeny. Br. J. Nutr. 90:283-293.

Gluckman, P. D., and C. S. Pinal. 2003. Regulation of fetal growth by the somatotrophic axis. J. Nutr. 133:1741S-1746S.

Gondret, F., L. Lefaucheur, L. Louveau, B. Lebret, X. Pichodo, and Y. Le Cozler. 2005. Influence of piglet birth weight on postnatal growth performance, tissue lipogenic capacity and muscle histological traits at market weight. Livest. Prod. Sci. 93:137-146. doi:DOI 10.1016/j.livprodsci.2004.09.009

Green, H., M. Morikawa, and T. Nixon. 1985. A dual effector theory of growth-hormone action. Differentiation. 29:195-198.

Guler, H. P., J. Zapf, C. Schmid, and E. R. Froesch. 1989. Insulin-like growth factors I and II in healthy man. Estimations of half-lives and production rates. Acta. Endocrinol. (Copenh). 121:753-758.

Haig, D., and C. Graham. 1991. Genomic imprinting and the strange case of the insulin-like growth factor II receptor. Cell. 64:1045-1046.

Han, B., J. Tong, M. J. Zhu, C. Ma, and M. Du. 2008. Insulin-like growth factor-1 (IGF-1) and leucine activate pig myogenic satellite cells through mammalian target of rapamycin (mTOR) pathway. Mol. Reprod. Dev. 75:810-817. doi:10.1002/mrd.20832

Handel, S. E., and N. C. Stickland. 1987. Muscle Cellularity and Birth-Weight. Anim. Prod. 44:311-317.

Hay, W. W., Jr. 2008. Strategies for feeding the preterm infant. Neonatology. 94:245-254. doi:10.1159/000151643

Hill, M. M., M. Andjelkovic, D. P. Brazil, S. Ferrari, D. Fabbro, and B. A. Hemmings. 2001. Insulin-stimulated protein kinase B phosphorylation on Ser-473 is independent of its activity and occurs through a staurosporine-insensitive kinase. J. Biol. Chem. 276:25643-25646. doi:10.1074/jbc.C100174200

Kim, S. W., W. L. Hurley, G. Wu, and F. Ji. 2009. Ideal amino acid balance for sows during gestation and lactation. J. Anim. Sci. 87:E123-132. doi:10.2527/jas.2008-1452

Kimball, S. R., and L. S. Jefferson. 2002. Control of protein synthesis by amino acid availability. Curr. Opin. Clin. Nutr. Metab. Care. 5:63-67.

Kimball, S. R., L. M. Shantz, R. L. Horetsky, and L. S. Jefferson. 1999. Leucine regulates translation of specific mRNAs in L6 myoblasts through mTOR-mediated changes in availability of eIF4E and phosphorylation of ribosomal protein S6. J. Biol. Chem. 274:11647-11652.

Kuang, S., K. Kuroda, F. Le Grand, and M. A. Rudnicki. 2007. Asymmetric self-renewal and commitment of satellite stem cells in muscle. Cell. 129:999-1010. doi:10.1016/j.cell.2007.03.044

Lanzi, R., A. C. Andreotti, A. Caumo, M. F. Manzoni, M. Losa, M. E. Malighetti, and A. E. Pontiroli. 1995. Assessment of growth hormone (GH) plasma clearance rate, half-life, and volume of distribution in acromegalic patients: the combined GH-octreotide infusion. J. Clin. Endocrinol. Metab. 80:3279-3283. doi:10.1210/jcem.80.11.7593438

Le Roith, D., C. Bondy, S. Yakar, J. L. Liu, and A. Butler. 2001. The somatomedin hypothesis: 2001. Endocr. Rev. 22:53-74. doi:10.1210/edrv.22.1.0419

Liu, J-L., and D. LeRoith. 1999. Insulin-Like Growth Factor I is essential for postnatal body growth in response to growth hormone. Endocrin. 140(5):5178-5184

Liu, J.-P., A. Baker, E. Perkins, A. Robertson, and Efstratiadis. 1993. Mice carrying null mutations of the genes encoding insulin-like growth factor I (Igf-1) and type 1 IGF receptor (Igf1r). Cell. 75:59-72.

Machlin, L. J. 1972. Effect of porcine growth hormone on growth and carcass composition of the pig. J. Anim. Sci. 35:794-800.

Maiter, D., T. Fliesen, L. E. Underwood, M. Maes, G. Gerard, M. L. Davenport, and J. M. Ketelslegers. 1989. Dietary protein restriction decreases insulin-like growth factor I independent of insulin and liver growth hormone binding. Endocrinology. 124:2604-2611. doi:10.1210/endo-124-5-2604

Mauro, A. 1961. Satellite cell of skeletal muscle fibers. J. Biophys. and Biochem. Cytol. 9:493-495.

McPherson, R. L., F. Ji, G. Wu, J. R. Blanton, Jr., and S. W. Kim. 2004. Growth and compositional changes of fetal tissues in pigs. J. Anim. Sci. 82:2534-2540.

Milligan, B. N., D. Fraser, and D. L. Kramer. 2002. Within-litter birth weight variation in the domestic pig and its relation to pre-weaning survival, weight gain, and variation in weaning weights. Livest. Prod. Sci. 76:181-191. doi:Pii S0301-6226(02)00012-X

Moss, F. P. 1968. The relationship between the dimensions of the fibres and the number of nuclei during normal growth of skeletal muscle in the domestic fowl. Am. J. Anat. 122:555-563.

Moss, F. P., and C. P. Leblond. 1971. Satellite cells as the source of nuclei in muscles of growing rats. Anat. Rec. 170:421-435.

Murphy, W. R., W. H. Daughaday, and C. Hartnett. 1956. The effect of hypophysectomy and growth hormone on the incorporation of labeled sulfate into tibial epiphyseal and nasal cartilage of the rat. J. Lab. Clin. Med. 47:715-722.

Nissen, P. M., I. L. Sorensen, M. Vestergaard, and N. Oksbjerg. 2005. Effects of sow nutrition on maternal and foetal serum growth factors and on foetal myogenesis. J. Anim. Sci. 80:299-306.

Oksbjerg, N., F. Gondret, and M. Vestergaard. 2004. Basic principles of muscle development and growth in meat-producing mammals as affected by the insulin-like growth factor (IGF) system. Domest. Anim. Endocrinol. 27:219-240. doi:DOI 10.1016/j.domaniend.2004.06.007

Oksbjerg, N., P. M. Nissen, M. Therkildsen, H. S. Moller, L. B. Larsen, M. Andersen, and J. F. Young. 2013. Meat Science and Muscle Biology Symposium: in utero nutrition related to fetal development, postnatal performance, and meat quality of pork. J. Anim. Sci. 91:1443-1453. doi:10.2527/jas.2012-5849

Oster, M., E. Murani, C. Metges, S. Ponsuksili, and K. Wimmers. 2012. Transcriptional response of skeletal muscle to a low-protein gestation diet in porcine offspring accumulates in growth- and cell cycle-regulating pathways. Physiol. Gen. 44:811-818.

Panzardi, A., M. L. Bernardi, A. P. Mellagi, T. Bierhals, F. P. Bortolozzo, and I. Wentz. 2013. Newborn piglet traits associated with survival and growth performance until weaning. Prev. Vet. Med. 110:206-213. doi:10.1016/j.prevetmed.2012.11.016

Perez-Perez, A., Y. Gambino, J. Maymo, R. Goberna, F. Fabiani, C. Varone, and V. Sanchez-Margalet. 2010. MAPK and PI3K activities are required for leptin stimulation of protein synthesis in human trophoblastic cells. Biochem. Biophys. Res. Commun. 396:956-960. doi:10.1016/j.bbrc.2010.05.031

Rehfeldt, C., I. Fiedler, G. Dietl, and K. Ender. 2000. Myogenesis and postnatal skeletal muscle cell growth as influenced by selection. Livest. Prod. Sci. 66:177-188.

Rehfeldt, C., and G. Kuhn. 2006. Consequences of birth weight for postnatal growth performance and carcass quality in pigs as related to myogenesis. J. Anim. Sci. 84 Suppl:E113-123.

Rehfeldt, C., P. M. Nissen, G. Kuhn, M. Vestergaard, K. Ender, and N. Oksbjerg. 2004. Effects of maternal nutrition and porcine growth hormone (pGH) treatment during gestation on endocrine and metabolic factors in sows, fetuses and pigs, skeletal muscle development, and postnatal growth. Domest. Anim. Endocrinol. 27:267-285. doi:10.1016/j.domaniend.2004.06.005

Rehfeldt, C., M. F. W. Te Pas, K. Wimmers, J. M. Brameld, P. M. Nissen, C. Berri, C. Rehfeldt, D. M. Power, B. Picard, N. C. Stickland, N. Oksbjerg, and L. M. P. Valente. 2011. Advances in research on the prenatal development of skeletal muscle in animals in relation to the quality of muscle-based food. II " Genetic factors related to animal performance and advances in methodology. Animal. 5:718-730.

Relaix, F., D. Montarras, S. Zaffran, B. Gayraud-Morel, D. Rocancourt, S. Tajbakhsh, A. Mansouri, A. Cumano, and M. Buckingham. 2006. Pax3 and Pax7 have distinct and overlapping functions in adult muscle progenitor cells. J. Cell Biol. 172:91-102.

Relaix, F., D. Rocancourt, A. Mansouri, and M. Buckingham. 2005. A Pax3/Pax7-dependent population of skeletal muscle progenitor cells. Nature. 435:948-953.

Renaville, R., M. Hammadi, and D. Portetelle. 2002. Role of the somatotropic axis in the mammalian metabolism. Domest. Anim. Endocrinol. 23:351-360.

Rodriguez-Zas, S. L., B. R. Southey, R. V. Knox, J. F. Connor, J. F. Lowe, and B. J. Roskamp. 2003. Bioeconomic evaluation of sow longevity and profitability. J. Anim. Sci. 81:2915-2922.

Rudnicki, M. A., P. N. Schnegelsberg, R. H. Stead, T. Braun, H. H. Arnold, and R. Jaenisch. 1993. MyoD or Myf-5 is required for the formation of skeletal muscle. Cell. 75:1351-1359.

Sabourin, L. A., and M. A. Rudnicki. 2000. The molecular regulation of myogenesis. Clin. Genet. 57:16-25.

Sarr, O., K. Yang, and T. R. Regnault. 2012. In utero programming of later adiposity: the role of fetal growth restriction. J. Pregnancy. 2012:134758. doi:10.1155/2012/134758

Schiaffino, S., and C. Mammucari. 2011. Regulation of skeletal muscle growth by the IGF1-Akt/PKB pathway: insights from genetic models. Skelet. Muscle. 1:4. doi:10.1186/2044-5040-1-4

Schneider, M. R., H. Lahm, M. Wu, A. Hoeflich, and E. Wolf. 2000. Transgenic mouse models for studying the functions of insulin-like growth factor-binding proteins. FASEB. J. 14:629-640.

Sikalidis, A. K., K. M. Mazor, M. J. Kang, H. Y. Liu, and M. H. Stipanuk. 2013. Total 4EBP1 is elevated in liver of rats in response to low sulfur amino acid intake. J. Amino Acids. 2013:864757-Article ID 864757.

Spangenburg, E. E., D. Le Roith, C. W. Ward, and S. C. Bodine. 2008. A functional insulin-like growth factor receptor is not necessary for load-induced skeletal muscle hypertrophy. J. Physiol. 586:283-291. doi:10.1113/jphysiol.2007.141507

Stalder, K. J. 2014. 2014 U. S. pork industry productivity analysis. http://old.pork.org/filelibrary/ipafull14. (Accessed 18 February 2015.)

Sterle, J. A., T. C. Cantley, W. R. Lamberson, M. C. Lucy, D. E. Gerrard, R. L. Matteri, and B. N. Day. 1995. Effects of recombinant porcine somatotropin on placental size, fetal growth, and IGF-I and IGF-II concentrations in pigs. J. Anim. Sci. 73:2980-2985.

Stewart, C. E., and J. M. Pell. 2010. Point: IGF-I is the major physiological regulator of muscle mass. J. Appl. Physiol. 108:1820-1821.

Stickland, N. C., S. Bayol, C. Ashton, C. Rehfeldt, M. F. W. t. Pas, M. E. Everts, and H. P. Haagsman. 2004. Manipulation of muscle fibre number during prenatal development Muscle Dev. Livest. Anim. : Physiol. Gen. Meat Qual.

Stitt, T. N., D. Drujan, B. A. Clarke, F. Panaro, Y. Timofeyva, W. O. Kline, M. Gonzalez, G. D. Yancopoulos, and D. J. Glass. 2004. The IGF-1/PI3K/Akt pathway prevents expression of muscle atrophy-induced ubiquitin ligases by inhibiting FOXO transcription factors. Mol. Cell. 14:395-403.

Su, G., M. S. Lund, and D. Sorensen. 2007. Selection for litter size at day five to improve litter size at weaning and piglet survival rate. J. Anim. Sci. 85:1385-1392. doi:Doi 10.2527/Jas.2006-631

Tajbakhsh, S., and M. Buckingham. 2000. The birth of muscle progenitor cells in the mouse: Spatiotemporal considerations. Curr. Top. Dev. Biol. 48:225-268.

Tanghe, S., S. Millet, J. Missotten, B. Vlaeminck, and S. De Smet. 2014. Effects of birth weight and maternal dietary fat source on the fatty acid profile of piglet tissue. Animal 8:1857-1866. doi:10.1017/S1751731114001724

Tavakkol, A., R. C. M. Simmen, and F. A. Simmen. 1988. Porcine insulin-like growth factor-I (pIGF-I): complementary deoxyribonucleic acid cloning and uterine expression of messenger ribonucleic acid encoding evolutionarily conserved IGF-I peptides. Mol. Endocrinol. 2:674-681.

Tran, H., J. W. Bundy, Y. S. Li, E. E. Carney-Hinkle, P. S. Miller, and T. E. Burkey. 2014. Effects of spray-dried porcine plasma on growth performance, immune response, total antioxidant capacity, and gut morphology of nursery pigs. J. Anim. Sci. 92:4494-4504. doi:10.2527/jas.2014-7620

Van der Meer, S. F. T., R. T. Jaspers, and H. Degens. 2011. Is the myonuclear domain size fixed? J. Musculoskel. Neuron. Interact. 11:286-297.

Varewijck, A. J., and J. A. Janssen. 2012. Insulin and its analogues and their affinities for the IGF1 receptor. Endocr. Relat. Cancer. 19:F63-75. doi:10.1530/ERC-12-0026

Wigmore, P. M., and N. C. Stickland. 1983. Muscle development in large and small pig fetuses. J. Anat. 137 (Pt 2):235-245.

Yakar, S., J. L. Liu, B. Stannard, A. Butler, D. Accili, B. Sauer, and D. LeRoith. 1999. Normal growth and development in the absence of hepatic insulin-like growth factor I. Proc. Natl. Acad. Sci. U. S. A. 96:7324-7329.

Yates, D. T., A. R. Macko, M. Nearing, X. Chen, R. P. Rhoads, and S. W. Limesand. 2012. Developmental programming in response to intrauterine growth restriction impairs myoblast function and skeletal muscle metabolism. J. Pregnancy. 2012:631038. doi:10.1155/2012/631038

Zammit, P. S., A. Cohen, M. E. Buckingham, and R. G. Kelly. 2008. Integration of embryonic and fetal skeletal myogenic programs at the myosin light chain 1f/3f locus. Dev. Biol. 313:420-433. doi:10.1016/j.ydbio.2007.10.044

Zammit, P. S., T. A. Partridge, and Z. Yablonka-Reuveni. 2006. The skeletal muscle satellite cell: the stem cell that came in from the cold. J. Histochem. Cytochem. 54:1177-1191. doi:10.1369/jhc.6R6995.2006

.

Chapter 2 - Impact of fetal size and longissimus muscle location on muscle fiber development, Pax7+ progenitor cell population, and myoblast activity

ABSTRACT

This **e**xperiment was conducted to determine the effect of fetal size on primary and secondary muscle fiber number and size, paired-homeobox transcription factor-7 (**Pax7**) + progenitor cell number, and porcine fetal myoblast (**PFM**) activity. Gravid gilts (n = 36; PIC 1050 × 327) were harvested at d-60 ± 2 of gestation. The smallest (**SM**), median (**ME**), and largest (**LG**) male fetuses were removed for muscle morphometric analysis based on crown-to-rump length. Gravid gilts (n = 24) were harvested at d-95 ± 1 of gestation. Fetal weight was used to categorize SM, ME, and LG fetuses. Whole muscle cross-sectional area (**CSA**) of longissimus thoracis at the 5th rib and longissimus lumborum at the first lumbar vertebrae were collected. Tissue samples corresponding to each location were cryopreserved, cut into 10-µm sections, and subjected to immunohistochemistry to identify primary and secondary muscle fibers. On d-60 of gestation, LG fetuses had greater whole muscle CSA than ME and SM fetuses ($P < 0.05$), and ME fetuses had greater ($P < 0.01$) whole muscle CSA than SM fetuses. Muscles of LG and ME fetuses possessed more primary muscle fibers than SM fetuses ($P = 0.03$), but were similar ($P = 0.83$) to each other. Primary muscle fiber CSA was similar for all fetal size categories ($P = 0.09$). Additionally, at d-60 of gestation, the number of total Pax7+ progenitor cells and Pax7+ progenitors per primary fiber were similar among fetal size categories ($P \geq 0.09$). On d-95 of gestation, LG fetuses had greater whole muscle CSA than ME and SM fetuses ($P < 0.01$), and ME fetuses had greater ($P < 0.01$) whole muscle CSA than SM fetuses. Total primary muscle

fiber number and CSA were not impacted by fetal size ($P > 0.20$). Secondary muscle fiber number was similar among fetal size categories ($P = 0.09$). Secondary muscle fiber CSA was greater in muscles of LG fetuses compared to SM and ME fetuses ($P < 0.01$). Additionally, muscles of ME fetuses exhibited greater ($P < 0.01$) secondary muscle fiber CSA than SM fetuses. Total number of Pax7+ progenitors in muscles of SM fetuses were less than those of LG and ME fetuses ($P < 0.01$), which were similar to each other ($P = 0.06$). These data indicate that SM and ME fetuses are on a delayed trajectory of myogenesis compared to LG fetuses. As fetal size increases, the total number of Pax7+ progenitors increases, which may be responsible for increased postnatal growth efficiency of large birthweight piglets.

KEYWORDS: fetal myoblast, fetus size, muscle progenitor, myogenesis, porcine

INTRODUCTION

Pre-natal myogenesis is a biphasic process, where primary muscle fibers develop by approximately d-55 of gestation to provide a surface for myoblasts to attach and differentiate into secondary muscle fibers (Wigmore and Stickland, 1983). After the conclusion of secondary myogenesis the remainder of muscle growth will occur through muscle hypertrophy (Wigmore and Stickland, 1983; Handel and Stickland, 1988). Postnatally, 50-99% of total muscle nuclear content is accumulated (Allen et al., 1979) through the proliferation and fusion of satellite cells (Moss and Leblond, 1971). These cells lie beneath the basal lamina and above the sarcolemma in a quiescent state until activated (Hawke and Gary, 2001) and originate from the somite (Gros et al., (2005). Myogenic progenitor cells that do not differentiate into myonuclei during embryonic or fetal myogenesis, will constitute the adult satellite cell pool (Buckingham, 2007; Bentzinger et al., 2012). Therefore, negative gestational events may affect the primary and secondary muscle fiber and progenitor cell establishment.

In pigs, genetic selection for hyperprolific sows has increased pigs born per sow from 12.3 in 2008 to 13.6 in 2013 (Stalder, 2014), but has resulted reduced piglet survivability (Fix et al., 2010) and an increase in low birth weight piglets (Milligan et al., 2002). Wigmore and Stickland (1983) reported smaller littermates have smaller muscles with fewer muscle fibers. The LM is a large muscle that originates in the from the epaxial dermomyotome and develops from the rostral to caudal region (Ordahl and Le Douarin, 1992; Tajbakhsh and Buckingham, 2000). It is unknown if the events of myogenesis are divergently affected by the intramuscular location and size of the fetus The objective of the current study was to characterize the effect of fetal size and LM intramuscular location on muscle fiber development, progenitor cell establishment, and procine fetal myoblast (**PFM**) activity.

MATERIALS AND METHODS

The experimental procedures were approved by the Kansas State University Institutional Animal Care and Use Committee.

Animal Management

All live animal procedures were conducted at the Kansas State University Swine Teaching and Research Center (Manhattan, KS). Gilts (n = 36; PIC 327 × 1050) received daily exposure to sexually mature boars and were moved to individual gestation stalls (2.88m^2) after the first recorded estrus. Nineteen days after their first recorded estrous cycle, gilts received 6.8 mL Matrix® (15 mg altrenogest; Merck Animal Health, Kenilworth, NJ) top dressed daily in their feed for 14 consecutive d. Gilts were heat checked with sexually mature boar exposure twice daily for 3 d following Matrix® therapy. After the onset of estrus gilts were a artificially inseminated (PIC 337 semen) 3 times in 12 h intervals. Pregnancy was confirmed via transcutaneous ultrasound 24 d after onset of estrus was first detected. Gilts were monitored

daily and limit fed (2.3 kg day^{-1}) a standard non-medicated gestation diet once daily, which met or exceeded daily nutritional requirements (NRC, 2012). On d-60 ± 2 of gestation, gravid gilts were transported to the Kansas State University Meats Laboratory (Manhattan, KS) and euthanized via electrical stunning and exsanguination. During evisceration the entire reproductive tract was removed and transported to an adjoining laboratory for fetus identification and removal. Each uterine horn was freed from surrounding connective tissue and mesometrium. Crown-rump length (poll to tail head) was collected through the placental membranes to identify the smallest (**SM**), median (**ME**), and largest (**LG**) male fetuses. The SM, ME, and LG male fetuses were removed for whole body morphometric data (data presented elsewhere) and muscle collection.

Gilts (*n* = 24 PIC 327 × 1050) were synchronized for estrus and bred as described above. On d-95 ± 1 of gestation, gravid gilts were euthanized, the reproductive tract was removed, and uterine processing occurred as described previously. Individual fetuses were removed from the uterus for measurement of body morphometric measurements (data presented elsewhere) and weighed. Male fetuses categorized as SM, ME, and LG for muscle collection were selected based on fetal body weight.

Muscle Collection

A 1-cm sample of the longissimus thoracis at the 5th rib and a 1-cm sample of the longissimus lumborum at the first lumbar vertebrae were collected from the right side of each fetus. Whole muscle cross-sectional area (**WMA**) was collected by blotting each sample on blotting paper, outlining blots with a marker, and scanning blots using a digital scanner (HP Deskjet 3050; Hewlett Packard, Palo Alto, CA). Scanned images were calibrated to a 2.54-cm line on each blot and WMA was measured using the Nikon NIS-Elements Basic Research image

analysis software (Nikon Instruments Inc., Mellville, NY). Following blotting, tissues were cryopreserved in optimal cutting temperature (**OCT**) tissue freezing medium (Fisher Scientific, Pittsburgh, PA) by submerging in supercooled isopentane (Fisher Scientific).

Histology

Ten-micrometer cryosections were collected onto positively charged, frost resistant slides (Midwest Scientific, Valley Park, MO) and subjected to immunohistochemistry. The methods of Town et al. (2004) and Paulk et al. (2014) were used with slight modifications. Briefly, cryosections were incubated in 5% horse serum, 0.2% TritonX-100 in phosphate buffered saline (**PBS**; Fisher Scientific) for 30 min to block for non-specific antigen binding sites. Subsequently, all sections were incubated in 1:500 α-dystrophin (Fisher Scientific), 1:10 hybridoma supernatant anti-slow myosin heavy chain (**BA-D5;** Developmental Studies Hybridoma Bank, Iowa City, IA), and 1:10 supernatant anti-Pax7 (**Pax7;** Developmental Studies Hybridoma Bank) primary antibody. After rinsing residual primary antibody with PBS, sections were incubated for 30 min in a secondary antibody solution containing 1:1,000 Alexa Fluor 594 goat anti-rabbit heavy and light chains (Invitrogen, Carlsbad, CA) for α-dystrophin, 1:1,000 Alexa Fluor 633 IgG2b for BA-D5 (Invitrogen), 1:1,000 Alexa Fluor 488 goat anti-mouse IgG1 (Invitrogen) for Pax-7, and 1:1,000 Hoechst 33342 dye (Fisher Scientific). Residual secondary antibody was rinsed with PBS, sections were covered in 9:1 glycerol (Fisher Scientific), and cover-slipped for imaging.

Immunohistochemistry Image Analyses

Four representative photomicrographs per sample were captured at 200× magnification, using a Nikon Eclipse TI-U inverted microscope equipped with an X-Cite 120XL epifluorescence illumination system, and DS-QiMc digital camera (Nikon Instruments Inc.). Primary muscle fibers stained positively for BA-D5, secondary muscle fibers stained negative

for BA-D5, α-dystrophin identified the periphery of all muscle fibers, Hoechst 33342 dye identified all nuclei, and Pax7 identified muscle progenitor cells. Cross-sectional areas (**CSA**) consisting of a minimum of 100 primary muscle fibers were collected from representative photomicrographs. At d-60 of gestation, developing secondary muscle fibers, total nuclei, and Pax7 positive (**Pax7+**) nuclei were enumerated. The ratio of secondary muscle fibers, fiber associated nuclei, and Pax7+ progenitor cells per primary muscle fiber were calculated. Total primary fiber number was calculated as WMA divided by average primary muscle fiber CSA. Total number of progenitor cells was calculated as WMA divided by the area of an image, then multiplied by the number of Pax7+ cells per image. Day-95 photomicrographs were analyzed similar to d-60 images; however, CSA of secondary muscle fibers were also collected, number of primary and secondary muscle fibers were calculated by multiplying the total fiber number by the percentage of each fiber type, and total fiber number were calculated as WMA divided by average muscle fiber CSA.

Porcine Fetal Myoblast Isolation

Porcine fetal myoblasts were isolated from fetuses of sows at d-95 ± 1 of gestation. After collection of muscle tissue for histology, whole left longissimus muscles were obtained from SM, ME and LG fetuses of 3 randomly chosen sows for isolation of porcine fetal myoblasts (**PFM**). A total of 9 pools of PFM were isolated (n = 3/size category).

The methods of Li et al. (2011) were followed for progenitor cell isolation with slight modifications. Briefly, muscles were excised of all visible connective tissue and minced with sterilized surgical scissors. Tissue was digested with 0.8 mg/mL of pronase XIV (Sigma Aldrich; St. Louis, MO) in PBS (Corning, Corning, NY**)** for 45 min at 37°C. To remove any residual pronase, samples were centrifuged at 1,500 × g for 4 min, liquid was decanted, and resulting

slurry was resuspended in PBS, shaken, and centrifuged again. This process was conducted a total of 4 times. The resulting slurry was resuspended in PBS, shaken well, and centrifuged at 500 × *g* for 10 minutes; this step was repeated 3 times. After each centrifugation step, supernatant containing progenitor cells were retained and cells were pelleted via centrifugation at 1,500 × *g* for 10 minutes. Cells were resuspended in PBS and passaged sequentially through 70- and 40-micrometer filters. After filtration, final pellets were resuspended in growth media (**GM**) consisting of high-glucose Dulbecco's Modified Eagle Medium (**DMEM**; Invitrogen, Carlsbad, CA) supplemented with 10% (vol/vol) fetal bovine serum (**FBS**; GE Healthcare, Pittsburgh, PA), 2% (vol/vol) porcine serum (**PS**; Sigma Aldrich), 100 U penicillan/mL, 100 μg of strepmycin/mL, and 20 μg of gentamicin/mL and plated on 100 mm^2 culture dishes (Eppendorf, Hauppauge, NY) for 24 h to allow all satellite cells to attach to the dish. Cells were rinsed of all additional cell debris, scraped from the culture dish, and cryopreserved in GM containing 10% volume dimethyl sulfoxide (Sigma Aldrich). Cells were stored in liquid nitrogen vapor until needed for the experiments.

Proliferation Assays

Parallel cultures of PFM (n = 3/size) were seeded at a density of 1×10^3 cells/cm^2 on tissue culture treated 12-well culture plates (Eppendorf) in GM. Myoblasts from each pool were plated in duplicate wells within each proliferation assay day and experiments were replicated 3 times.

Twenty-four, 48, 72, and 96 h after initiation of experiments, cultures were immunostained for Pax7, Myf-5, and bromodeoxyuridine (**BrdU**; Sigma Aldrich). For the detection of cells traversing S-phase, 5 μM BrdU, a thymidine analog, was added to media 2 h before fixation (Allen et al., 1979). Temporal characterization of the muscle lineage markers was conducted as previously described (Li et al., 2011). Cells were fixed with 4% (wt/vol)

formaldehyde (Polysciences, Warrington, PA) in PBS. Cultures were incubated in 0.5% Triton-X 100 (Fisher Scientific, Waltham, MA) in PBS for 10 min to permeabilize the nuclear membrane, followed by a 7 min incubation in 4 *N* hydrochloric acid (Fisher Scientific) to denature DNA for immunostaining. Next, cultures were incubated in 5% horse serum (Fisher Scientific) and 0.2% Triton-X 100 in PBS for 30 min to block non-specific antigen binding. Cultures were incubated with a primary antibody solution containing, 1:250 anti-BrdU (Santa Cruz Biotechnology, Dallas, TX), 1:10 supernatant anti-Pax7 (Developmental Studies Hybridoma Bank), and 1:50 anti-Myf5 (Santa Cruz Biotechnology) for 1 h. Next, cells were incubated with goat anti-rat AlexaFluor 594 (1:1000; Invitrogen), goat anti-mouse AlexaFluor 488 (1:1000; Invitrogen) and goat anti-rabbit AlexaFluor 633 (1:1000; Invitrogen) to detect BrdU, Pax7, and Myf-5, respectively. Hoechst 33324 (Invitrogen) was included at 10µg/mL for detection of nuclei.

Cells were visualized and photomicrographs were captured using the system described above. Utilizing an extra-long working distance objective, a minimum of 10 microscopic fields at 200× magnification were analyzed per sample utilizing NIS-Elements Imaging Software (Basic Research, 3.3; Nikon Instruments Inc.). Within representative photomicrographs area and mean intensity of each myoblast at each wavelength of light was measured using the automated measurement tool in NIS-Elements Imaging Software. Myoblasts were determined positive for Pax7, Myf-5 or BrdU when the mean intensity for the wavelength corresponding to each antibody was greater than the background for that specific wavelength. Proliferation rate was determined by the proportion of cells traversing the S-phase (BrdU+ cells) at each time point. Additionally, cells were classified into 3 categories based on Pax7 and Myf-5 expression, cells only expressing Pax7 (**Pax7+**), only expressing Myf-5 (**Myf-5+**), and cells co-expressing Pax7 and Myf-5.

Differentiation Assays

Plate designs, cell seeding, and sample replication were similar as described for proliferation assays. Cultures were maintained in GM media for 96 h resulting in approximately 70% confluency. At this time, myoblasts were treated with one of three treatments, the first consisting of high-glucose DMEM (Invitrogen, Carlsbad, CA) supplemented with 2% (vol/vol) PS (Sigma Aldrich), 100 U penicillan/mL, 100 μg of strepmycin/mL, and 20 μg of gentamicin/mL (**LS**) to induce differentiation through serum starvation (Pirkmajer and Chibalin, 2011). The second treatment consisted of the LS treatment supplemented 10% (vol/vol) fetal bovine serum (**HS**; Fisher Scientific), and the third treatment was the LS treatment supplemented with 100 ng/mL insulin-like growth factor-1 (**IGF-1**). The treatments were replenished 48 h after initial application, and cultures were fixed with 4% (wt/vol) formaldehyde (Polysciences) in PBS 96 h after application of DM. Cultures were incubated in 5% horse serum, 0.2% Triton-X 100 in PBS for 30 min to block non-specific antigen binding sites, incubated for 1 h with a primary antibody solution containing 1:2 supernatant anti-sarcomeric myosin (MF20; Developmental Studies Hybridoma Bank), and incubated with 1:1,000 goat anti-mouse AlexaFluor 594 (Invitrogen). Hoechst 33324 (Invitrogen) was included at 10μg/mL for detection of nuclei. Following immunostaining cultures were imaged as described above. The differentiation capacity was calculated as number of nuclei present in multinucleated sarcomeric myosin positive myotubes divided by total number of nuclei.

Protein Synthesis Assays

Porcine fetal myoblasts were plated similarly to the proliferation assay to assess effects of fetal size on myotube growth and protein synthesis after differentiation. Duplicate sets of plates were cultured in parallel for immunostaining and protein isolation. Myoblasts again were,

maintained in GM media for 96 h, resulting in approximately 70% confluency, then were treated with LS media for 96 h. Media was replaced with LS media supplemented with 10 μM cytosine β-D-arabinofuranoside (Sigma Aldrich) for 24 h to eliminate any proliferating mononuclear cells (Hinterberger and Barald, 1990). After elimination of proliferating cells, treatments were applied for 72 h, as described for differentiation assays, after which time myotubes were either immunostained with sarcomeric myosin (Developmental Studies Hybridoma Bank; MF20) or subjected to protein isolation.

Protein was extracted from progenitor cells at the conclusion of the protein synthesis assay according to the methods of Wang et al. (2012). Cells were scraped from the bottom of each well in 300 μL of lysis buffer (50 *M* Tris-HCL, 150 *M* NaCl, 1 *M* EDTA, 0.5% Triton X-100, 1 *M* phenlymethanessulfonyl fluoride, 1 *M* $NaVO_4$; Fisher Scientific) containing a complete protease inhibitor (Sigma Aldrich) and homogenized through a 21 gauge needle. Homogenates were centrifuged at 14,000 × *g* for 15 min at 4°C. Sample protein concentrations were quantified using Pierce's BCA Protein Assay Kit (Thermo Scientific).

Western blotting was performed following methods of Phelps et al. (2016) with slight modifications. Three micrograms of protein were heated in 4× sample loading buffer (40% vol/vol glycerol, 4% vol/vol β-mercaptoethanol, 0.08% wt/vol sodium dodecyl sulfate; Fisher Scientific) at 95ºC for 3 min. Protein utilized for evaluation of mTOR and AKT was loaded onto two separate 7.5% separating polyacrylamide gels with 3.5% stacking gels and separated at 40 mA. Proteins were transferred to a nitrocellulose membrane (Amersham Hybond-ECL; GE Healthcare) using blotting paper saturated with transfer buffer (25m*M* Tris, 192 m*M* glycine, and 5% vol/vol methanol) and a Semi-dry Transfer Unit (Hoefer, Holliston, MA). Blots were incubated with 5% nonfat dry milk in TBS-T (10 m*M* Tris, pH 8.0, 150 m*M* NaCl, 0.1% Tween-

20) for 30 min at room temperature to block nonspecific antigen sites. Subsequently, one blot was incubated with an p-mTOR and p-AKT antibody (1:1,000 and 1:2,000, respectively, in 1% nonfat dry milk in TBS-T; Cell Signaling, Beverly, MA) and the other blot was incubated with total mTOR and total AKT antibody (1:1,000 in 1% nonfat dry milk in TBS-T; Cell Signaling), overnight at 4ºC. Protein utilized for evaluation of RPS, 4EBP-1, MAFbx, and MURF-1 were loaded onto two separate 10% separating polyacrylamide gels with 3.5% stacking gels and separated at 40 mA. Proteins were transferred and blocked as described above with a transfer buffer (25m*M* Tris, 192 m*M* glycine, 2 mM EDTA and 15% vol/vol methanol) catered to smaller molecular weight proteins. Subsequently, one blot was incubated with an p-RPS, p-4EBP-1, and MURF-1 primary antibodies (1:1,000, 1:1,000, and 1:2,000, respectively, in 1% nonfat dry milk in TBS-T; Cell signaling, Beverly, MA) and the other blot was incubated with total RPS, total 4EBP-1, and MAFbx primary antibodies (1:1,000 in 1% nonfat dry milk in TBS-T; Cell Signaling), overnight at 4ºC.

Following primary antibody incubation, blots were incubated with an anti-rabbit horse radish peroxidase linked secondary antibody (1:1,000 in 5% nonfat dry milk in TBS-T; Cell Signaling) at room temperature for 1 h. Blots were developed using an enhanced chemiluminescence kit (ECL Plus, Amersham, Pittsburgh, PA) and visualized using the ChemiDoc-It 415 Imaging System (UVP, Upland, CA). Band intensities were quantified using VisionWorksLS Image Acquisition and Analysis Software (UVP; Upland, CA). Values are reported as the abundance of each protein that was equalized to a pooled sample ran on each blot and as the ratio of phosphorylated protein (relative abundance of phosphorylated protein / relative abundance of total protein × 100).

Statistical Analyses

All histology data were analyzed as a 2 × 3 factorial design using the GLIMMIX procedure of SAS (SAS Institute Inc., Cary, NC). Random effect was litter of fetuses, and fixed effects included fetal size (**Size**), muscle location (**LOC**), and the Size × LOC interaction. Proliferation assays were analyzed as a completely randomized design with repeated measures. The random effect was the pool of PFM. Fixed effects included size of the fetus from which PFM were isolated (**Size**), and time point of the assay (**Time**) was the repeated measure. The differentiation and protein synthesis assays were analyzed as a 3 × 3 factorial design, with main effects of Size and treatment (**Trt**), and random effect was the pool of PFM. Pair-wise comparisons between the least-square means of the factor levels, including planned interaction comparison, were computed using the PDIFF option of the LSMEANS statement. Differences were considered significant at $\alpha \leq 0.05$.

RESULTS

Fetal body weight

At d-60 and 95 of gestation Size affected fetal body weight ($P < 0.01$). At d-60 of gestation the SM fetuses exhibited a reduced fetal body weight compared to ME and LG fetuses ($P < 0.01$), which were similar to each other ($P = 0.06$). At d-95 of gestation SM fetuses had a reduced average fetal body weight compared to ME and LG fetuses ($P < 0.01$), and ME fetuses had a reduced ($P < 0.01$) average body weight compared to LS fetuses.

Muscle Fiber Morphometrics

At d-60 of gestation, the end of primary myogenesis and beginning of secondary myogenesis, muscle fiber morphology consisted of primary muscle fibers surrounded by small developing secondary muscle fibers (Fig. 2.2). Primary muscle fibers exhibited characteristically

hollow-center morphology, which previously has been used to identify primary muscle fibers (Wigmore and Stickland, 1983). Fiber associated nuclei were located on the periphery of muscle fibers or centrally located, and Pax7 positive muscle progenitor cells were typically located on the periphery of muscle fibers. At d-95 of gestation, the end of secondary myogenesis, primary muscle fibers again stained positively for the primary antibody, BA-D5, while secondary fibers stained negative (Fig. 2.3). When stained with a myosin heavy chain IIA antibody (SC-71), all secondary fibers stained positive, while primaries were negative. These findings are in agreement with Town et al. (2004), who described a similar staining pattern. Finally, unlike d-60, myonuclei and Pax7+ nuclei located on the periphery of muscle fibers.

At d-60 of gestation there were no Size × LOC interactions for WMA or any of the muscle fiber characteristics evaluated ($P \geq 0.06$; Table 2.1). There were no LOC effects on WMA, primary muscle fiber number, or secondary fibers per primary fiber ($P \geq 0.17$); however, LOC did affect primary muscle fiber CSA ($P < 0.01$). Primary muscle fiber CSA in longissimus thoracis was greater ($P < 0.01$) than primary muscle fiber area in longissimus lumborum. Size did affect ($P < 0.01$) WMA, with LG fetuses having greater WMA compared to ME and SM fetuses ($P \leq 0.05$), and ME fetuses having greater ($P < 0.01$) WMA compared to SM fetuses. Size also affected primary muscle fiber number and secondary fibers per primary fiber ($P \leq 0.03$). The SM fetuses had fewer primary fibers compared to ME and LG fetuses ($P \leq 0.03$), which did not differ ($P = 0.84$) from each other. The LG fetuses had more secondary fibers per primary fiber than SM and ME fetuses ($P \leq 0.02$), which did not differ ($P = 0.32$) from each other.

At d-95 of gestation there were no Size × LOC interactions for WMA or any of the muscle fiber characteristics measured ($P \geq 0.68$). The main effect of LOC affected WMA and all

muscle fiber characteristics measured ($P \leq 0.02$), except for primary muscle fiber number ($P = 0.36$). The longissimus lumborum had a greater WMA, secondary fiber number, secondary fibers per primary, and total fiber number fiber compared to the longissimus thoracis ($P \leq 0.02$). In contrast, the longissimus thoracis had a greater primary fiber CSA, secondary fiber CSA, and average muscle fiber CSA compared to the longissimus lumborum ($P \leq 0.02$). There were Size effects on WMA, secondary fiber CSA, and average muscle fiber CSA ($P \leq 0.02$); however, Size did not affect the other muscle fiber measures ($P \geq 0.11$). The LG fetuses had a greater WMA compared to SM and ME fetuses ($P \leq 0.02$), and ME fetuses had greater ($P < 0.01$) WMA than SM fetuses. The LG and ME fetuses had similar ($P = 0.06$) secondary muscle fiber CSA, but both categories had larger secondary fibers than SM fetuses ($P < 0.01$). The LG fetuses had greater average muscle fiber CSA of all fibers compared to SM and ME fetuses ($P \leq 0.04$), and ME fetuses had greater ($P < 0.01$) average muscle fiber CSA compared to SM fetuses.

Nuclei and Progenitor Cell Numbers

At d-60 of gestation there were no Size × LOC interactions or Size effects for nuclei per primary fiber or either of progenitor cell parameters evaluated ($P \geq 0.09$; Table 2.2); however, LOC affected all measures ($P \leq 0.02$). The Longissimus thoracis possessed more nuclei per primary fiber, Pax7+ progenitor cells per primary fiber, and total of Pax7+ progenitor cells compared to the Longissimus lumborum ($P \leq 0.02$).

At d-95 of gestation there were no Size × LOC interactions for any of the nuclear or progenitor cell measures ($P \geq 0.28$; Table 2.2). There was a LOC effect for nuclei per fiber and both progenitor cell parameters evaluated ($P \leq 0.02$), with the Longissimus thoracis exhibiting a more nuclei per fiber, more Pax7+ progenitors per fiber, but fewer total Pax7+ progenitor cells compared to the Longissimus lumborum. There were no Size effects on nuclei per fiber, or

Pax7+ progenitors per fiber ($P \geq 0.39$); however size did affect ($P < 0.01$) the total Pax7+ progenitor cells. The SM fetuses had fewer Pax7+ progenitor cells than ME and LG fetuses ($P \leq 0.03$), which did not differ ($P = 0.06$) from each other.

Porcine Fetal Myoblast Activity

Among PFM obtained from fetuses at d-95 of gestation there were no Time × Size interactions or Size effects for any of the criteria evaluated during the proliferation assay ($P \geq 0.15$, Table 2.3). Time did not affect the percentage of PFM that were only Pax7+ or Myf-5+ ($P \geq 0.08$); however, Time affected the proliferation rate, nuclear area, and the percentage of PFM that co-expressed Pax7 and Myf-5 ($P < 0.01$). The percentage of cells proliferating at 24 and 72 h were greater than those proliferating at 48 and 96 h ($P \leq 0.05$). The percentage of cells proliferating at 24 h was similar ($P = 0.12$) to 72 h, and percentage of cells proliferating at 48 h was similar ($P = 0.20$) to 96 h. At 24 h the nuclear area of PFM was smaller compared to all other time points ($P < 0.01$). Nuclear area at 48 h was similar ($P = 0.54$) to 72 h, and 96-h PFM nuclear area was greater than 48 and 72 h ($P < 0.01$). At 24 h, there was a greater percentage of PFM that co-expressed Pax7 and Myf-5 compared to all other periods ($P < 0.01$), and at 48 h there was a greater ($P < 0.01$) percentage of PFM co-expressing Pax7 and Myf-5 compared to 96 h. The percentage of PFM co-expressing Pax7 and Myf-5 at 72 h was similar to the percentage of PFM co-expressing Pax7 and Myf-5 at 48 and 96 h ($P = 0.08$).

There were no Trt × Size interactions for differentiation capacity or mTOR pathway proteins ($P \geq 0.06$; Table 2.4). There was an effect of Trt on the myotube diameter and the abundance of phosphorylated AKT ($P \leq 0.03$); however, Trt did not affect any of the other parameters ($P \geq 0.12$). The HS treated myotubes had smaller diameters than the other treatments ($P \leq 0.05$), which were similar in diameter to each other ($P = 0.55$). The IGF-1 treated myotubes

had a greater ($P = 0.01$) abundance of phosphorylated AKT compared to LS treated myotubes. However, HS treated myotubes had a similar abundance of phosphorylated AKT when compared to other treatments ($P = 0.06$). Size did not affect any of the parameters measured ($P \geq 0.06$), except for the abundance of phosphorylated 4EBP-1 ($P < 0.01$). Myotubes derived from LG fetuses had greater abundance of phosphorylated 4EBP-1 than the other sizes ($P < 0.01$), which had a similar ($P = 0.86$) abundance of phosphorylated 4EBP-1.

DISCUSSION

Effect of Fetal Size on Muscle Fiber Development

Pre-natal myogenesis is a biphasic process, where primary muscle fibers develop first to provide a surface for myoblasts to attach and differentiate into secondary muscle fibers (Wigmore and Stickland, 1983). Piglets from large litters are subject to naturally occurring intrauterine growth restriction (**IUGR**), which can be detrimental to muscle fiber development (Wigmore and Stickland, 1983; Wu et al., 2006; Wang et al., 2013). Prenatal effects impact postnatal growth, as piglets with fewer muscle fibers that are smaller exhibit decreased average daily gain from birth to weaning (Dwyer et al., 1993; Paredes et al., 2013). Previous literature focusing on d-60 of gestation indicated smaller fetuses had a similar number of primary muscle fibers with smaller diameters compared to their normal birth weight litter mates (Wang et al., 2013). In agreement, Wigmore and Stickland (1983) observed that total muscle fiber number in the semitendinosus muscle was similar for large and small fetuses within a litter, but fibers were larger in the large fetuses. In the current study at d-60 of gestation, which represents the transition between primary and secondary myogenesis, WMA of SM fetuses was 13% and 21% smaller than those of ME and LG fetuses, respectively. Additionally, WMA of ME fetuses was 7% smaller than LG fetuses. Differences in WMA between the size categories were due to

primary muscle fiber number and number of secondary fibers formed, but not primary muscle fiber CSA. When compared to ME and LG fetuses, SM fetuses had 12% and 13% fewer primary muscle fibers, respectively. Small fetuses did not differ from ME fetuses in secondary fiber development; however, SM fetuses had 13% fewer secondary fibers than LG fetuses. When ME fetuses were compared to LG, ME fetuses had a similar number of primary fibers, but 9% fewer secondary fibers. Therefore, differences in WMA between SM and ME fetuses was primarily due to the number of primary fibers formed, the difference in WMA between a SM and LG fetus was due to the combination of primary and secondary fiber formation, and the WMA difference between ME and LG fetuses was due to secondary fiber formation.

In the pig, secondary myogenesis is concluded between d-85 and d-90 of gestation and muscle fibers present at this time represent the totality of muscle fibers available to support postnatal muscle growth (Wigmore and Stickland, 1983). Wang et al. (2013) reported that fetuses of normal body weights had more and larger muscle fibers at d-90 of gestation compared to fetuses that had experienced IUGR; however, primary and secondary fibers were not distinguished. Wigmore and Stickland (1983) reported that over the course of gestation the smallest littermate had fewer muscle fibers with a smaller fiber CSA compared to the largest littermate. In the current study at d-95 of gestation, differences in WMA of the fetal size categories were maintained, but these differences were catalyzed by secondary fiber CSA. Small fetus WMA was 20% and 31% smaller than ME and LG fetuses, respectively, while WMA of ME fetuses was 9% smaller than that of LG fetuses. Compared to ME and LG fetuses, SM fetuses had 12% and 17% smaller secondary muscle fibers, respectively. This resulted in SM fetuses having a 13% and 18% smaller average fiber CSA than ME and LG fetuses, respectively. Fetuses classified as ME had 4% smaller secondary muscle fiber CSA compared to LG fetuses,

which resulted in ME fetuses having a 5% smaller average fiber CSA. Therefore, because primary and secondary fiber number and primary fiber CSA did not influence WMA differences, but secondary fiber CSA did, this would indicate smaller pigs are on a delayed trajectory of muscle fiber development compared to their larger littermates.

Effect of Fetal Size on Myonuclei and Progenitor Cell Populations

Postnatal muscle growth and ultimate protein deposition is determined through transcriptional signals from myonuclei (Moss, 1968a). During periods of rapid growth, additional myonuclei are added to fibers to support growth via satellite cell incorporation (Buckingham, 2007). Resident muscle progenitors proliferate extensively during embryonic myogenesis and proliferation is slowed at the conclusion of fetal myogenesis as protein synthesis peaks (Schultz, 1996; Davis and Fiorotto, 2009). The muscle progenitor cells that do not differentiate into myonuclei during embryonic and fetal myogenesis will constitute the satellite cell pool (Bentzinger et al., 2012). Because myonuclei and satellite cells originate from the dermomyotome during gestation (Gros et al., 2005), detrimental effects of IUGR on muscle fiber development may also affect myonuclei and progenitor cell establishment. Previous literature indicates that nuclear density was not affected by size at birth; however, satellite cell content was greater in larger littermates (Brown and Stickland, 1993). At d-60 of gestation in the current study, nuclei per primary fiber and Pax7+ progenitor cell populations were similar among all fetal size categories. This trend continued through d 95 of gestation for nuclei per fiber and Pax7+ progenitors per fiber; however, SM fetuses had 13% and 25% fewer total Pax7+ progenitor cells than ME and LG fetuses, respectively. Because d-95 marks the end of secondary muscle fiber development, the remaining progenitor cells present must establish the satellite cell pool that will catalyze postnatal muscle growth and repair. Therefore, these data indicate

negative effects of IUGR slowing progenitor cell establishment and help explain origins of differences found by Brown and Strickland (1993).

Effect of Muscle Location on Muscle Fiber Development

The Longissimus is a large muscle that originates from the epaxial dermomyotome and develops in the rostral to caudal direction (Ordahl and Le Douarin, 1992; Tajbakhsh and Buckingham, 2000). To date there has not been research that has evaluated myogenesis of different regions of the Longissimus muscle of the pig. Therefore, data were analyzed to explore if the size related delayed trajectory of myogenesis selectively affected the development of the Longissimus thoracis and Longissimus lumborum. At both gestational time points, myogenic development of both muscle locations were affected similarly by all fetal sizes; however, locational differences were found.

The Longissimus thoracis had 15% larger primary fibers than the Longissimus lumborum at d 60 of gestation; however, these differences were not enough to drive WMA differences. This was most likely due to the two areas not exhibiting differences in primary and secondary fiber formation. By d-95 of gestation, the Longissimus thoracis had larger primary and secondary muscle fiber CSA than the Longissimus lumborum, resulting in a 12% increase in average muscle fiber CSA. Even though the Longissimus lumborum had smaller average muscle fiber CSA, the location had 18% more total fibers than the Longissimus thoracis, which was driven by an 18% increase in secondary fiber number. This ultimately led to the Longissimus lumborum having a 7% larger WMA than the Longissimus thoracis. These data indicate a divergent pattern of muscle fiber hyperplasia and hypertrophy between two locations of the same muscle and that increases in muscle fiber number are more powerful than increases in fiber CSA when determining WMA differences.

At d-60 of gestation the longissimus thoracis contained 15% more nuclei per primary fiber, 13% more total Pax7+ progenitor cells, and 19% more Pax7+ progenitors per primary fiber than the longissimus lumborum. Carried out to d-95 of gestation, the larger size of the Longissimus lumborum resulted in 11% increase in the number of total Pax7+ progenitor cells. When put on a per fiber basis, the longissimus thoracis contained 21% more nuclei per fiber and 15% more Pax7+ progenitors per fiber than the longissimus lumborum. These data illustrate that increased muscle fiber hypertrophy experienced by the longissimus thoracis is mediated through increased number of nuclei per fiber and Pax7+ progenitor cells per fiber. The developmental differences in WMA and muscle fiber development within the longissimus thoracis and longissimus lumborum are supported by changes in prevalence of nuclei and Pax7+ progenitor cells.

Effect of Fetal Size on Porcine Fetal Myoblast Activity

As myoblasts differentiate to create muscle fibers, a subset of myoblasts will retain the expression of the paired box proteins and the ability to proliferate (Relaix et al., 2005). These myoblasts make up the postnatal satellite cell pool (Bentzinger et al., 2012). The majority of myonuclei are accumulated postnatally and satellite cell differentiation serves as the sole source to increase myonuclei needed during postnatal muscle hypertrophy (Moss and Leblond, 1971; Allen et al., 1979). Satellite cell proliferation is required to replenish the satellite cell pool needed for postnatal muscle growth, and rate of satellite cell proliferation is indicative of muscle growth potential (Hawke and Garry, 2001). Nissen and Oksbjerg (2009) isolated satellite cells from the lightest, medium, and greatest birth weight gilts within a litter at 6 wk of age and reported cells from the lightest gilt tended to have fewer viable cells over the course of a proliferation assay, indicating satellite cells from the lightest gilt proliferated more slowly. In the

current study, proliferation rate was evaluated using the thymidine analog, BrdU, to identify all cells that traversed the S-phase within the 2 h prior to fixation. In contrast to previous results, the proliferation rate of PFM was similar among all fetal sizes and all fetal sizes had similar proliferation rates over Time. The activity of myogenic progenitor cells is mediated through transition of myogenic transcription factors (Zammit et al., 2006), and as cell size increases the cells proliferative ability decreases (Dolfi et al., 2013). *In vitro* proliferative satellite cells can be characterized into three sub-classes of cells that express Pax7, Myf-5, and co-express Pax7 and Myf-5 (Li et al., 2011). The PFM in the current study are phenotypically and transcriptionally similar. This is indicated by PFM from different fetal size categories having a similar nuclear area, and temporal expression of Pax7 and Myf-5.

Satellite cells must proliferate to replenish their population during periods of growth, but in order to contribute to muscle growth a portion of the population must terminally differentiate and fuse into muscle fibers (Moss 1968a; Schultz 1996). Nissen and Oksbjerg (2009) observed that dispite the lightest birth weight gilt having an elevation of an indicator of proliferation, there was no increase in satellite cell fusion. Additionally, Nissen and Oksbjerg (2009) indicated protein synthesis and degradation characteristics of satellite cell derived myotubes were not affected by the growth rate of the gilt from which the satellite cells were isolated. Differentiation capacity and myotube diameter were also similar between fetal size categories in the current study.

Even though protein synthesis characteristics were largely similar among PFM from different fetal size categories, it is interesting that LG fetuses had 53% and 56% more phosphorylated 4E-BP than ME and SM fetuses, respectively. Even though fetal size did not influence growth of myotubes, or proteins of mTOR pathway signaling that modulate protein

synthesis, this indicates that there is less negative regulation of protein synthesis in PFM from LG fetuses. Collectively, these observations indicates there are within litter variation in metabolic capabilities of progenitor cells, but in both studies have not resulted in phenotypic detriments of myotubes derived from either PFM or satellite cells (Nissen and Oksbjerg, 2009). Additionally, growth factors play an integral role in differentiation and protein synthesis of skeletal muscle cells (Stitt et al., 2004; Sotiropouluos et al., 2006; Han et al., 2008). Stitt et al. (2004) indicated that IGF-1 supplementation to C2C12 muscle cell line induces muscle hypertrophy through mTOR pathway signaling. Additionally, Han et al. (2008) indicated that IGF-1 also promoted protein synthesis of adult porcine satellite cells through the mTOR signaling pathway. In the current study, LS and IGF-1 treated myotubes exhibited 17% and 14% greater myotube diameter than HS treated myotubes, respectively. Increase in myotube diameter does not appear to be mediated through mTOR pathway signaling. The addition of 100 ng/mL IGF-1 resulted in a 51% increase in abundance of phosphorylated AKT compared to the LS treatment, but the mTOR signaling cascade did not continue downstream as previously characterized in myogenic cells from adult animals (Stitt et al., 2004; Han et al., 2008). Fetal serum IGF-1 concentration does not begin to increase until the conclusion of gestation (Li et al., 1991), which may explain why mTOR pathway signaling was not fully stimulated in the current study. Additionally, when treatments increased myotube diameter and abundance of phosphorylated AKT, effects were similar for all fetal size categories. This indicates that if PFM from different size categories have equivalent ability to stimulate muscle growth when provided a similar environment.

Figure 2.1. Fetal body weights of fetuses within size categories at d-60 and d-95 of gestation.

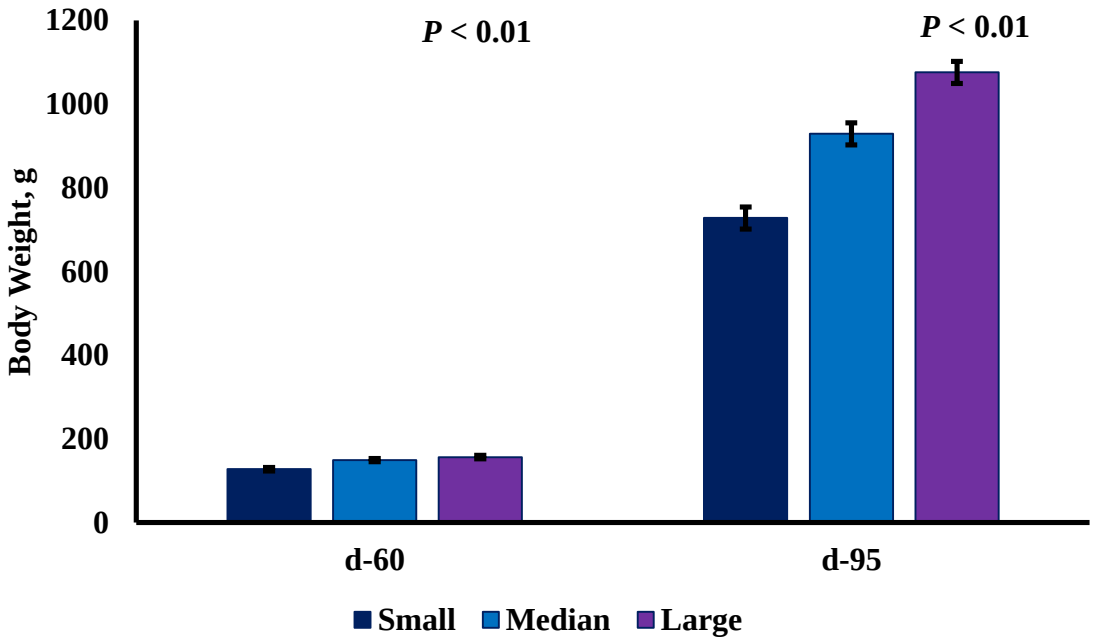

Figure 2.2. Cross section of longissimus muscle of a porcine fetus at d-60 ± 2 of gestation. A) Hosescht 33342, identifies all nuclei; B) a Pax7 antibody identifies a subset of nuclei as Pax7+ progenitor cells; C) an α-dystrophin antibody identifies periphery of muscle fibers (red), and BA-D5 positively stains primary muscle fibers (orange); D) merged image of all antibodies. Scale bars = 100 µm.

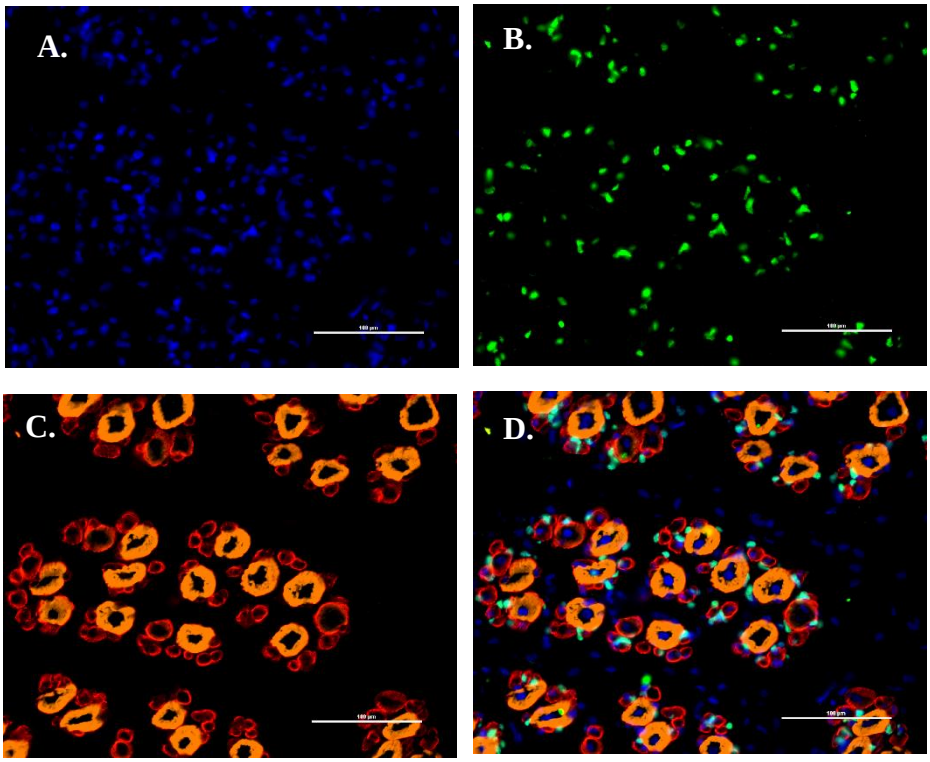

Figure 2.3. Cross section of longissimus muscle of a porcine fetus at d-95 or 96 of gestation. A) Hosescht 33342, identifies all nuclei; B) a Pax7 antibody identifies a subset of nuclei as Pax7+ progenitor cells; C) an α-dystrophin antibody identifies periphery of muscle fibers (red), and BA-D5 positively stains primary muscle fibers (orange); D) merged image of all antibodies. Scale bars = 100 µm.

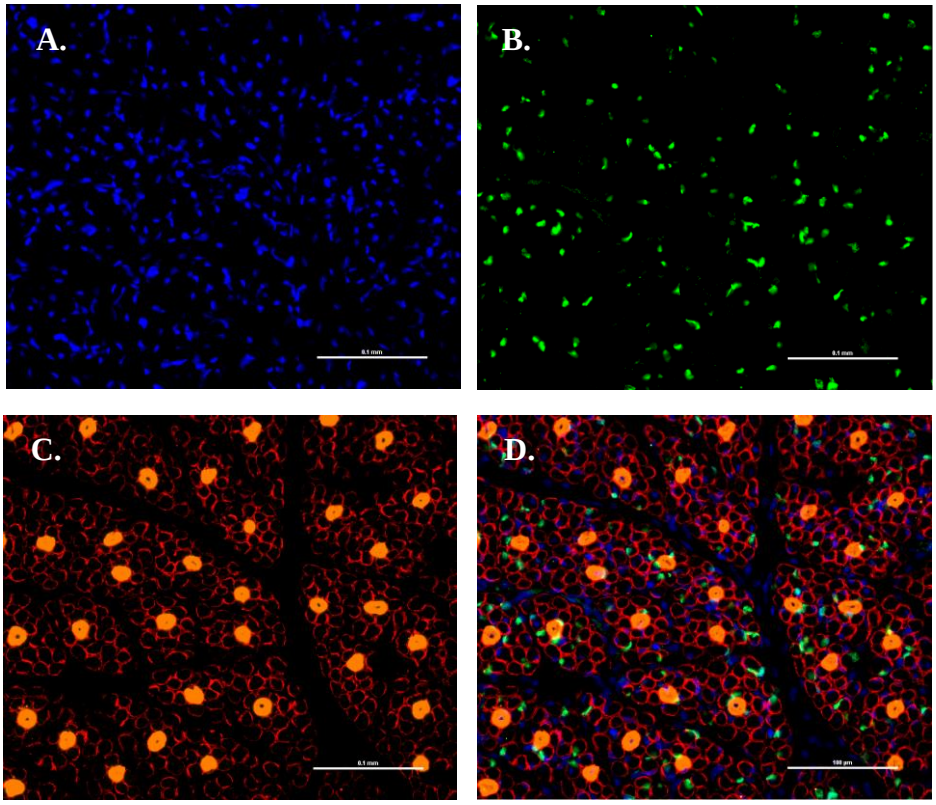

Table 2.1. Whole muscle and muscle fiber characteristics of the longissimus lumborum and longissimus thoracis from the smallest (**SM**), median (**ME**), and largest (**LG**) male fetuses within litters at d-60 and d-95 of gestation

	Longissimus thoracis			Longissimus lumborum				*P*-value		
	Small	Median	Large	Small	Median	Large	SEM	Size × LOC	LOC	Size
D-60 fetuses										
Whole muscle CSA[1], mm^2	51.6	60.1	67.0	53.0	58.3	60.0	2.3	0.15	0.17	< 0.01
Fiber characteristics										
Primary fiber number[2]	109,395	112,794	126,077	105,702	127,425	116,483	7,779	0.09	0.93	0.03
Primary fiber CSA, µm^2	514	570	556	466	481	483	18	0.50	< 0.01	0.09
Secondary muscle fibers per primary muscle fiber[3]	2.3	2.3	2.8	2.4	2.5	2.5	0.1	0.06	0.85	< 0.01
D-95 fetuses										
Whole muscle CSA,	127.5	148.4	163.4	132.6	163.5	176.1	6.8	0.68	0.02	< 0.01
Fiber characteristics										
Primary fiber number[2]	76,152	72,445	76,944	80,869	76,359	79,614	5,554	0.98	0.36	0.66
Primary fiber CSA, µm^2	169	168	176	160	164	166	8	0.70	0.02	0.20
Secondary fiber number[4]	1,430,697	1,495,323	1,550,986	1,710,049	1,827,795	1,944,870	91,443	0.77	< 0.01	0.09
Secondary fiber CSA, µm^2	84	93	98	73	83	86	3	0.76	< 0.01	< 0.01
Secondary fibers per primary fiber[3]	19.5	20.9	21.5	23.0	25.1	26.2	1.3	0.89	< 0.01	0.11
Total fiber number[5]	1,506,574	1,567,559	1,627,722	1,790,643	1,903,946	2,024,275	94,679	0.79	< 0.01	0.10
Average muscle fiber CSA, µm^2	90	97	103	75	87	89	3	0.68	< 0.01	< 0.01

[1]CSA = cross-sectional area.

[2]The total number of primary muscle fibers was calculated as the whole muscle cross-sectional area divided by the average primary muscle fiber CSA.

[3]Represents the ratio of secondary muscle fibers that were present per primary muscle fiber.

[4]Total number of primary muscle fibers was calculated by multiplying the total number of muscle fibers by the percentage of fibers that were secondary muscle fibers.

[5]The total number of muscle fibers was calculated as the whole muscle cross-sectional area divided by the average muscle fiber CSA.

Table 2.2. Nuclei and Pax7 positive progenitor cell number from the longissimus lumborum and longissimus thoracis from the smallest (**SM**), median (**ME**), and largest (**LG**) male fetuses within litters at d-60 and d-95 of gestation

	Longissimus thoracis			Longissimus lumborum				*P*-value		
	Small	Median	Large	Small	Median	Large	SEM	Size × LOC[1]	LOC	Size
D-60 fetuses										
Nuclei per primary fiber[2]	4.9	5.4	5.3	4.4	4.2	4.5	0.2	0.24	< 0.01	0.37
Pax7+ progenitor cell number[3]	26,966	29,837	33,857	24,814	27,221	26,611	2,464	0.37	0.02	0.09
Pax7+ progenitors per primary fiber[4]	2.0	2.1	2.1	1.7	1.6	1.7	0.1	0.62	< 0.01	0.85
D-95 fetuses										
Nuclei per fiber[2]	1.1	1.2	1.1	0.9	0.9	0.8	0.1	0.63	< 0.01	0.90
Pax7+ progenitor cell number[3]	74,928	89,891	93,115	86,628	93,133	108,673	6,541	0.44	0.01	< 0.01
Pax7+ progenitors per fiber[4]	0.18	0.22	0.21	0.17	0.16	0.18	0.02	0.28	0.02	0.39

[1]LOC = location effect.

[2]Represents the average number of nuclei associated with each muscle fiber.

[3]The total number of progenitor cells was calculated as the whole muscle cross-sectional area divided by the area of an image, then multiplied by the number of Pax7+ cells per image.

[4]Represents the average number of Pax7+ progenitor cells associated with each muscle fiber.

Table 2.3. Proliferation rate, nuclear area, and temporal expression of Pax7 and Myf-5 of porcine fetal myoblasts (PFM) harvested from the longissimus muscle of the smallest (**SM**), median (**ME**), and largest (**LG**) male fetuses within litters at d-95 of gestation[1]

					P-value		
Size	SM	ME	LG	SEM	Time × Size	Time	Size
Proliferation rate[2], %							
24 h	50.0	48.0	52.7	4.8	0.94	< 0.01	0.15
48 h	40.1	33.2	38.3				
72 h	46.7	38.7	48.5				
96 h	30.6	31.3	35.9				
Nuclear area[3], μm^2							
24 h	125.5	123.0	132.3	6.7	0.33	< 0.01	0.86
48 h	141.5	137.8	142.2				
72 h	137.8	148.6	141.7				
96 h	163.0	164.6	157.2				
Pax7+[4], %							
24 h	0.0	0.0	0.0	0.7	0.57	0.08	0.44
48 h	0.5	0.3	0.3				
72 h	0.4	0.6	0.3				
96 h	2.5	0.2	1.5				
Myf5+[5], %							
24 h	16.46	13.54	31.4	4.6	0.23	0.10	0.25
48 h	22.76	28.44	30.3				
72 h	28.74	30.07	24.0				
96 h	26.99	31.25	31.4				
Pax7+ and Myf5+[6], %							
24 h	83.5	86.0	67.7	6.7	0.48	< 0.01	0.38
48 h	70.6	61.6	90.1				
72 h	57.7	48.4	57.2				
96 h	45.0	46.5	46.1				

[1]Porcine fetal myoblasts from the SM, ME, and LG male fetuses maintained in 10% fetal bovine serum, 2% porcine serum in DMEM supplemented with 100 U penicillan/mL, 100 μg of strepmycin/mL, and 20 μg of gentamicin/mL . Parallel cultures were exposed to 5 μM bromodeoxyuridine (BrdU) and immunostained daily.

[2]Number of BrdU positive PFM divided by the total number of PFM present within 10 representative photomicrographs.

[3]Represents the average nuclear area of PFM.

[4]Represents the percentage of all PFM that solely immunostained Pax7 positive.

[5]Represents the percentage of all PFM that solely immunostained Myf-5 positive.

[6]Represents the percentage of all PFM that co-expressed Pax7 and Myf-5.

Table 2.4. Differentiation capacity, myotube development, and mammalian target of rapamycin (mTOR) signaling of longissimus muscle porcine fetal myoblasts from the smallest (**SM**), median (**ME**), and largest (**LG**) male fetuses harvested within litters at d-95 of gestation and exposed to different growth media cocktails[1]

	Low Serum			High Serum			IGF-1				*P*-value[2]		
	SM	ME	LG	SM	ME	LG	SM	ME	LG	SEM	Trt × Size	Trt	Size
Differentiation capacity[3], %	32.2	41.1	38.3	37.5	38.0	32.0	36.0	40.5	31.2	3.8	0.52	0.88	0.15
Myotube diameter[4], µm	34.3	30.3	29.3	25.9	25.3	26.6	31.4	28.2	30.8	2.4	0.78	0.03	0.42
mTOR pathway signaling[5]													
AKT													
Total, AU[6]	0.83	0.77	0.84	0.97	1.43	1.38	0.78	2.13	1.14	0.56	0.74	0.46	0.45
Phosphorylated[7], AU	0.39	0.54	0.76	0.82	1.07	0.96	1.03	1.15	1.27	0.27	0.97	0.03	0.46
Ratio phosphorylated, AU	53	100	101	139	100	111	132	124	96	40	0.75	0.53	0.98
mTOR													
Total, AU	0.93	0.78	1.46	2.44	1.26	1.65	0.91	1.69	1.22	0.47	0.23	0.15	0.83
Phosphorylated[8], AU	0.75	0.75	1.24	1.59	1.14	0.99	1.27	1.81	0.96	0.50	0.57	0.52	0.90
Ratio phosphorylated, AU	107	82	110	100	132	86	125	86	86	25	0.50	0.93	0.72
RPS													
Total, AU	0.92	0.43	2.17	2.21	1.19	2.72	2.79	0.89	1.21	0.84	0.56	0.46	0.17
Phosphorylated[9], AU	1.05	1.10	1.25	2.41	1.91	1.94	1.30	1.32	1.20	0.59	0.98	0.13	0.95
Ratio phosphorylated, AU	89	74	55	172	80	73	88	130	59	26	0.18	0.27	0.06
4E-BP													
Total, AU	1.17	0.76	2.26	2.44	2.70	1.24	0.85	0.90	2.68	0.74	0.18	0.43	0.55
Phosphorylated[10], AU	1.00	0.72	1.24	0.94	0.84	1.74	0.65	1.17	2.87	0.33	0.09	0.12	< 0.01
Ratio phosphorylated, AU	63	101	135	123	142	97	95	156	54	38	0.43	0.76	0.38
MAFbx, AU	0.89	1.26	1.04	1.15	1.88	1.14	1.33	0.68	1.81	0.38	0.20	0.59	0.80
MURF-1, AU	0.85	0.62	1.40	1.20	2.00	0.93	0.82	0.93	1.45	0.30	0.06	0.23	0.45

[1]Differentiating and differentiated porcine fetal myoblasts were treated with a low serum treatment containing 2% porcine serum in DMEM supplemented with 100 U penicillan/mL, 100 µg of strepmycin/mL, and 20 µg of gentamicin/mL, a high serum treatment was the low serum treatment with the addition of 10% fetal bovine serum, and the IGF-1 treatment was the low serum treatment with the addition of 100 ng/mL IGF-1.

[2]Trt = treatment effect.

[3]Percentage of all PFM that have incorporated into multinucleated sarcomeric myosin positive myotubes.

[4]Average diameter of multinucleated myotubes from 10 representative photomicrographs.

[5]AKT = protein kinase B, mTOR = mammalian target of rapamycin, RPS = ribosomal protein S6, 4E-BP = eukaryotic translation initiation factor 4E binding protein, MAFbx = muscle atrophy F-box, and MURF-1 = muscle ring finger-1.

[6]AU = Arbitrary Unit

[7]AKT phosphorylated at Ser^{473}

[8]mTOR phosphorylated at Ser^{2448}

[9]RPS phosphorylated at $Ser^{235/236}$

[10]4E-BP phosphorylated at $Thr^{37/46}$

REFERENCES

Allen, R. E., R. A. Merkel, and R. B. Young. 1979. Cellular aspects of muscle growth: myogenic cell proliferation. J. Anim. Sci. 49:115-127.

Bell, A. W., and P. L. Greenwood. 2016. Prenatal origins of postnatal variation in growth, development and productivity of ruminants. Anim. Prod. Sci. 56:1217-1232. doi:10.1071/AN15408

Bentzinger, C. F., Y. X. Wang, and M. A. Rudnicki. 2012. Building muscle: molecular regulation of myogenesis. Cold Spring Harb. Perspect. Biol. 4. doi:10.1101/cshperspect.a008342

Brown, S. C., and N. C. Stickland. 1993. Satellite cell content in muscles of large and small mice. J. Anat. 183 (Pt 1):91-96.

Buckingham, M. 2007. Skeletal muscle progenitor cells and the role of Pax genes. C. R. Biol. 330:530-533. doi:10.1016/j.crvi.2007.03.015

Campbell, R. G., N. C. Steele, T. J. Caperna, J. P. Mcmurtry, M. B. Solomon, and A. D. Mitchell. 1989. Interrelationships between sex and exogenous growth-hormone administration on performance, body-composition and protein and fat accretion of growing-pigs. J. Anim. Sci. 67:177-186.

Davis, T. A., and M. L. Fiorotto. 2009. Regulation of muscle growth in neonates. Curr Opin Clin Nutr. Metab. Care. 12:78-85. doi:10.1097/MCO.0b013e32831cef9f

Dolfi, S. C., L. L. Chan, J. Qiu, P. M. Tedeschi, J. R. Bertino, K. M. Hirshfield, Z. N. Oltvai, and A. Vazquez. 2013. The metabolic demands of cancer cells are coupled to their size and protein synthesis rates. Cancer. Metab. 1:20. doi:10.1186/2049-3002-1-20

Dwyer, C. M., J. M. Fletcher, and N. C. Stickland. 1993. Muscle cellularity and postnatal growth in the pig. J. Anim. Sci. 71:3339-3343.

Fix, J. S., J. P. Cassady, J. W. Holl, W. O. Herring, M. S. Culbertson, and M. T. See. 2010. Effect of piglet birth weight on survival and quality of commercial market swine. Livest. Sci. 132:98-106. doi:DOI 10.1016/j.livsci.2010.05.007

Gondret, F., L. Lefaucheur, L. Louveau, B. Lebret, X. Pichodo, and Y. Le Cozler. 2005. Influence of piglet birth weight on postnatal growth performance, tissue lipogenic capacity and muscle histological traits at market weight. Livest. Prod. Sci. 93:137-146. doi:DOI 10.1016/j.livprodsci.2004.09.009

Han, B., J. Tong, M. J. Zhu, C. Ma, and M. Du. 2008. Insulin-like growth factor-1 (IGF-1) and leucine activate pig myogenic satellite cells through mammalian target of rapamycin (mTOR) pathway. Mol. Reprod. Dev. 75:810-817. doi:10.1002/mrd.20832

Handel, S. E., and N. C. Stickland. 1988. Catch-up growth in pigs - a relationship with muscle cellularity. Anim. Prod. 47:291-295.

Hawke, T. J., and D. J. Garry. 2001. Myogenic satellite cells: physiology to molecular biology. J. Appl. Physiol. 91:534-551.

Hinterberger, T. J., and K. F. Barald. 1990. Fusion between myoblasts and adult muscle-fibers promotes remodeling of fibers into myotubes in vitro. Development. 109:139-148.

Lee, C. Y., F. W. Bazer, T. D. Etherton, and F. A. Simmen. 1991. Ontogeny of insulin-like growth factors (IGF-I and IGF-II) and IGF-binding proteins in porcine serum during fetal and postnatal development. Endocrin. 128:2336-2344.

Li, J., J. M. Gonzalez, D. K. Walker, M. J. Hersom, A. D. Ealy, and S. E. Johnson. 2011. Evidence of heterogeneity within bovine satellite cells isolated from young and adult animals. J. Anim. Sci. 89:1751-1757. doi:10.2527/jas.2010-3568

Ma, G. D., H. Y. Wang, X. F. Gu, W. Li, X. L. Zhang, L. L. Cui, Y. Li, Y. Zhang, B. Zhao, and K. S. Li. 2014. CARP, a myostatin-downregulated gene in CFM Cells, is a novel essential positive regulator of myogenesis. Int. J. Biol. Sci. 10:309-320. doi:10.7150/ijbs.7475

Moss, F. P. 1968a. The relationship between the dimensions of the fibres and the number of nuclei during normal growth of skeletal muscle in the domestic fowl. Am. J. Anat. 122:555-563.

Moss, F. P. 1968b. The relationship between the dimensions of the fibres and the number of nuclei during restricted growth and compensatory growth of skeletal muscle. Am. J. Anat. 122:565-571.

Moss, F. P., and C. P. Leblond. 1971. Satellite cells as the source of nuclei in muscles of growing rats. Anat. Record. 170:421-435.

Nissen, P. M., and N. Oksbjerg. 2009. In vitro primary satellite cell growth and differentiation within litters of pigs. Animal. 3:703-709. doi:10.1017/S1751731109003929

NRC. 2012. Nutrient requirements of swine. 11th rev. ed. Natl. Acad. Press, Washington, DC.

Ordahl, C. P., and N. M. Le Douarin. 1992. Two myogenic lineages within the developing somite. Development. 114:339-353.

Paredes, S. P., C. Kalbe, A. J. Jansman, M. W. Verstegen, H. M. van Hees, D. Losel, W. J. Gerrits, and C. Rehfeldt. 2013. Predicted high-performing piglets exhibit more and larger skeletal muscle fibers. J. Anim. Sci. 91:5589-5598. doi:10.2527/jas.2013-6908

Paulk, C. B., M. D. Tokach, J. L. Nelssen, D. D. Burnett, M. A. Vaughn, K. J. Phelps, S. S. Dritz, J. M. Derouchey, R. D. Goodband, J. C. Woodworth, T. A. Houser, K. D. Haydon, and J. M. Gonzalez. 2014. Effect of dietary zinc and ractopamine-HCl on pork chop muscle fiber type distribution, tenderness, and color characteristics. J. Anim. Sci. doi:10.2527/jas.2013-7318

Phelps, K. J., J. S. Drouillard, M. B. Silva, L. D. Miranda, S. M. Ebarb, C. L. Van Bibber-Krueger, T. G. O'Quinn, and J. M. Gonzalez. 2016. Effect of extended postmortem aging and steak location on myofibrillar protein degradation and Warner-Bratzler shear force of beef M. semitendinosus steaks. J. Anim. Sci. 94:412-423. doi:10.2527/jas.2015-9862

Pipalia, T. G., J. Koth, S. D. Roy, C. L. Hammond, K. Kawakami, and S. M. Hughes. 2016. Cellular dynamics of regeneration reveals role of two distinct Pax7 stem cell populations in larval zebrafish muscle repair. Dis. Model. Mech. 9:671-684. doi:10.1242/dmm.022251

Pirkmajer, S., and A. V. Chibalin. 2011. Serum starvation: caveat emptor. Am. J. Physiol. Cell Physiol. 301:C272-279. doi:10.1152/ajpcell.00091.2011

Quiniou, N., J. Dagorn, and D. Gaudre. 2002. Variation of piglets birth weight and consequences on subsequent performance. Livest. Prod. Sci. 78:63-70. doi:Pii S0301-6226(02)00181-1

Relaix, F., D. Rocancourt, A. Mansouri, and M. Buckingham. 2005. A Pax3/Pax7-dependent population of skeletal muscle progenitor cells. Nature. 435:948-953.

Schultz, E. 1996. Satellite cell proliferative compartments in growing skeletal muscles. Dev. Biol. 175:84-94. doi:10.1006/dbio.1996.0097

Sotiropoulos, A., M. Ohanna, C. Kedzia, R. K. Menon, J. J. Kopchick, P. A. Kelly, and M. Pende. 2006. Growth hormone promotes skeletal muscle cell fusion independent of

insulin-like growth factor 1 up-regulation. Proc. Natl. Acad. Sci. U. S. A. 103:7315-7320. doi:10.1073/pnas.0510033103

Stitt, T. N., D. Drujan, B. A. Clarke, F. Panaro, Y. Timofeyva, W. O. Kline, M. Gonzalez, G. D. Yancopoulos, and D. J. Glass. 2004. The IGF-1/PI3K/Akt pathway prevents expression of muscle atrophy-induced ubiquitin ligases by inhibiting FOXO transcription factors. Mol. Cell. 14:395-403.

Tajbakhsh, S., and M. Buckingham. 2000. The birth of muscle progenitor cells in the mouse: spatiotemporal considerations. Curr. Top. Dev. Biol. 48:225-268.

Town, S. C., C. T. Putman, N. J. Turchinsky, W. T. Dixon, and G. R. Foxcroft. 2004. Number of conceptuses in utero affects porcine fetal muscle development. Reproduction. 128:443-454. doi:10.1530/rep.1.00069

Wang, T., C. Liu, C. Feng, X. Wang, G. Lin, Y. Zhu, J. Yin, D. Li, and J. Wang. 2013. IUGR alters muscle fiber development and proteome in fetal pigs. Front. Biosci. 18:598-607.

Wigmore, P. M., and N. C. Stickland. 1983. Muscle development in large and small pig fetuses. J. Anat. 137 (Pt 2):235-245.

Wu, G., F. W. Bazer, J. M. Wallace, and T. E. Spencer. 2006. Board-invited review: intrauterine growth retardation: implications for the animal sciences. J. Anim. Sci. 84:2316-2337. doi:10.2527/jas.2006-156

Yates, D. T., A. R. Macko, M. Nearing, X. Chen, R. P. Rhoads, and S. W. Limesand. 2012. Developmental programming in response to intrauterine growth restriction impairs myoblast function and skeletal muscle metabolism. J. Pregnancy. 2012:631038. doi:10.1155/2012/631038

Zammit, P. S., T. A. Partridge, and Z. Yablonka-Reuveni. 2006. The skeletal muscle satellite cell: the stem cell that came in from the cold. J. Histochem. Cytochem. 54:1177-1191. doi:10.1369/jhc.6R6995.2006

Chapter 3 - Effect of porcine plasma supplementation on proliferation and differentiation characteristics of porcine fetal myoblasts in vitro

ABSTRACT

This experiment was conducted to determine effects of porcine plasma supplementation on porcine fetal myoblast (**PFM**) proliferation, differentiation, protein synthesis, and mammalian target of rapamycin (**mTOR**) pathway signaling. Porcine fetal myoblasts were isolated from whole left LM of the smallest (**SM**), median (**ME**), and largest (**LG**) fetus from each litter at d-60 ± 2 of gestation (n = 3/size category). Proliferation assays were conducted as a 4 × 3 × 3 factorial arrangement with time of culture (24, 48, 72, 96 h), fetus size, and media treatment as main effects. Treatments consisted of: high serum which consisted high-glucose Dulbecco's Modified Eagle Medium supplemented with 10% (vol/vol) fetal bovine serum (**FBS**), 2% (vol/vol) porcine serum, 100 U penicillan/mL, 100 µg of strepmycin/mL, and 20 µg of gentamicin/mL (**HS**), low serum which consisted of HS without 10% FBS (**LS**), and LS supplemented with 10% (wt/vol) porcine plasma (**PP**). Cultures were immunostained for Pax7, Myf-5, and bromodeoxyuridine (**BrdU**). Differentiation and protein synthesis synthesis assays were conducted as 2 × 2 × 3 factorial designs with serum concentration, PP, and fetus size as the main effects. Treatment and Size affected proliferation rate, and percent of PFM that co-expressed Pax7 and Myf-5 (P < 0.01). The HS-PFM had a greater proliferation rate compared to the LS- and PP-PFM (P < 0.01), and PP-PFM had a greater (P < 0.01) proliferation rate compared to LS-PFM. The LS-PFMt had a lower percentage of PFM co-expressing Pax7 and Myf-5 than HS- and PP-PFM (P < 0.01), which were similar (P = 0.31). Small and ME fetuses'

PFM had a greater proliferation rate than LG fetuses' PFM ($P < 0.04$), and which were similar ($P = 0.09$). Small fetuses' PFM had a greater ($P = 0.01$) percentage of cells co-expressing Pax7 and Myf-5 compared to LG fetuses' PFM, and ME fetuses' PFM had a similar percentage of cells co-expressing Pax7 and Myf-5 as SM and LG fetus PFM ($P \geq 0.16$). There was an effect of PP and Size on myotube diameter ($P < 0.01$). The PPP-PFM had a decreased ($P < 0.01$) myotube diameter compared to PPN-PFM. Small fetuses' PFM had a greater myotube diameter compared to ME and LG fetuses' PFM ($P < 0.01$), and ME fetuses' PFM had a greater ($P = 0.01$) myotube diameter compared to LG fetuses' PFM. Supplementation of porcine plasma to PFM promotes the proliferation and at d-60 of gestation SM fetuses' PFM appear to have to potential for compensatory proliferation when in an optimal nutrient environment.

KEYWORDS: differentiation, porcine fetal myoblasts, porcine plasma, proliferation,

INTRODUCTION

Stimulating efficient growth of skeletal muscle of swine will improve the overall efficiency of pork production. Muscle is a dynamic tissue accounting for approximately 40% of the body mass and 65% of fetal glucose usage (Yates et al., 2012). Muscle mass is determined by the number and size of individual muscle fibers (Oksbjerg et al., 2013), with the number of muscle fibers being determined prior to birth. Prenatal myogenesis is the proliferation, commitment, and differentiation of embryonic and fetal myoblasts into mature muscle cells, and occurs in two waves (Biressi et al., 2007; Bentzinger et al., 2012). In pigs, primary muscle fibers develop between d 25 and 50 of gestation, followed by development of secondary muscle fibers through d 90 of gestation (Wigmore and Stickland, 1983; Handel and Stickland, 1987). Placental insufficiency results in fetal nutrient restriction, and decreased piglet survival (Rehfeldt et al.,

2011) and as characterized in chapter 2 leads to a delayed trajectory of myogenesis of smaller fetuses within litters.

Quiescent myogenic progenitor cells highly express paired box transcription factor-7 (**Pax7**) and transition to express myogenic factor-5 (**Myf-5**) as they mature (Zammit et al., 2006). Additionally, there are a subclass of daughter cells that co-express Pax7 and Myf-5, which exhibit advanced proliferative characteristics (Kuang et al., 2007; Li et al., 2011). Compounds such as insulin-like growth factor-1 (**IGF-1**) play a central role in proliferation and differentiation of satellite cells *in vitro* and *in vivo* (Engert et al., 1996; Stitt et al., 2004), providing a potential avenue to augment muscle growth. In addition to effects of IGF-1 on cell cycle progression and proliferation, IGF-1 stimulates cellular differentiation and protein synthesis (Han et al., 2008; Stitt et al., 2004; Rommel et al., 2001). The feed additive, porcine plasma, possesses elevated levels of IGF-1 and amino acids (de Rodas et al., 1995). Additionally, porcine plasma stimulated proliferation of jejunal epithelial cells when supplemented with 2.5 to 10% porcine plasma *in vitro* (Tran et al., 2014), suggesting that porcine plasma can directly affect cellular activity and tissue development. Therefore, the objective of the current study was to determine the effect of porcine plasma supplementation *in vitro* on porcine fetal myoblast (**PFM**) proliferation, differentiation, and protein synthesis.

MATERIALS AND METHODS

The experimental procedures were approved by the Kansas State University Institutional Animal Care and Use Committee.

Progenitor cell isolation

At d-60 ± 2 of gestation, based on crown-rump-length, whole left LM were collected from the smallest (**SM**), median (**ME**), and largest (**LG**) fetuses of litters of 3 randomly chosen sows based on crown-to-rump length. These muscles were utilized for PFM isolation with a total

of 9 pools (n = 3/size category). The methods of Li et al. (2011) were be followed for PFM isolation with slight modifications. Briefly, muscles were excised of all visible connective tissue and minced with sterilized surgical scissors. The tissue was digested with 0.8 mg/mL of pronase XIV (Sigma Aldrich; St. Louis, MO) in Phosphate Buffered Saline (**PBS**, Corning, Corning, NY) for 45 min at 37°C. To remove any residual pronase, samples were centrifuged at 1,500 × *g* for 4 min, liquid was decanted, and resulting slurry was resuspended in PBS, shaken, and centrifuged again. This process was repeated 4 times. The resulting slurry was resuspended in PBS, shaken, and centrifuged at 500 × *g* for 10 min; this step was repeated 3 times. After each centrifugation step, supernatant containing satellite cells were retained and cells were pelleted via centrifugation at 1,500 × *g* for 10 min. Cells were resuspended in PBS and passaged sequentially through 70- and 40-µm filters. After filtration, final satellite cell pellets were resuspended in growth media (**GM**) consisting of high-glucose Dulbecco's Modified Eagle Medium (**DMEM**; Invitrogen, Carlsbad, CA) supplemented with 10% (vol/vol) fetal bovine serum (**FBS**; GE Healthcare, Pittsburgh, PA), 2% (vol/vol) porcine serum (**PS**; Sigma Aldrich), 100 U penicillan/mL, 100 µg of strepmycin/mL, and 20 µg of gentamicin/mL and plated on 100 mm^2 culture dishes (Eppendorf, Hauppauge, NY) for 24 h to allow all myoblasts to attach to the dish. Cells were rinsed of all additional cell debris, scraped from the culture dishes, and cryopreserved in GM containing 10% volume dimethyl sulfoxide (Sigma Aldrich). Cells were stored in liquid nitrogen vapor until needed for experiments.

Proliferation Assay

Parallel cultures of PFM were seeded at a density of 1×10^3 cells/cm^2 on tissue culture treated 12-well culture plates (Eppendorf) coated with 5 µg/cm^2 entactin-collagen IV-laminin (**ECL**; Millipore, Billerica, MA). Within each size category for each proliferation assay day, 2

culture plates were utilized to seed a pool of PFM on 6 wells. Cells in 2 of the 6 wells were treated with one of three treatments 12-h post-plating: high serum which consisted of GM (**HS**), low serum which consisted of GM without 10% FBS (**LS**), and LS supplemented with 10% (wt/vol) porcine plasma (**PP**). Experiments were replicated 3 times.

Twenty-four, 48, 72, and 96 h after treatments were applied, proliferation assay cultures were immunostained for Pax7, Myf-5, and bromodeoxyuridine (**BrdU**; Sigma Aldrich). For detection of cells traversing S-phase, BrdU, a thymidine analog, was added to media 2 hours prior to immunostaining (Allen et al., 1979). Temporal characterization of the muscle lineage markers was conducted as previously described (Li et al., 2011). Briefly, cells were fixed with 4% (wt/vol) formaldehyde (Polysciences, Warrington, PA) in PBS. Cultures were incubated in 0.5% Triton-X 100 (Fisher Scientific, Waltham, MA) in PBS for 10min to permeabilize the nuclear membrane, followed by a 7-min incubation in 4 N hydrochloric acid (Fisher Scientific) to denature the DNA for immunostaining. Cultures were incubated in 5% horse serum (Fisher Scientific) in 0.2% Triton-X in PBS (blocking solution) for 30 min to block non-specific antigen binding. Cultures were incubated with a primary antibody solution containing, 1:250 anti-BrdU (Santa Cruz Biotechnology, Dallas, TX), 1:10 supernatant anti-Pax7 (Developmental Studies Hybridoma Bank, University of Iowa, Iowa City, IA), and 1:50 anti-Myf5 (Santa Cruz Biotechnology) diluted in blocking solution for 1 h. Next, cells were incubated with goat anti-rat AlexaFluor 594 (1:1000; Invitrogen), goat anti-mouse AlexaFluor 488 (1:1000; Invitrogen) and goat anti-rabbit AlexaFluor633 (1:1000; Invitrogen) to detect BrdU, Pax7, and Myf-5, respectively. Hoechst 33324 (Invitrogen) was utilized at 10 µg/mL for detection of nuclei.

Cells were visualized using an Eclipse TI-U microscope equipped with an X-Cite 120XL epiflouresence illumination system (Nikon Instruments Inc., Melville, NY). Photomicrographs

were captured using a Nikon DS-QiMc digital camera (Nikon Instruments Inc.). A minimum of 5 microscopic fields at 200-fold magnification were analyzed per each sample well for a total of 10 total microscopic fields utilizing NIS-Elements Imaging Sofware (Basic Research, 3.3; Nikon Instruments Inc.). Proliferation rate was determined as the proportion of cells that immunostained positive for BrdU at each time point. Additionally, cells were classified into 3 categories based on Pax7 and Myf-5 expression: cells only expressing Pax7 (**Pax7+**), only expressing Myf-5 (**Myf-5+**), and cells co-expressing Pax7 and Myf-5 (**Pax7/Myf-5**).

Differentiation Assay

Parallel cultures of PFM were seeded at a density of 1×10^3 cells/cm^2 on tissue culture treated 12-well culture plates (Eppendorf) coated with 5 µg/cm^2 ECL (Millipore, Billerica, MA). Each pool of PFM was seeded on 16 wells. All PFM were maintained in GM for 96 h prior to application of treatments, at which time half of the 16 wells were treated with either HS or LS media. Of the wells that contained HS and LS media, half of each were treated with porcine plasma 10% wt/vol (**PPP**) or 0% wt/vol (**PPN**) porcine plasma. Treatments were replenished 48 h after initial application, and cultures were either immunostained or subjected to protein isolation 96 h after application of treatments. Cultures utilized for immunostaining were fixed with 4% (wt/vol) formaldehyde (Polysciences) in PBS. Cultures were incubated in 5% horse serum, 0.2% Triton-X 100 in PBS for 30 min to block non-specific antigen binding sites, incubated for 1 h with a primary antibody solution containing 1:2 supernatant anti-sarcomeric myosin (**MF20**; Developmental Studies Hybridoma Bank), and incubated with 1:1,000 goat anti-mouse AlexaFluor 594 (Invitrogen). Hoechst 33324 (Invitrogen) was included at 10 µg/mL for the detection of nuclei. Following immunostaining cultures were imaged as described above. The differentiation capacity was calculated as the number of nuclei present in multinucleated

sarcomeric myosin positive myotubes, divided by the total number of nuclei in the photomicrograph.

Protein Synthesis Assay

Porcine fetal myoblasts were plated in the same arrangement as the differentiation assay and maintained in GM for 96 h. Media was replaced with LS media to induce differentiation for an additional 96 h, at which time media was replaced with LS media supplemented with 10 µM cytosine β-D-arabinofuranoside (Sigma Aldrich) for 24 h to eliminate any proliferating mononuclear cells (Hinterberger and Barald, 1990). Cells were subsequently exposed to treatments described for the differentiation assay for 72 h, after which cultures were either immunostained with MF20 (Developmental Studies Hybridoma Bank) or subjected to protein isolation. Cultures were immunostained as described for the differentiation assay. To determine average myotube diameter, a minimum of 100 measurements were taken perpendicular to the length of each myotube, using the length measurement tool in NIS Elements Imaging Software (Nikon Instruments Inc.).

Western Blot Analysis

Protein was extracted from progenitor cells at conclusion of the differentiation assay, according to methods of Wang et al. (2012). Briefly, cells were scraped from the bottom of each well in 300 µL of lysis buffer (50 *M* Tris-HCL, 150 *M* NaCl, 1 *M* EDTA, 0.5% Triton X-100, 1 *M* phenlymethanessulfonyl fluoride, 1 *M* $NaVO^4$; Fisher Scientific) containing a complete protease inhibitor (Sigma Aldrich) and homogenized through a 21-gauge needle. Homogenates were centrifuged at 14,000 × *g* for 15 min at 4°C. Sample protein concentrations were quantified using Pierce's BCA Protein Assay Kit (Thermo Scientific). Three micrograms of protein was heated in 4× sample loading buffer (40% vol/vol glycerol, 4% vol/vol β-mercaptoethanol, 0.08%

wt/vol Sodium dodecyl sulfate; Fisher Scientific) at 95ºC for 3 min. Samples were loaded onto four 7.5% separating polyacrylamide gels with 3.5% stacking gels and separated at 40 mA. Proteins were transferred to a nitrocellulose membrane (Amersham Hybond-ECL; GE Healthcare) using blotting paper saturated with transfer buffer (25mM Tris, 192 mM glycine, and 5% vol/vol methanol) and a Semi-dry Transfer Unit (Hoefer, Holliston, MA). Blots were incubated with 5% nonfat dry milk in TBS-T (10 mM Tris, pH 8.0, 150 mM NaCl, 0.1% Tween-20) for 30 min at room temperature to block nonspecific antigen sites. After the nitrocellulose membranes were blocked, the first blot was incubated with an p-mTOR, p-AKT (Ser^{473}), p-FOXO-1, and p-4EBP-1 antibodies (1:1000, 1:2000, 1:500, and 1:1000, respectively, in 1% nonfat dry milk in TBS-T; Cell signaling, Beverly, MA), the second blot was incubated with total mTOR, total AKT antibody, total FOXO-1, and total 4EBP-1 (1:1000 in 1% nonfat dry milk in TBS-T; Cell Signaling). The third blot was incubated with an p-S6 kinase, p-AKT (Thr^{308}; 1:1000 in 1% nonfat dry milk in TBS-T; Cell Signaling) and MAFbx antibodies (1:500, in 1% nonfat dry milk in TBS-T; Santa Cruz Biotechnology) The fourth blot was incubated with total S6 kinase (1:1000 in 1% nonfat dry milk in TBS-T; Cell Signaling) and MURF-1 antibodies (1:2000, in 1% nonfat dry milk in TBS-T; Santa Cruz Biotechnology) overnight at 4ºC. Following primary antibody incubation blots were incubated with an anti-rabbit horse radish peroxidase linked secondary antibody (1:1000 in 5% nonfat dry milk in TBS-T; Cell Signaling) at room temperature for 1 h. Blots were developed using an enhanced chemiluminescence kit (ECL Plus, Amersham, Pittsburgh, PA) and visualized using the ChemiDoc-It 415 Imaging System (UVP). Band intensities were quantified using VisionWorksLS Image Acquisition and Analysis Software (UVP; Upland, CA). Values are reported as abundance of total and phosphorylated protein that was equalized to a pooled sample on each blot and as a ratio of

protein phosphorylation (normalized phosphorylated band intensity / normalized total band intensity × 100).

Statistical Analyses

The proliferation assay was analyzed as a 3 × 3 × 4 factorial arrangement, with repeated measures. The fixed effects included treatment (**Trt**), fetal size (**Size**), and Time served as the repeated measurement. The random effect was pool of cells. The PFM differentiation and protein synthesis assays were analyzed as a 2 × 2 × 3 factorial design. Fixed effects were type of serum in the media (**Serum**), and porcine plasma supplementation status (**PP**), and Size. The random effect was pool of cells. Statistical analyses were performed using the GLIMMIX Procedures of SAS 9.4 (Cary, NC). Pair-wise comparisons between the least square means of the factor levels, were computed using the PDIFF option of the LSMEANS statement. Differences were considered significant at $\alpha \leq 0.05$.

RESULTS

Proliferation Assay

There were no TRT × Time × Size, Trt × Size, or Size × Time interactions for any proliferation characteristics evaluated ($P \geq 0.12$; Table 3.1). There were TRT × Time interactions for proliferation rate, percentage of Pax7+ PFM, and the percentage of Pax7/Myf-5+ PFM ($P \leq 0.05$), but the interaction did not affect ($P = 0.21$) the percentage of Myf-5+ PFM. At 24 h, HS-PFM had a greater proliferation rate than LS- and PP-PFM ($P \leq 0.02$), and PP-PFM had greater ($P < 0.01$) proliferation than LS-PFM. At 48 h, HS-PFM had a greater proliferation rate than LS- and PP-FM ($P \leq 0.02$), At 72 h, HS-PFM had similar ($P = 0.44$) proliferation rate compared to PP-PFM, which was greater than LS PFM ($P < 0.01$). At 96 h, HS-PFM proliferation rate was

greater than PP- and LS-PFM ($P \leq 0.02$), and PP-PFM proliferation rate was greater ($P < 0.01$) LS-PFM.

At 24 h, PP-PFM had a greater percentage of Pax7+ compared to HS- and LS-PFM ($P \leq 0.02$), which were similar to each other ($P = 0.75$). At 48 and 72 h, percentage of Pax7+ PFM were similar among all treatments ($P \geq 0.12$). At 96 h, LS-PFM had a greater ($P = 0.03$) percentage of Pax7+ cells compared to HS-PFM, and PP-PFM has a similar percentage of Pax7+ cells compared to HS and LS PFM ($P \geq 0.28$). At all-time points HS- and PP-PFM had a greater percentage Pax7/Myf-5+ cells compared to LS-PFM ($P < 0.01$), and were similar to each other ($P = 0.10$).

Time affected proliferation rate, percentage of Myf-5+ PFM, and percentage of Pax7/Myf-5+ PFM ($P < 0.01$), but did not affect ($P = 0.13$) percentage of PFM that were Pax7+. The percentage of proliferative PFM was decreased at 96 h compared to other time points ($P < 0.01$), which were similar ($P \geq 0.16$). At 24 h there was a greater percentage of Myf-5+ PFM than all other time points ($P \leq 0.03$), which did not differ from each other ($P \geq 0.22$). At 48 and 72 h there was a greater percentage of Pax7/Myf-5+ PFM than at 24 and 96 h ($P < 0.01$), which were similar to each other ($P = 0.38$). The percentage of Pax7/Myf-5+ PFM were similar ($P = 0.27$) at 48 and 72 h.

There was a Trt effect for proliferation rate, percentage of Myf-5+ PFM, and Pax7/Myf-5+ PFM ($P \leq 0.03$), but Trt did not affect ($P = 0.12$) the percentage of Pax7+ PFM. The HS-PFM had a greater proliferation rate compared to both the LS and PP treatments ($P < 0.01$), and PP-PFM had a greater ($P < 0.01$) proliferation rate compared to LS-PFM. The LS-PFM had a greater percentage of Myf-5+ PFM compared to the HS- and PP-PFM ($P \leq 0.03$), which were similar (P

= 0.55). The LS treatment had less Pax7/Myf-5+ PFM than HS- and PP-PFM ($P < 0.01$), which were similar ($P = 0.31$).

Size of the fetus PFM were isolated from affected proliferation rate, percentage of Myf-5+ PFM, and the percentage of Pax7/Myf-5+ PFM ($P \leq 0.03$); however, Size did not affect percentage of Pax7+ PFM ($P \geq 0.21$). The SM and ME fetuses' PFM had a greater proliferation rate than LG fetuses ($P < 0.04$), and were similar ($P = 0.09$) to each other. Small fetuses' PFM had a smaller percentage of Myf-5+ PFM compared to ME and LG fetuses' PFM ($P < 0.01$), which were similar ($P = 0.10$). Small fetuses' PFM had a greater ($P = 0.01$) percentage of Pax7/Myf-5+ PFM compared to LG fetuses'. Median fetuses' had a similar percentage of Pax7/Myf-5+ PFM as SM and LG fetuses' PFM ($P \geq 0.16$).

Differentiation Assay

The Serum × PP × Size, or PP × Size interactions did not affect differentiation capacity or mTOR pathway signaling ($P \geq 0.15$; Table 3.2). There was a Serum × PP interaction for differentiation capacity, and the abundance of total AKT, Ser^{473} phosphorylated AKT, phosphorylated 4E-BP, total FOXO, MAFbx, and MURF-1 ($P \leq 0.05$). When in the presence of HS, PPP increased ($P < 0.01$) differentiation capacity compared to PPN; however, in the presence of LS, PPP decreased ($P < 0.01$) differentiation capacity compared to PPN. When in the presence of HS PPP decreased abundance of total AKT, Ser^{473} phosphorylated AKT, phosphorylated 4E-BP, and total FOXO compared to PPN ($P \leq 0.01$), but PP did not influence the abundance of total AKT in the presence of LS ($P \geq 0.18$). In the presence of LS PPP increased abundance of MAFbx and MURF-1 compared to PPN ($P \leq 0.05$), but PP did not influence MAFbx or MURF-1 abundance in the presence of HS ($P \geq 0.22$).

The Serum × Size interaction affected the abundance of total AKT ($P = 0.02$); however, the Serum × Size interaction did not affect differentiation capacity or any of the mTOR pathway signaling proteins evaluated ($P \geq 0.12$). Large fetuses' PFM in the presence of HS media had a greater ($P < 0.01$) abundance of total AKT compared LG fetuses' PFM in the presence of LS media, but SM and ME fetuses' PFM were not affected by the serum status of the media ($P \geq 0.21$).

There was an effect of Serum on differentiation capacity, the abundance of total AKT, Ser^{473} phosphorylated AKT, Thr^{308} phosphorylated AKT, total mTOR, and total FOXO ($P \leq 0.03$), but Serum did not influence the remainder of the mTOR pathway signaling proteins evaluated ($P \geq 0.07$). The HS-PFM had greater ($P < 0.01$) differentiation capacity and abundance of total AKT, Ser^{473} phosphorylated AKT, Thr^{308} phosphorylated AKT, total mTOR, and total FOXO ($P \leq 0.03$) than LS-PFM.

There was a PP effect on the abundance of total AKT, Thr^{308} phosphorylated AKT, total S6 Kinase, phosphorylated S6 Kinase, phosphorylated 4E-BP, total FOXO, MAFbx and the ratios of Ser^{473} phosphorylated AKT, Thr^{308} phosphorylated AKT, and phosphorylated FOXO ($P \leq 0.05$), but PP did not affect differentiation capacity or any of the other mTOR pathway signaling proteins evaluated ($P \geq 0.13$). The PPP-PFM had decreased abundance of total AKT, phosphorylated 4E-BP, and total FOXO compared to PPN-PFM ($P \leq 0.05$). The PPP-PFM had increased ($P < 0.01$) abundance of Thr^{308} phosphorylated AKT, and increased ratios of Ser473 phosphorylated AKT, Thr308 phosphorylated AKT, and phosphorylated FOXO compared to PPN-PFM ($P \leq 0.05$) compared to PPN-PFM. Additionally, PPP-PFM had an increased abundance of total S6 Kinase, and phosphorylated S6 Kinase compared to PPN-PFM ($P \leq 0.04$).

Size affected differentiation capacity, abundance of total AKT, Ser^{473} phosphorylated AKT, phosphorylated S6 Kinase, and the ratio of Thr^{308} phosphorylated AKT ($P \leq 0.03$), but Size did not affect the remainder of the mTOR pathway signaling proteins evaluated ($P \geq 0.07$). Large-PFM had greater differentiation capacity than SM- and ME-PFM ($P < 0.01$), and ME-PFM had a greater ($P = 0.01$) differentiation capacity compared to SM-PFM. The LG-PFM had a greater abundance of total AKT and Ser^{473} phosphorylated AKT than SM- or ME-PFM ($P \leq 0.04$), which were similar to each other ($P \geq 0.15$). Median-PFM had a greater abundance of phosphorylated S6 Kinase compared to SM- and LG-PFM ($P \leq 0.04$), which were similar to each other ($P = 0.21$). Small-PFM had a greater ratio of Thr308 phosphorylated AKT compared to ME- and LG-PFM ($P \leq 0.04$), which were similar to each other ($P = 0.72$).

Protein Synthesis Assay

The Serum × PP × Size interaction affected the abundance of phosphorylated mTOR, the abundance of MURF-1, and the ratio of phosphorylated S6 Kinase ($P \leq 0.03$; Table 3.3); however the three way interaction did not affect myotube diameter or any of the other mTOR pathway signaling proteins evaluated ($P \geq 0.12$). Small-PFM in the presence of LS-PPP media had elevated ($P = 0.02$) abundance of phosphorylated mTOR compared SM-PFM cultured in LS-PP media, but SM-PFM cultured in HS-PP+ media had decreased ($P = 0.04$) abundance of phosphorylated mTOR compared SM-PFM cultured in HS-PPN media. In contrast, ME- and LG-PFM had similar abundance of phosphorylated mTOR regardless of serum or porcine plasma status of the media ($P \geq 0.20$). Large-PFM cultured in HS-PPP media had a decreased ($P < 0.01$) abundance of MURF-1 compared to when they were cultured in HS-PPN media; however, LG-PFM cultured in LS-PPP media had elevated ($P = 0.03$) abundance of MURF-1 compared to when they were cultured in LS-PPN media. The SM- and ME-PFM had a similar abundance of

phosphorylated mTOR regardless of serum or porcine plasma status of the media ($P \geq 0.41$). Small-PFM cultured in HS-PPP media had increased ($P < 0.01$) ratio of phosphorylated S6 Kinase compared to when they were cultured in LS-PPN media, but SM-PFM were not affected by porcine plasma status in the presence of LS media ($P = 0.42$). The ME- and LG-PFM had a similar ratio of phosphorylated S6 Kinase regardless of serum or porcine plasma status of the media ($P \geq 0.08$).

There were PP × Size interactions for myotube diameter and the ratio of phosphorylated S6 Kinase ($P \leq 0.03$), but this interaction did not influence any of the other mTOR pathway signaling proteins evaluated ($P \geq 0.16$). Small- and ME-PFM cultured in PPN media had greater myotube diameter compared to when they were cultured with PPP media ($P < 0.01$), but PP status did not influence the myotube diameter of LG-PFM ($P = 0.17$). Small-PFM cultured with PPN media had a greater ($P < 0.01$) ratio of S6 Kinase phosphorylation compared to when they were cultured in PPP, but PP status did not affect the ratio of S6 Kinase of ME- and LG-PFM ($P \geq 0.59$).

The Serum × Size interaction affected ($P = 0.01$) the abundance of phosphorylated S6 Kinase, but did not affect myotube diameter or any of the other mTOR pathway signaling proteins evaluated ($P \geq 0.07$). Small-PFM cultured in the presence of HS had a greater ($P = 0.01$) abundance of phosphorylated S6 Kinase than when they were cultured in the presence of LS; however, ME-PFM cultured in the presence of HS had decreased ($P = 0.05$) abundance of phosphorylated S6 Kinase compared to when they cultured in LS media. Additionally, serum status of the media did not influence phosphorylated S6 Kinase abundance of LG-PFM ($P = 0.35$).

There were Serum × PP interactions for myotube diameter, abundance of Ser^{473} phosphorylated AKT, and abundance of MURF-1 ($P \leq 0.03$), but this interaction did not influence the other mTOR pathway signaling proteins evaluated ($P \geq 0.09$). The combination of LS-PPN resulted in a greater ($P < 0.01$) myotube diameter compared to LS-PPP, but porcine plasma status did not influence myotube diameter in the presence of HS media ($P = 0.57$). The combination of HS-PPP resulted in decreased ($P < 0.01$) abundance of Ser^{473} phosphorylated AKT compared to HS-PPN, but PP status did not influence myotube diameter in the presence of LS media ($P = 0.25$). Porcine fetal myoblasts cultured in HS-PPN media had increased ($P = 0.01$) abundance of MURF-1 compared to LS-PPN media; however, MURF-1 abundance was not affected by serum status when the media was PP+ ($P = 0.82$).

The main effect of Serum influenced the abundance of Ser^{473} phosphorylated AKT, total S6 Kinase, phosphorylated 4E-BP, and MAFbx ($P \leq 0.03$), but Serum did not affect myotube diameter, or any of the other mTOR pathway signaling proteins evaluated ($P \geq 0.06$). Porcine fetal myoblasts cultured in HS media had an increased abundance of Ser^{473} phosphorylated AKT, total S6 Kinase, phosphorylated 4E-BP, and MAFbx compared to PFM cultured in LS media ($P \leq 0.03$). There was a PP effect for myotube diameter, the ratio of Thr^{308} phosphorylated AKT, and the abundance of phosphorylated FOXO ($P \leq 0.05$), but did not affect any of the other mTOR pathway signaling proteins evaluated ($P \geq 0.09$). The PPP-PFM had a decreased ($P < 0.01$) myotube diameter compared to PPN-PFM. The PPP-PFM had a greater ratio of Thr^{308} phosphorylated AKT, and abundance of phosphorylated FOXO compared to PPN-PFM ($P \leq 0.05$). Size affected myotube diameter, the abundance of total AKT, Ser^{473} phosphorylated AKT, phosphorylated mTOR, MAFbx and MURF-1, and the ratios of Ser^{473} and Thr^{308} phosphorylated AKT ($P \leq 0.05$). Size did not affect any of the other mTOR pathway signaling proteins evaluated

($P \geq 0.06$). Small-PFM had a greater myotube diameter compared to ME- and LG-PFM ($P < 0.01$), and ME-PFM had a greater ($P = 0.01$) myotube diameter compared to LG-PFM. Large-PFM had a greater abundance of total AKT and Ser^{473} phosphorylated AKT compared to SM- and ME-PFM ($P \leq 0.01$), which were similar to each other ($P \geq 0.39$). Large-PFM had decreased ratio of Ser^{473} phosphorylated AKT compared to SM- and ME-PFM ($P \leq 0.03$), which were similar ($P = 0.21$). Small-PFM had a greater ratio of Thr^{308} phosphorylated AKT compared to ME- and LG-PFM ($P \leq 0.01$), which were similar ($P = 0.87$). Small-PFM had a greater ($P = 0.01$) abundance of phosphorylated mTOR compared to ME-PFM, and LG had a similar abundance of phosphorylated mTOR compared to SM- and ME-PFM ($P \geq 0.09$). Large-PFM had a greater ($P = 0.02$) abundance of MAFbx compared ME-PFM, and SM-PFM had a similar abundance of MAFbx compared to ME- and LG-PFM ($P \geq 0.18$). Large-PFM had a greater abundance of MURF-1 compared to SM- and ME-PFM ($P < 0.01$), which were similar ($P = 0.87$).

DISCUSSION

Effect of Fetal Size on Porcine Fetal Myoblast Activity

Development of all the muscle fibers an animal will have is completed prenatally, and occurs in two waves of coordinated proliferation and differentiation forming primary and secondary muscle fibers (Wigmore and Stickland, 1983). Development of primary muscle fibers is occurs between d-25 and 50 of gestation, at which time secondary myogenesis begins and is concluded at approximately d-90 of gestation (Wigmore and Stickland, 1983; Handel and Stickland, 1987). In the pig, intrauterine growth restriction develops as a result of placental insufficiency from d-30 to 45 of gestation until term of the pregnancy (Wu et al., 2006; Kim et al., 2009). This placental insufficiency results in developmental variation among littermates, and

with skeletal muscle accounting for 65% of fetal glucose utilization it serves as a prime site for nutrient preservation (Foxcroft et al., 2006; Yates et al., 2012). The proliferation and differentiation of PFM will establish the secondary muscle fiber and satellite cell populations (Bentzinger et al., 2012).

In utero myoblast proliferation is a pertinent event during prenatal myogenesis to develop muscle fibers needed for postnatal growth, muscle fiber development is complete near d-90 of gestation (Handel and Stickland, 1987; Rehfeldt et al., 1993; Stickland et al., 2004). Myogenic cells undergo a transition of transcription factor expression from Pax7 to Myf-5 during myogenesis. While undergoing this transition myogenic cells can be characterized into three sub-classes of cells that express Pax7, Myf-5, or co-express Pax7 and Myf-5 (Li et al., 2011). Cells that solely express Pax7 are activated and moderately proliferative. Cells mature into the population of cells that are co-express Pax7 and Myf-5, which are the most proliferative of the three populations of myogenic cells. As Pax7 expression subsides, the rate of proliferation is lessened, and cells that solely expressing Myf-5 are committed to myogenic differentiation (Zammit et al., 2006).

Nissen and Oksbjerg (2009) observed that porcine satellite cells from the lightest weight gilt at 6 weeks of age tended to proliferate slower *in vitro*; however in the current study, the proliferation rate of SM-PFM was 7% and 3% greater than LG- and ME-PFM, respectively. The population of the SM-PFM had 6% and 4% fewer Myf-5+ PFM compared to LG- and ME-PFM, respectively. This resulted in SM-PFM having 7% and 4% more Pax7/Myf-5+ PFM. These data indicate SM-PFM are able to proliferate more rapidly when the plane of nutrition is similar to ME- and LG-PFM, suggesting that improving placental efficiency at d-60 of gestation may allow for compensatory myogenesis to alleviate myogenic detriments described in chapter 2.

At d-60 of gestation porcine fetal myoblasts are both proliferating and differentiating into secondary muscle fibers (Wigmore and Stickland, 1983; Oksbjerg et al., 2013). Previously, Nissen and Oksbjerg (2009) observed that porcine satellite cells from the gilt with the greatest body weight within the litter had increased levels of creatine phosphokinase compared to the porcine satellite cells from the lightest body weight gilt within the litter, suggesting the lightest gilts' satellite cells are delayed in differentiation. In contrast, the same study found differentiation capacity of the heaviest and lightest weight gilts' satellite cells were not different (Nissen and Oksbjerg, 2009). In the current study LG-PFM had a 9% and 13% greater differentiation capacity compared to ME- and SM-PFM, respectively. Median-PFM had a 4% greater differentiation capacity compared to SM-PFM. Large-PFM had a 37% and 62% greater abundance of total AKT compared to ME- and SM-PFM, respectively. In addition to having more total AKT, LG-PFM had 52% and 54% greater abundance of Ser^{473} phosphorylated AKT compared to ME- and SM-PFM, respectively. Small-PFM, however, had 32% and 37% greater ratio of Thr^{308} phosphorylated AKT compared to LG- and ME-PFM, respectively. This data indicates that LG-PFM exhibit accelerated differentiation, which may explain the advanced myogenic trajectory of LG fetuses observed in chapter 2.

Wang et al. (2013) observed that piglets that have experienced intrauterine growth restriction have smaller muscle fibers at d-60 and d-90 of gestation. Postnatally, lighter birth weight piglets were able to deposit a similar percentage lean mass compared to heavier birth weight piglets, which is achieved through an increase in muscle fiber hypertrophy (Gondret et al., 2005). In the current study, SM-PFM had a 10% and 6% greater myotube diameter compared to LG- and ME-PFM, respectively, and ME-PFM had a 4% greater myotube diameter compared to LG fetuses' PFM. Large-PFM had a 48% and 65% greater abundance of total AKT compared

to ME- and SM-PFM. Additionally, LG-PFM had a 43% and 58% greater abundance of Ser^{473} phosphorylated AKT compared to ME- and SM-PFM, respectively. Large-PFM had 41% greater abundance of MAFbx compared to ME-PFM. Large-PFM had a 69% and 71% greater abundance of MURF-1 compared to ME- and SM-PFM, respectively. Small-PFM had a 17% and 42% greater ratio of Ser^{473} and Thr^{308} phosphorylated AKT compared to LG-PFM, respectively. The greater myotube diameter of SM-PFM appears to be mediated through AKT being more active and decreased abundance of the ubiquitin ligases compared to LG-PFM. These data indicates that when nutrient availability is similar, SM-PFM will preferentially proliferate to compensate for detriments in myoblast number, and once differentiated will undergo expedited muscle hypertrophy.

Effect of Porcine Plasma on Porcine Fetal Myoblast Activity

The effects of porcine plasma on characteristics of porcine fetal myoblasts *in vitro* has not yet been evaluated; however, Tran et al. (2014) indicated that porcine plasma increased proliferation of porcine intestinal epithelial cells. The current study focused on the potential of porcine plasma supplementation to stimulate fetal skeletal muscle development *in vitro* and serve as a potential intervention to negate the detriments of skeletal muscle development experienced in smaller fetuses. The lack of PP × Size interactions for proliferation and differentiation assays indicate that PFM from all fetuses reacted similarly to the porcine plasma product. There was an interaction for myotube diameter where SM and ME-PFM supplemented with porcine plasma had smaller myotubes compared to SM and ME-PFM that were not supplemented with porcine plasma, and porcine plasma supplementation to LG-PFM did not influence myotube diameter. These data illustrate divergent effects of porcine plasma on PFM from different fetal size

categories, where porcine plasma supplementation of SM- and ME-PFM appears to repartition nutrients away from myotube development for promotion of other cellular events.

In proliferation assays of the current study, the HS treatment serves as a positive control and porcine plasma was supplemented to the LS treatment, which served as a negative control. The PP treatment resulted in proliferative characteristics more similar to the HS treatment than the LS treatment. Over the course of the proliferation assay on average PP-PFM had a 19% greater proliferation rate compared to the LS treatment over all. Additionally, the temporal expression profile of Pax7 and Myf-5 of PP-PFM was more similar to the HS-PFM than the LS-PFM. On average over the course of the proliferation assay the PP-PFM had a 27% increase in the percentage of Pax7/Myf-5+ PFM and a 10% decrease in the percentage of Myf-5+ PFM compared to the LS treatment. Even though treatment affected PFM from all fetal size categories similarly, supplementation of porcine plasma stimulated mitotic activity, retention of Pax7 expression, and promoted proliferation of porcine fetal myoblast.

The ultimate fate of myogenic precursor cells is to undergo differentiation, contributing to the pool of muscle fibers prenatally (Moss and Leblond, 1971; Biressi et al., 2007). Currently, there are no studies that have evaluated myogenic differentiation in response to porcine plasma; however, it is known that porcine plasma is a composite material that contains high levels of amino acids and an elevated concentration of IGF-1 (Coffey and Cromwell, 1995; de Rodas et al., 1995). The protein IGF-1 has been implicated in promoting myogenic differentiation and protein synthesis through mTOR pathway signaling (Schiaffino and Mammucari, 2011). Schiaffino and Mammucari (2011) identified AKT as the branch point for IGF-1R mediated protein synthesis, where phosphorylation of AKT promotes downstream phosphorylation of mTOR, S6 Kinase, 4E-BP, and FOXO to ultimately promote protein synthesis and inhibit protein

degradation. Supplementation of porcine plasma did not impact the percentage of PFM that differentiated. The PPP-PFM had a 61% and 28% decrease in the abundance of total AKT and phosphorylated 4E-BP compared to PPN-PFM, but porcine plasma supplementation did result in a 39% and 56% increase in the abundance and ratio of Thr^{308} phosphorylated AKT, respectively. Porcine plasma also resulted in a 28% increase in the ratio of Ser^{473} phosphorylated AKT. The PPP-PFM had a 45% and 32% increase in the abundance of total and phosphorylated S6 Kinase compared to PPN-PFM, respectively. Additionally, PPP-PFM had a 38% decrease in total FOXO abundance and a 29% increase in the ratio of phosphorylated FOXO. Even though porcine plasma did not affect the differentiation capacity of PFM, the profile of proteins of mTOR pathway signaling indicate that PPP-PFM were likely in a positive balance for protein synthesis.

In previous reports IGF-1 supplementation *in vitro* has resulted in increases in average myotube diameter and also stimulated upregulation and phosphorylation of mTOR pathway signaling proteins involved in protein synthesis (Rommel et al., 2001; Han et al., 2008). Han et al. (2008) observed that porcine satellite cells supplemented with IGF-1 had increased abundance of Ser^{473} phosphorylated AKT, phosphorylated mTOR, phosphorylated 4E-BP, and phosphorylated S6 Kinase. Additionally, amino acids promote myogenic differentiation and protein synthesis (Kimball et al., 1999; Kimball and Jefferson, 2002). The addition of methionine and leucine to a myogenic cells resulted in an increase in the phosphorylation of S6 kinase at the Thr^{389} phosphorylation site, resulting in an in S6 kinase activation (Tesseraud et al., 2003). In the current study, differentiated PFM that were treated with PPP media had 5% smaller myotube diameter compared to PPN; however, PPP-PFM had a 4% greater ratio of Thr^{308} phosphorylated AKT and a 50% greater abundance of phosphorylated FOXO compared to PPN-PFM. These data indicate the mixture of amino acids and IGF-1 contained in porcine plasma stimulated fetal

myoblasts to proliferate more and synthesize protein less. Therefore, it is possible PPP cultures may have been delayed in synthesizing protein, which resulted in them having smaller myotube diameters but mTOR signaling consistent with increased protein synthesis.

Until the current investigation, research involving porcine plasma supplementation have focused on the overall gains, gut health, and immunity (Coffey and Cromwell, 1995; de Rodas et al., 1995; Everts et al., 2001; Tran et al., 2014). Porcine plasma supplementation during the nursery phase increases ADG and feed intake (Everts et al., 2001), and stimulates the proliferation of intestinal epithelial cells, promoting gut health and nutrient absorption (Tran et al., 2014). The current study suggest porcine plasma is able to promote proliferation during prenatal myogenesis, eliciting positive effects on skeletal muscle development. Additionally, the current data suggests that SM fetuses' PFM at d-60 of gestation have the ability to proliferate more rapidly and produce larger myotubes in an equal nutrient environment as simulated *in vitro.* Evaluation of the PP × Size interaction indicates that porcine plasma affects all size categories of fetuses similarly, but PPP actually resulted in a decrease in myotube diameter of SM- and ME-PFM compared to PPN media. These data indicate porcine plasma supplementation may be able to stimulate myoblast proliferation and at d-60 of gestation may serve as a prime time point to preferentially stimulate myogenesis lower body weight fetuses.

Table 3.1. Proliferation rate and temporal expression of Pax7 and Myf-5 of porcine fetal myoblasts (**PFM**) harvested from the longissimus muscle of the smallest (**SM**), median (**ME**), and largest (**LG**) male fetus at d-60 of gestation[1]

Treatment	HS			LS			PP				*P*-value[2]					
Size	SM	ME	LG	SM	ME	LG	SM	ME	LG	SEM	Trt × Size	Size × Time	Trt × Time	Time	Trt	Size
Proliferation rate[3], %																
24 h	44.6	53.4	48.9	32.5	27.7	24.8	42.2	35.0	30.5	5.1	0.29	0.99	< 0.01	< 0.01	< 0.01	< 0.01
48 h	48.8	47.6	43.0	27.7	21.1	20.7	38.2	36.8	30.5							
72 h	46.6	47.3	40.3	20.7	10.8	9.7	51.4	45.1	44.1							
96 h	41.6	41.5	35.3	11.9	5.6	5.9	34.4	32.7	28.0							
Pax7+[4], %																
24 h	0.5	0.6	0.0	0.2	0.6	1.2	2.7	0.0	5.9	1.2	0.34	0.31	0.05	0.13	0.12	0.73
48 h	1.2	0.2	0.1	0.0	0.1	0.4	0.0	0.2	0.0							
72 h	0.4	0.2	0.1	0.1	3.8	1.1	0.7	0.0	0.0							
96 h	0.4	0.1	0.6	2.1	1.1	3.8	0.0	1.6	2.4							
Myf5+[5], %																
24 h	33.8	30.9	30.9	36.3	43.3	44.2	28.8	35.1	31.4	5.1	0.67	0.12	0.21	0.01	0.03	< 0.01
48 h	17.4	21.8	25.1	28.7	36.3	42.3	24.7	24.1	28.7							
72 h	18.8	17.5	25.2	37.7	36.3	44.0	16.7	17.2	31.1							
96 h	22.1	28.6	26.1	31.7	38.3	32.9	24.0	36.3	27.2							
Pax7+ and Myf5+[6], %																
24 h	55.5	61.6	61.7	45.4	39.9	37.2	66.2	60.3	54.5	5.2	0.31	0.83	< 0.01	< 0.01	< 0.01	0.03
48 h	77.2	74.7	71.3	63.8	48.9	42.8	70.1	73.8	68.6							
72 h	75.7	79.3	75.7	47.6	34.7	32.3	79.3	80.3	67.9							
96 h	74.4	65.0	67.3	28.8	24.0	23.3	58.1	59.2	61.6							

[1]Porcine fetal myoblasts from the SM, ME, and LG male fetuses maintained in a high serum media containing 10% fetal bovine serum, 2% porcine serum in DMEM supplemented with 100 U penicillan/mL, 100 µg of strepmycin/mL, and 20 µg of gentamicin/mL (**HS**), or a low serum media containing 2% porcine serum in DMEM supplemented with 1× antibiotic/mL and 1× gentamicin/mL (**LS**), or in LS media supplemented with 10% (wt/vol) porcine plasma (**PP**). Parallel cultures were exposed to 5 µM bromodeoxyuridine (**BrdU**) and immunostained daily.

[2]Trt = treatment effect. All Trt × Size × Time interactions were not significant $P > 0.05$.

[3]Number of BrdU positive PFM divided by the total number of PFM present within 10 representative photomicrographs.

[4]Represents the percentage of all PFM that solely immunostained Pax7 positive.

[5]Represents the percentage of all PFM that solely immunostained Myf-5 positive.

[6]Represents the percentage of all PFM that co-expressed Pax7 and Myf-5.

Table 3.2. Differentiation capacity, and mammalian target of rapamycin (**mTOR**) signaling of longissimus muscle porcine fetal myoblasts from the smallest (**SM**), median (**ME**), and largest (**LG**) male fetus harvested at d-60 of gestation and exposed to different growth media cocktails[1]

Serum	HS			HS			LS			LS				*P*-value[2]		
PP	PPN			PPP			PPN			PPP						
Size	SM	ME	LG	SM	ME	LG	SM	ME	LG	SM	ME	LG	SEM	Serum	PP	Size
Differentiation capacity[3, 12], %	38.0	38.9	45.6	43.7	51.4	59.6	50.7	55.6	64.1	38.6	44.4	55.5	4.2	< 0.01	0.97	< 0.01
mTOR pathway signaling[4]																
AKT																
Total[5, 12, 13], AU	1.6	2.9	5.0	0.4	0.8	2.1	0.8	1.4	1.6	0.7	0.8	0.5	0.8	< 0.01	< 0.01	< 0.01
Phosphorylated[6, 12], AU	2.5	2.3	4.2	0.9	1.3	2.9	0.7	1.0	1.7	1.0	0.7	2.3	0.74	< 0.01	0.13	< 0.01
Ratio phosphorylated, AU	153	117	113	272	186	197	185	110	155	128	191	185	52.6	0.57	0.03	0.52
Phosphorylated[7], AU	1.3	1.0	1.5	2.4	2.5	2.0	1.5	1.0	0.8	1.1	1.8	1.7	0.36	0.01	< 0.01	0.91
Ratio phosphorylated, AU	97	126	77	384	157	208	167	92	114	313	227	254	51.5	0.50	< 0.01	0.03
mTOR																
Total, AU	1.2	1.4	2.4	1.1	1.6	1.8	0.7	1.1	1.1	0.8	0.9	0.93	0.41	0.01	0.62	0.10
Phosphorylated[8], AU	1.0	1.2	2.0	1.7	1.4	1.3	1.4	1.2	0.9	1.5	1.6	0.7	0.35	0.24	0.72	0.81
Ratio phosphorylated, AU	142	147	134	192	143	135	328	139	163	187	173	129	54.2	0.21	0.60	0.11
S6 Kinase																
Total, AU	0.9	1.0	1.5	1.7	1.1	1.9	0.5	0.8	1.2	1.6	2.1	2.5	0.38	0.67	< 0.01	0.07
Phosphorylated[9], AU	0.7	1.3	1.3	0.9	2.8	1.8	1.1	2.2	1.2	1.4	2.9	1.7	0.69	0.32	0.04	< 0.01
Ratio phosphorylated, AU	183	188	112	81	102	98	119	130	269	155	150	123	57.8	0.39	0.17	0.93
4E-BP																
Total, AU	1.2	1.2	1.3	1.0	1.3	1.6	1.0	1.4	1.3	1.0	1.2	1.4	0.29	0.65	0.88	0.24
Phosphorylated[10, 12], AU	2.3	1.8	1.9	0.7	1.1	1.5	1.2	1.4	1.3	1.3	1.3	1.3	0.39	0.25	0.04	0.93

Ratio phosphorylated, AU	165	192	214	127	117	213	177	117	152	168	128	157	54.0	0.47	0.56	0.47
FOXO																
Total[12], AU	2.4	2.1	4.3	1.5	1.7	1.8	1.4	1.8	1.6	1.1	1.9	1.9	0.67	0.03	0.05	0.11
Phosphorylated[11], AU	1.3	0.8	1.2	1.4	1.2	1.5	1.4	1.4	1.1	1.1	2.2	1.3	0.34	0.41	0.24	0.86
Ratio phosphorylated, AU	126	95	107	203	196	128	185	152	94	226	195	127	46.7	0.43	0.05	0.09
MAFbx[12], AU	1.1	2.1	4.1	3.1	2.5	3.2	1.0	1.0	0.9	2.9	3.2	3.6	0.72	0.14	< 0.01	0.12
MURF-1[12], AU	1.6	2.5	5.2	2.3	1.6	2.7	0.9	2.5	1.3	2.5	2.5	2.3	0.93	0.07	0.59	0.17

[1]Differentiating porcine fetal myoblasts were treated with a high serum media containing 10% fetal bovine serum, 2% porcine serum in DMEM supplemented with 100 U penicillan/mL, 100 µg of strepmycin/mL, and 20 µg of gentamicin/mL (**HS**), or a low serum media containing 2% porcine serum in DMEM supplemented with 100 U penicillan/mL, 100 µg of strepmycin/mL, and 20 µg of gentamicin/mL (**LS**). The HS and LS media was supplemented with 10% (wt/vol) porcine plasma (**PPP**), or 0% (wt/vol) porcine plasma (**PPN**).

[2]PP = Porcine plasma effect. All PP × Size, and Serum × PP × Size interactions were not significant $P > 0.05$.

[3]Percentage of all PFM that have incorporated into multinucleated sarcomeric myosin positive myotubes.

[4]AKT = protein kinase B, mTOR = mammalian target of rapamycin, S6 Kinase = p70 S6 kinase, 4E-BP = eukaryotic translation initiation factor 4E binding protein, FOXO = forkhead box O1, MAFbx = muscle atrophy F-box, and MURF-1 = muscle ring finger-1.

[5]AU = Arbitrary Unit.

[6]AKT phosphorylated at Ser^{473}.

[7]AKT phosphorylated at Thr^{308}.

[8]mTOR phosphorylated at Ser^{2448}.

[9]S6 Kinase phosphorylated at Thr^{389}.

[10]4E-BP phosphorylated at $Thr^{37/46}$.

[11]FOXO phosphorylated at Ser^{319}.

[12]Serum × PP interaction $P < 0.05$.

[13]Serum × Size interaction $P < 0.05$.

Table 3.3. Myotube diameter, and mammalian target of rapamycin (**mTOR**) signaling of longissimus muscle porcine fetal myoblasts from the smallest (**SM**), median (**ME**), and largest (**LG**) male fetus harvested at d-60 of gestation and exposed to different growth media cocktails[1]

Serum	HS			HS			LS			LS				*P*-value[2]		
PP	PPN			PPP			PPN			PPP						
Size	SM	ME	LG	SM	ME	LG	SM	ME	LG	SM	ME	LG	SEM	Serum	PP	Size
Myotube diameter[3, 12, 14], %	35.5	33.1	30.0	34.2	32.9	32.5	37.8	34.2	31.2	30.7	29.9	30.7	0.94	0.12	< 0.01	< 0.01
mTOR pathway signaling[4]																
AKT																
Total, AU[5,]	1.1	1.3	2.9	0.5	0.7	2.6	1.7	1.0	2.4	0.2	2.0	1.8	0.88	0.91	0.30	0.01
Phosphorylated[6, 12], AU	1.8	2.9	3.7	0.8	1.1	2.1	0.9	0.7	1.2	0.7	0.9	3.0	0.66	0.02	0.20	< 0.01
Ratio phosphorylated, AU	310	215	117	191	167	157	171	224	110	274	184	141	49.0	0.72	0.84	0.01
Phosphorylated[7], AU	1.4	1.5	1.5	2.3	1.5	1.6	1.6	1.4	0.8	1.2	1.8	0.9	0.53	0.22	0.45	0.55
Ratio phosphorylated, AU	259	151	181	352	242	247	203	165	149	408	148	158	79.5	0.36	0.05	0.01
mTOR																
Total, AU	2.0	1.7	2.6	2.1	1.9	1.9	2.7	1.7	2.7	1.7	1.6	1.7	0.41	0.88	0.11	0.20
Phosphorylated[8, 15], AU	2.4	1.3	1.6	1.5	1.7	1.5	1.4	1.2	1.4	2.3	1.2	1.7	0.27	0.47	0.55	0.03
Ratio phosphorylated, AU	147	128	92	117	107	100	97	154	101	202	106	147	27.3	0.27	0.59	0.37
S6 Kinase																
Total, AU	1.5	1.3	2.7	1.5	1.1	1.9	0.8	1.5	0.9	1.0	1.3	1.6	0.36	0.03	0.81	0.06
Phosphorylated[9, 13], AU	2.9	0.7	1.8	2.1	1.4	1.0	1.2	1.7	0.9	0.9	2.6	0.8	0.55	0.33	0.88	0.22
Ratio phosphorylated[14, 15], AU	184	66	75	57	103	103	156	135	122	127	125	73	28.6	0.09	0.09	0.10
4E-BP																
Total, AU	1.6	1.7	1.8	1.5	1.7	1.8	1.3	1.8	1.9	2.1	1.3	1.8	0.37	0.91	0.87	0.64
Phosphorylated[10], AU	2.5	1.5	2.6	1.9	2.1	2.3	1.7	1.2	1.8	1.2	1.4	1.7	0.41	0.01	0.61	0.24

Ratio phosphorylated, AU	151	118	145	152	128	137	139	116	103	116	126	133	24.8	0.27	0.82	0.62
FOXO																
Total, AU	1.1	1.3	1.3	1.3	1.2	1.1	1.2	1.4	1.4	0.9	1.5	1.4	0.27	0.51	0.64	0.32
Phosphorylated[11], AU	1.3	1.7	1.2	2.3	2.2	1.5	1.5	1.6	1.2	2.3	2.2	2.1	0.45	0.60	0.01	0.32
Ratio phosphorylated, AU	128	141	136	166	127	135	172	177	152	170	99	192	37.6	0.30	0.89	0.64
MAFbx, AU	3.3	2.2	4.7	3.6	3.2	3.6	1.7	0.9	2.9	2.8	2.5	3.6	0.83	0.03	0.19	0.05
MURF-1[12, 15], AU	1.3	1.3	6.8	1.4	1.6	3.5	0.7	1.2	2.1	1.4	1.0	4.5	0.96	0.06	0.97	< 0.01

[1]Differentiated porcine fetal myoblasts were treated with a high serum media containing 10% fetal bovine serum, 2% porcine serum in DMEM supplemented with 100 U penicillan/mL, 100 µg of strepmycin/mL, and 20 µg of gentamicin/mL (**HS**), or a low serum media containing 2% porcine serum in DMEM supplemented with 100 U penicillan/mL, 100 µg of strepmycin/mL, and 20 µg of gentamicin/mL (**LS**). The HS and LS media was supplemented with 10% (wt/vol) porcine plasma (**PPP**), or 0% (wt/vol) porcine plasma (**PPN**).

[2]PP = Porcine plasma effect.

[3]Average diameter of multinucleated myotubes from 10 representative photomicrographs.

[4]AKT = protein kinase B, mTOR = mammalian target of rapamycin, S6 Kinase = p70 S6 kinase, 4E-BP = eukaryotic translation initiation factor 4E binding protein, FOXO = forkhead box O1, MAFbx = muscle atrophy F-box, and MURF-1 = muscle ring finger-1.

[5]AU = Arbitrary Unit

[6]AKT phosphorylated at Ser^{473}

[7]AKT phosphorylated at Thr^{308}

[8]mTOR phosphorylated at Ser^{2448}

[9]S6 Kinase phosphorylated at Thr^{389}

[10]4E-BP phosphorylated at $Thr^{37/46}$

[11]FOXO phosphorylated at Ser^{319}

[12]Serum × PP interaction $P < 0.05$

[13]Serum × Size interaction $P < 0.05$

[14]PP × Size interaction $P < 0.05$

[15]Serum × PP × Size interaction $P < 0.05$

REFERENCES

Allen, R. E., R. A. Merkel, and R. B. Young. 1979. Cellular aspects of muscle growth: myogenic cell proliferation. J. Anim. Sci. 49:115-127.

Bentzinger, C. F., Y. X. Wang, and M. A. Rudnicki. 2012. Building muscle: molecular regulation of myogenesis. Cold Spring Harb. Perspect. Biol. 4. doi:10.1101/cshperspect.a008342

Biressi, S., and T. A. Rando. 2010. Heterogeneity in the muscle satellite cell population. Semin. Cell Dev. Biol. 21:845-854. doi:10.1016/j.semcdb.2010.09.003

Biressi, S., E. Tagliafico, G. Lamorte, S. Monteverde, E. Tenedini, E. Roncaglia, S. Ferrari, S. Ferrari, M. G. Cusella-De Angelis, S. Tajbakhsh, and G. Cossu. 2007. Intrinsic phenotypic diversity of embryonic and fetal myoblasts is revealed by genome-wide gene expression analysis on purified cells. Dev. Biol. 304:633-651. doi:10.1016/j.ydbio.2007.01.016

Coffey, R. D., and G. L. Cromwell. 1995. The impact of environment and antimicrobial agents on the growth response of early-weaned pigs to spray-dried porcine plasma. J. Anim. Sci. 73:2532-2539.

de Rodas, B. Z., K. S. Sohn, C. V. Maxwell, and L. J. Spicer. 1995. Plasma protein for pigs weaned at 19 to 24 days of age: effect on performance and plasma insulin-like growth factor I, growth hormone, insulin, and glucose concentrations. J. Anim. Sci. 73:3657-3665.

Dolfi, S. C., L. L. Chan, J. Qiu, P. M. Tedeschi, J. R. Bertino, K. M. Hirshfield, Z. N. Oltvai, and A. Vazquez. 2013. The metabolic demands of cancer cells are coupled to their size and protein synthesis rates. Cancer Metab. 1:20. doi:10.1186/2049-3002-1-20

Engert, J. C., E. B. Berglund, and N. Rosenthal. 1996. Proliferation precedes differentiation in IGF-I-stimulated myogenesis. J. Cell Biol. 135:431-440.

Everts, H., M. J. A. Nabuurs, R. Margry, A. J. van Dijk, and A. C. Beynen. 2001. Growth performance of weanling pigs fed spray-dried animal plasma: a review. Livest. Prod. Sci. 68:263-274.

Foxcroft, G. R., W. T. Dixon, S. Novak, C. T. Putman, S. C. Town, and M. D. Vinsky. 2006. The biological basis for prenatal programming of postnatal performance in pigs. J. Anim. Sci. 84 Suppl:E105-112.

Han, B., J. Tong, M. J. Zhu, C. Ma, and M. Du. 2008. Insulin-like growth factor-1 (IGF-1) and leucine activate pig myogenic satellite cells through mammalian target of rapamycin (mTOR) pathway. Mol. Reprod. Dev. 75:810-817. doi:10.1002/mrd.20832

Handel, S. E., and N. C. Stickland. 1987. Muscle cellularity and birth-weight. Anim. Prod. 44:311-317.

Hinterberger, T. J., and K. F. Barald. 1990. Fusion between myoblasts and adult muscle-fibers promotes remodeling of fibers into myotubes *in vitro*. Development. 109:139-148.

Kimball, S. R., and L. S. Jefferson. 2002. Control of protein synthesis by amino acid availability. Curr. Opin. Clin. Nutr. Metab. Care. 5:63-67.

Kimball, S. R., L. M. Shantz, R. L. Horetsky, and L. S. Jefferson. 1999. Leucine regulates translation of specific mRNAs in L6 myoblasts through mTOR-mediated changes in availability of eIF4E and phosphorylation of ribosomal protein S6. J. Biol. Chem. 274:11647-11652.

Kuang, S., K. Kuroda, F. Le Grand, and M. A. Rudnicki. 2007. Asymmetric self-renewal and commitment of satellite stem cells in muscle. Cell. 129:999-1010. doi:10.1016/j.cell.2007.03.044

Li, J., J. M. Gonzalez, D. K. Walker, M. J. Hersom, A. D. Ealy, and S. E. Johnson. 2011. Evidence of heterogeneity within bovine satellite cells isolated from young and adult animals. J. Anim. Sci. 89:1751-1757. doi:10.2527/jas.2010-3568

Moss, F. P., and C. P. Leblond. 1971. Satellite cells as the source of nuclei in muscles of growing rats. Anatomical Records 170:421-435.

Oksbjerg, N., P. M. Nissen, M. Therkildsen, H. S. Moller, L. B. Larsen, M. Andersen, and J. F. Young. 2013. Meat Science and Muscle Biology Symposium: in utero nutrition related to fetal development, postnatal performance, and meat quality of pork. J. Anim. Sci. 91:1443-1453. doi:10.2527/jas.2012-5849

Pardee, A. B. 1989. G1 events and regulation of cell proliferation. Science. 246:603-608.

Rehfeldt, C., I. Fiedler, R. Weikard, E. Kanitz, and K. Ender. 1993. It is possible to increase skeletal muscle fibre number in utero. Biosci. Rep. 13:213-220.

Rehfeldt, C., M. F. W. Te Pas, K. Wimmers, J. M. Brameld, P. M. Nissen, C. Berri, C. Rehfeldt, D. M. Power, B. Picard, N. C. Stickland, N. Oksbjerg, and L. M. P. Valente. 2011. Advances in research on the prenatal development of skeletal muscle in animals in relation to the quality of muscle-based food. II. Genetic factors related to animal performance and advances in methodology. Anim. 5:718-730.

Rommel, C., S. C. Bodine, B. A. Clarke, R. Rossman, L. Nunez, T. N. Stitt, G. D. Yancopoulos, and D. J. Glass. 2001. Mediation of IGF-1-induced skeletal myotube hypertrophy by

PI(3)K/Akt/mTOR and PI(3)K/Akt/GSK3 pathways. Nat. Cell Biol. 3:1009-1013. doi:10.1038/ncb1101-1009

Schiaffino, S., and C. Mammucari. 2011. Regulation of skeletal muscle growth by the IGF1-Akt/PKB pathway: insights from genetic models. Skelet. Mus. 1:4. doi:10.1186/2044-5040-1-4

Sikalidis, A. K., K. M. Mazor, M. J. Kang, H. Y. Liu, and M. H. Stipanuk. 2013. Total 4EBP1 is elevated in liver of rats in response to low sulfur amino acid intake. J. of Amino Acids 2013:864757-Article ID 864757.

Stickland, N. C., S. Bayol, C. Ashton, C. Rehfeldt, M. F. W. t. Pas, M. E. Everts, and H. P. Haagsman. 2004. Manipulation of muscle fibre number during prenatal development. Muscle Development of Livestock Animals : Physiology, Genetics and Meat Quality.

Stitt, T. N., D. Drujan, B. A. Clarke, F. Panaro, Y. Timofeyva, W. O. Kline, M. Gonzalez, G. D. Yancopoulos, and D. J. Glass. 2004. The IGF-1/PI3K/Akt pathway prevents expression of muscle atrophy-induced ubiquitin ligases by inhibiting FOXO transcription factors. Mol. Cell 14:395-403.

Tesseraud, S., K. Bigot, and M. Taouis. 2003. Amino acid availability regulates S6K1 and protein synthesis in avian insulin-insensitive QM7 myoblasts. FEBS Lett. 540:176-180. doi:10.1016/s0014-5793(03)00260-6

Tran, H., J. W. Bundy, Y. S. Li, E. E. Carney-Hinkle, P. S. Miller, and T. E. Burkey. 2014. Effects of spray-dried porcine plasma on growth performance, immune response, total antioxidant capacity, and gut morphology of nursery pigs. J. Anim. Sci. 92:4494-4504. doi:10.2527/jas.2014-7620

Wang, X. Q., W. J. Yang, Z. Yang, G. Shu, S. B. Wang, Q. Y. Jiang, L. Yuan, and T. S. Wu. 2012. The differential proliferative ability of satellite cells in Lantang and Landrace pigs. PLoS One 7:e32537. doi:10.1371/journal.pone.0032537

Wigmore, P. M., and N. C. Stickland. 1983. Muscle development in large and small pig fetuses. J. Anat. 137 (Pt 2):235-245.

Yates, D. T., A. R. Macko, M. Nearing, X. Chen, R. P. Rhoads, and S. W. Limesand. 2012. Developmental programming in response to intrauterine growth restriction impairs myoblast function and skeletal muscle metabolism. J Pregnancy 2012:631038. doi:10.1155/2012/631038

Zammit, P. S., T. A. Partridge, and Z. Yablonka-Reuveni. 2006. The skeletal muscle satellite cell: the stem cell that came in from the cold. J. Histochem. Cytochem. 54:1177-1191. doi:10.1369/jhc.6R6995.2006

Chapter 4 - Effect of porcine plasma supplementation on proliferation and differentiation characteristics of neonatal porcine satellite cells *in vitro*

ABSTRACT

This experiment was conducted to determine the effect of porcine plasma supplementation on porcine satellite cell (**PSC**) proliferation, differentiation, protein synthesis, and mammalian target of rapamycin (**mTOR**) pathway signaling. Piglets (n = 3) nearest to the average birth weight of the litter were randomly chosen and euthanized within 24 h of birth. Left LM were pooled, minced, subjected to a protease digestion, and isolated using differential centrifugation. Proliferation assays were conducted as 4 × 3 factorial arrangement with time of culture (24, 48, 72, 96 h) and media treatment were main effects. Treatments consisted of: high serum which consisted high-glucose Dulbecco's Modified Eagle Medium supplemented with 10% (vol/vol) fetal bovine serum, 2% (vol/vol) porcine serum, 100 U penicillan/mL, 100 µg of strepmycin/mL, and 20 µg of gentamicin/mL (**HS**); low serum which consisted of HS without 10% FBS (**LS**), and LS supplemented with 10% (wt/vol) porcine plasma (**PP**). Cultures were immunostained for Pax7, Myf-5, and bromodeoxyuridine (**BrdU**). Differentiation and protein synthesis assays were conducted as 2 × 2 factorial designs with serum concentration (HS or LS) and PP (0, **PPP**; or 10%, **PPN** wt/vol) as main effects. Treatment affected the proliferation rate of PSC ($P < 0.01$). The proliferation rate of PP-PSC was decreased compared to the HS- and LS-PSC ($P < 0.01$), and HS-PSC had a greater ($P < 0.01$) proliferation rate compared to LS-PSC. There was a PP × Serum interaction for differentiation capacity ($P < 0.01$). Porcine satellite cells cultured in LS-PPP had greater differentiation capacity compared to LS-PPN-PSC ($P < 0.01$),

and the HS-PPP-PSC had a greater ($P < 0.01$); however, the difference was more pronounced in the LS treatment. The main effect of porcine plasma affected the differentiation capacity, abundance of total and phosphorylated S6 Kinase, ratio of Thr^{308} phosphorylated AKT, ratio of phosphorylated mTOR, total AKT abundance, and total mTOR abundance in differentiated PSC ($P < 0.04$). The PPP-PSC had greater differentiation capacity, abundance of total, and phosphorylated S6 Kinase compared to PPN-PSC ($P \leq 0.04$). The PPP-PSC had greater ratio of Thr^{308} phosphorylated AKT and phosphorylated mTOR ($P \leq 0.03$); however, PPP-PSC had decreased abundance of total AKT and mTOR ($P \leq 0.01$). Porcine plasma affected myotube diameter, the abundance of phosphorylated 4E-BP, and the ratio of phosphorylated 4E-BP of differentiated PSC ($P \leq 0.02$). The PPP-PSC had a greater ($P < 0.01$) myotube diameter compared to PPN-PSC. Additionally, PPP-PSC had an increase ($P = 0.01$) in the abundance of phosphorylated 4E-BP compared to PPN-PSC. Supplementation of PP to PSC promotes the differentiation and growth of myotubes by stimulating downstream proteins of mTOR pathway signaling in an mTOR independent fashion.

KEYWORDS: differentiation, porcine plasma, porcine satellite cells, proliferation

INTRODUCTION

Stimulating efficient growth of skeletal muscle of swine will improve the overall efficiency of pork production. In mature animals the majority of myonuclei result from proliferation and fusion of satellite cells into existing muscle fibers that provide the DNA template required for protein synthesis (Moss and Leblond, 1971; Dodson et al., 1987). Compounds such as insulin-like growth factor-1 (**IGF-1**) play a central role in proliferation and differentiation of satellite cells *in vitro* and *in vivo* (Engert et al., 1996; Stitt et al., 2004), providing a potential avenue to augment muscle growth. Required for initiation and progression

through the cell cycle (Pardee, 1989), IGF-1 promotes the proliferation of satellite cells *in vitro* (Engert et al., 1996). Additionally, IGF-1stimulates protein synthesis. The supplementation of IGF-1 to porcine satellite cells isolated from 6 week old pigs resulted in increases in the abundance of protein synthesis proteins and decreases in protein degradation proteins involved in the mammalian target of rapamycin (**mTOR**) pathway signaling (Han et al., 2008; Rommel et al., 2001; Stitt et al., 2004)

The feed additive, porcine plasma (**PP**), possesses elevated levels of IGF-1 (de Rodas et al., 1995); therefore, supplementation of porcine plasma may elicit a similar mTOR pathway signaling phosphorylation cascade (Schiaffino and Mammucari, 2011). Supplementation of PP during the nursery phase improves ADG and G:F (Coffey and Cromwell, 1995; de Rodas et al., 1995; Everts et al., 2001). Porcine plasma stimulated proliferation of jejunal epithelial cells *in vitro* (Tran et al., 2014), suggesting that PP can directly affect cellular activity during tissue development. Therefore, the objective of the current study was to determine the effect of porcine plasma supplementation *in vitro* on porcine satellite cell (**PSC**) proliferation, differentiation, and protein synthesis.

MATERIAL AND METHODS

The experimental procedures were approved by the Kansas State University Institutional Animal Care and Use Committee.

Porcine Satellite Cell Isolation

Porcine satellite cells were isolated from neonatal piglets less than 24-h old. Whole left LM were obtained from 9 piglets weighing near the average of the litter which it was born were pooled for isolation of PSC. A total of 3 pools of PSC were isolated.

The methods of Li et al. (2011) were be followed for progenitor cell isolation with slight modifications. Briefly, muscles were excised of all visible connective tissue and minced with

sterilized surgical scissors. The tissue was digested with 0.8 mg/mL of pronase XIV (Sigma Aldrich; St. Louis, MO) in Phosphate Buffered Saline (**PBS**, Corning, Corning, NY**)** for 45 min at 37°C. To remove any residual pronase, samples were centrifuged at 1,500 × *g* for 4 min, liquid was decanted, and the resulting slurry was resuspended in PBS, shaken, and centrifuged again. This process was conducted a total of 4 times. The resulting slurry was resuspended in PBS, shaken well, and centrifuged at 500 × *g* for 10 minutes; this step was repeated 3 times. After each centrifugation step, supernatant containing satellite cells was retained and cells were pelleted via centrifugation at 1,500 × *g* for 10 minutes. Cells were resuspended in PBS and passaged sequentially through 70- and 40-micrometer filters. After filtration, the final satellite cell pellet was resuspended in growth media (**GM**) consisting of high-glucose Dulbecco's Modified Eagle Medium (**DMEM**; Invitrogen, Carlsbad, CA) supplemented with 10% (vol/vol) fetal bovine serum (**FBS**; GE Healthcare, Pittsburgh, PA), 2% (vol/vol) porcine serum(**PS**; Sigma Aldrich), 100 U penicillan/mL, 100 µg of strepmycin/mL, and 20 µg of gentamicin/mL and plated on 100 mm^2 culture dishes (Eppendorf, Hauppauge, NY) for 24 hours to allow all satellite cells to attach to the dish. Cells were rinsed of all additional cell debris, scraped from the culture dish, and cryopreserved in GM containing 10% volume dimethyl sulfoxide (Sigma Aldrich). Cells were stored in liquid nitrogen vapor until needed for the experiments.

Proliferation Assay

Parallel cultures of PSC (n = 3) were seeded at a density of 1×10^3 cells/cm^2 on tissue culture treated 12-well culture plates (Eppendorf). Two culture plates were utilized to seed each pool of PSC on 6 wells. Cells in 2 of the 6 wells were treated with one of three treatments 12-h post-plating: high serum which consisted of GM (**HS**), low serum which consisted of GM without 10% FBS (**LS**), and LS supplemented with 10% (wt/vol; **PP**). Treatments were then

applied to 2 of the 6 wells as described above. Experiments for both types of cells were replicated 3 times.

Twenty-four, 48, 72, and 96 h after treatments were applied proliferation assay cultures were immunostained for Pax7, Myf-5, and bromodeoxyuridine (**BrdU**; Sigma Aldrich). For the detection of cells traversing S-phase, BrdU, a thymidine analog, was added to media 2 hours before fixation (Allen et al., 1979). Temporal characterization of the muscle lineage markers was conducted as previously described (Li et al., 2011). Briefly, cells were fixed with 4% (wt/vol) formaldehyde (Polysciences, Warrington, PA) in PBS. Cultures were incubated in 0.5% Triton-X 100 (Fisher Scientific, Waltham, MA) in PBS for 10 minutes to permeabilize the nuclear membrane, followed by a 7 min incubation in 4 *N* hydrochloric acid (Fisher Scientific) to denature the DNA for immunostaining. Next, cultures were incubated in 5% horse serum (Fisher Scientific) and 0.2% Triton-X in PBS for 30 min to block non-specific antigen binding. Cultures were incubated with a primary antibody solution containing, 1:250 anti-BrdU (Santa Cruz Biotechnology, Dallas, TX), 1:10 supernatant anti-Pax7 (Developmental Studies Hybridoma Bank, University of Iowa, Iowa City, IA), and 1:50 anti-Myf5 (Santa Cruz Biotechnology) diluted in blocking solution for 1 hour. Next, cells were incubated with goat anti-rat AlexaFluor 594 (1:1000; Invitrogen), goat anti-mouse AlexaFluor 488 (1:1000; Invitrogen) and goat anti-rabbit AlexaFluor633 (1:1000; Invitrogen) to detect BrdU, Pax7, and Myf-5, respectively. Hoechst 33324 (Invitrogen) was included at 10µg/mL for the detection of nuclei.

Cells were visualized using an Eclipse TI-U microscope equipped with an X-Cite 120XL epiflouresence illumination system (Nikon Instruments Inc., Melville, NY). Photomicrographs were captured using a Nikon DS-QiMc digital camera (Nikon Instruments Inc.). A minimum of 10 microscopic fields at 200-fold magnification were analyzed per sample utilizing NIS-

Elements Imaging Sofware (Basic Research, 3.3; Nikon Instruments Inc.). Proliferation indicies were determined by the proportion of cells traversing the S-phase at each time point. Additionally, cells were classified into 3 categories based on Pax7 and Myf-5 expression, cells only expressing Pax7 (**Pax7+**), only expressing Myf-5 (**Myf-5+**), and cells co-expressing Pax7 and Myf-5 (**Pax7/Myf-5+**).

Differentiation Assay

Parallel cultures of PSC (n = 3) were seeded at a density of 1×10^3 cells/cm^2 on tissue culture treated 12-well culture plates (Eppendorf) coated with 5 μg/cm^2 entactin-collagen IV-laminin (**ECL**; Millipore, Billerica, MA) . Four culture plates were utilized to seed a pool of PFM on 16 wells. All PFM were maintained in GM for 96 h prior to application of treatments, at which time half of the 16 wells were treated with either HS or LS media. Of the wells that contained HS and LS half of each were treated with porcine plasma 0 (**PPN**) or 10% wt/vol (**PPP**). The treatments were replenished 48 h after initial application, and cultures were either immunostained or subjected to protein isolation 96 h after application of treatments. For immunostaining cultures were fixed with 4% (wt/vol) formaldehyde (Polysciences) in PBS. Cultures were incubated in 5% horse serum, 0.2% Triton-X 100 in PBS for 30 min to block non-specific antigen binding sites, incubated for 1 h with a primary antibody solution containing 1:2 supernatant anti-sarcomeric myosin (**MF20**; Developmental Studies Hybridoma Bank), and incubated with 1:1,000 goat anti-mouse AlexaFluor 594 (Invitrogen). Hoechst 33324 (Invitrogen) was included at 10 μg/mL for the detection of nuclei. Following immunostaining cultures were imaged as described above. The differentiation capacity was calculated as the number of nuclei present in multinucleated sarcomeric myosin positive myotubes divided by the total number of nuclei.

Protein Synthesis Assay

The PSC were plated in the same arrangement as the differentiation assay and maintained in GM for 96 h. Media was replaced with LS media to induce differentiation for an additional 96 h and media was replaced with LS media supplemented with 10 μM cytosine β-D-arabinofuranoside (Sigma Aldrich) for 24 h to eliminate any proliferating cells (Hinterberger and Barald, 1990). Cells were subsequently exposed to the treatments described for the differentiation assay for an acuter period of 180 min or 72 h. After which time cultures were either immunostained with sarcomeric myosin (Developmental Studies Hybridoma Bank; MF20) or subjected to protein isolation as described above. To determine average myotube diameter, a minimum of 100 measurements were taken perpendicular to the length of each myotube, using the length measurement tool in NIS Elements Imaging Software (Nikon Instruments Inc.).

Western Blot Analysis

Protein was extracted from progenitor cells at the conclusion of the differentiation assay, according to the methods of (Wang et al., 2012). Briefly, cells were scraped from the bottom of each well in 300 μL of lysis buffer (50 *M* Tris-HCL, 150 *M* NaCl, 1 *M* EDTA, 0.5% Triton X-100, 1 *M* phenlymethanessulfonyl fluoride, 1 *M* $NaVO_4$; Fisher Scientific) containing a complete protease inhibitor (Sigma Aldrich) and homogenized through a 21 gauge needle. Homogenates were centrifuged at 14,000 × *g* for 15 min at 4°C. Sample protein concentrations were quantified using Pierce's BCA Protein Assay Kit (Thermo Scientific). Three micrograms of protein was heated in 4× sample loading buffer (40% vol/vol glycerol, 4% vol/vol β-mercaptoethanol, 0.08% wt/vol Sodium dodecyl sulfate; Fisher Scientific) at 95ºC for 3 min. Samples were loaded onto four separate 7.5% separating polyacrylamide gels with 3.5% stacking gels and separated at 40 mA. Proteins were transferred to a nitrocellulose membrane (Amersham Hybond-ECL; GE

Healthcare) using blotting paper saturated with transfer buffer (25m*M* Tris, 192 m*M* glycine, and 5% vol/vol methanol) and a Semi-dry Transfer Unit (Hoefer, Holliston, MA). Blots were incubated with 5% nonfat dry milk in TBS-T (10 mM Tris, pH 8.0, 150 mM NaCl, 0.1% Tween-20) for 30 min at room temperature to block nonspecific antigen sites. After the nitrocellulose membranes were blocked, the first blot was incubated with an p-mTOR, p-AKT (Ser^{473}), p-FOXO-1, and p-4EBP-1 antibodies (1:1000, 1:2000, 1:500, and 1:1000, respectively, in 1% nonfat dry milk in TBS-T; Cell signaling, Beverly, MA), the second blot was incubated with total mTOR, total AKT antibody, total FOXO-1, and total 4EBP-1 (1:1000 in 1% nonfat dry milk in TBS-T; Cell Signaling). The third blot was incubated with an p-S6 kinase, p-AKT (Thr^{308}), (1:1000 in 1% nonfat dry milk in TBS-T; Cell Signaling) and MAFbx antibodies (1:500, in 1% nonfat dry milk in TBS-T; Santa Cruz Biotechnology), and the fourth blot was incubated with total S6 kinase (1:1000 in 1% nonfat dry milk in TBS-T; Cell Signaling), and MURF-1 antibodies (1:2000, in 1% nonfat dry milk in TBS-T; Santa Cruz Biotechnology) overnight at 4ºC. Following primary antibody incubation blots were incubated with an anti-rabbit horse radish peroxidase linked secondary antibody (1:1000 in 5% nonfat dry milk in TBS-T; Cell Signaling) at room temperature for 1 h. Blots were developed using an enhanced chemiluminescence kit (ECL Plus, Amersham, Pittsburgh, PA) and visualized using the ChemiDoc-It 415 Imaging System (UVP, Upland, CA). Band intensities were quantified using VisionWorksLS Image Acquisition and Analysis Software (UVP; Upland, CA). Values are reported as the abundance of each protein that was equalized to a pooled sample on each blot and as a ratio of protein phosphorylation (normalized phoshphorylated band intensity / normalized total band intensity × 100).

Statistical Analyses

The proliferation assay was analyzed as a 3 × 4 factorial arrangement, with repeated measures. The random effect was pool of cells. The fixed effects included treatment (**Trt**), and Time served as the repeated measurement. The PSC differentiation and protein synthesis assays were analyzed as a 2 × 2 factorial design. The random effect was pool. The fixed effects were serum status (**Serum**), and porcine plasma supplementation status (**PP**). All statistical analysis was performed using the GLIMMIX Procedures of SAS 9.4 (Cary, NC). Pair-wise comparisons between the least square means of the factor levels, including planned interaction comparisons, were computed using the PDIFF option of the LSMEANS statement. Differences were considered significant at $\alpha \leq 0.05$.

RESULTS

Proliferation Assay

There were Time × Trt interactions for PSC proliferation rate and percentage of Pax7+ PSC ($P \leq 0.05$; Table 4.1); however, the percent of Myf-5+ and Pax7/Myf-5+ PSC were not affected by the interaction ($P \geq 0.09$). Proliferation rate of PP-PSC at 48 h was similar to proliferation rate at 24 and 72 h ($P \geq 0.07$), and was greater ($P = 0.05$) than at 96 h. Overall, at all time points the HS-PSC had a greater proliferation rate than the LS- and PP-PSC ($P < 0.01$), and the LS-PSC had a greater ($P < 0.01$) proliferation rate than the PP-PSC, and all treatments had a similar Pax7+ percentage, within time period at 48, 72, and 96 h, ($P \geq 0.16$).

Time affected all proliferation characteristics assessed ($P < 0.01$). The proliferation rate of PSC was greater at 24 h compared to 48, 72, and 96 h ($P < 0.01$), which were similar to each other ($P \geq 0.79$). At 24 h, there was a greater percentage of Pax7+ PSC compared to all other time points ($P < 0.01$). Forty-eight hour PSC had a greater percentage of Pax7+ PSC than cells at

72 and 96 h ($P < 0.01$), which were similar to each other ($P = 0.94$). At 24 h, there were fewer Myf-5+ PSC compared to all other time points ($P < 0.01$), which were similar to each other ($P \geq 0.07$). At 24 h, the percentage of the Pax7/Myf-5+ PCS was greater than at 48 and 72 h ($P \leq 0.01$), and was similar ($P = 0.09$) to 96 h. At 72 h there were fewer Pax7/Myf-5+ PSC than at the 48 and 96 h ($P \leq 0.01$), which were similar to each other ($P = 0.33$).

The main effect of Trt affected proliferation rate, percentage of Myf-5+ PSC, and the percentage of Pax7/Myf-5+ PSC ($P \leq 0.03$); however, Trt did not affect percentage of Pax7+ PSC ($P \geq 0.06$). The PSC exposed to the HS treatment had greater proliferation rate compared to all other treatments ($P < 0.01$), and LS-PSC had a greater ($P < 0.01$) proliferation rate than PP-PSC. The HS-PSC had a decreased percentage of Myf-5+ PSC compared to LS- and PP-PSC ($P < 0.01$), which were similar to each other ($P = 0.06$). The HS PSC had a greater percentage of Pax7/Myf-5+ PSC compared to LS and PP treatments ($P \leq 0.04$), which were similar to each other ($P = 0.29$).

Differentiation Assay

There was a PP × Serum interaction for differentiation capacity of PSC ($P < 0.01$; Table 4.2); however, the interaction did not affect any mTOR signaling pathway proteins ($P \geq 0.13$). Porcine satellite cells cultured in LS-PPP had greater differentiation capacity compared to LS-PPN ($P < 0.01$), and the HS-PPP had a greater ($P < 0.01$) differentiation capacity compared to HS-PPN; however, the difference was more pronounced in the LS treatment. Serum affected the abundance of total mTOR, total s6 Kinase, and MAFbx ($P \leq 0.05$); however, Serum did not affect differentiation capacity or any of the other mTOR signaling pathway proteins evaluated ($P \geq 0.06$). The HS-PSC had a greater abundance of total mTOR, total S6 Kinase, and MAFbx compared to LS-PSC ($P \leq 0.05$).

There was a PP effect for differentiation capacity, the abundance of total AKT, Ser^{473} phosphorylated AKT, total mTOR, total S6 Kinase, phosphorylated S6 Kinase, and MAFbx, and the ratios of Thr^{308} phosphorylated AKT, and phosphorylated mTOR ($P \leq 0.04$), with no effect on any of the other mTOR pathway signaling proteins evaluated ($P \geq 0.08$). The PPP-PSC had an increased ($P < 0.01$) percentage of cells that fused into multinucleated myotubes compared to PPN-PSC. The PPP-PSC had a decreased abundance of total AKT and total mTOR compared to PPP-PSC ($P \leq 0.01$). The PPP-PSC had a greater abundance of S6 kinase and MAFbx compared to PPN-PSC ($P \leq 0.03$), and PPP-PSC had a greater ratio of phosphorylated mTOR and Thr^{308} AKT compared to PPN-PSC ($P \leq 0.03$).

Protein Synthesis Assay

Differentiated PSC derived myotubes were subjected to a 72 h treatment period and protein synthesis characteristics were assessed. There were PP × Serum interactions for the abundance of phosphorylated S6 Kinase and 4E-BP, and the ratio of phosphorylated FOXO ($P \leq 0.03$; Table 4.3); however, myotube diameter and all other mTOR pathway signaling proteins were not affected ($P \geq 0.13$). In the presence of HS media PPP-PSC had similar ($P = 0.46$) abundance of phosphorylated S6 Kinase compared to PPN-PSC, but in LS media PPP-PSC had increased ($P = 0.01$) abundance of phosphorylated S6 Kinase. In the presence of HS media the PPP-PSC had an increased abundance of phosphorylated 4E-BP and ratio of phosphorylated FOXO compared to PPN-PSC ($P \leq 0.04$), but in LS media PPP-PSC had a similar abundance of phosphorylated 4E-BP and ratio of phosphorylated FOXO compared to PPN-PSC ($P \geq 0.26$).

Serum affected myotube diameter, the abundance of total AKT, Ser^{473} phosphorylated AKT, Thr^{308} phosphorylated AKT, and ratios of Ser^{473} phosphorylated AKT and mTOR ($P \leq 0.04$); however, the remainder of the mTOR pathway signaling proteins evaluated were not

affected ($P \geq 0.06$). The LS-PSC had a greater ($P < 0.01$) myotube diameter compared to HS-PSC. The HS-PSC had a greater abundance of total AKT, Ser^{473} phosphorylated AKT, and Thr^{308} phosphorylated AKT compared to LS-PSC ($P \leq 0.04$). Additionally, HS-PSC had a greater ratio of Ser^{473} phosphorylated AKT, and phosphorylated mTOR compared to LS-PSC ($P \geq 0.03$).

There was a PP effect on myotube diameter, abundance of total AKT, Ser^{473} phosphorylated AKT, and phosphorylated 4E-BP, as well as the ratio of 4E-BP phosphorylation ($P \leq 0.02$). The PPP-PSC had a greater ($P < 0.01$) myotube diameter than PPN-PSC. The PPP-PSC had a decreased abundance of total AKT and Ser^{473} phosphorylated AKT compared to PPN-PSC ($P \leq 0.01$). Additionally, the PPP-PSC had a greater abundance and ratio of phosphorylated 4E-BP ($P \geq 0.02$).

One-hundred and Eighty Minute Protein Synthesis Assay

Following an 180-min treatment period of differentiated PSC there were PP × Serum interactions for the abundance of Ser^{473} phosphorylated AKT, the ratio of Ser^{473} phosphorylated AKT, and the abundance of total 4E-BP ($P \leq 0.02$; Table 4.4), while myotube diameter and the remainder of the mTOR pathway signaling proteins were not affected ($P \geq 0.06$). When in the presence of HS the PPP-PSC had decreased abundance and ratio of Ser^{473} phosphorylated AKT compared to PPN-PSC ($P \leq 0.01$), but in the presence of LS PPP-PSC had a greater abundance and ratio of Ser^{473} phosphorylated AKT compared to PPN-PSC ($P = 0.01$).

Serum affected the abundance and ratio of Ser^{473} phosphorylated AKT ($P \leq 0.02$), but did not affect myotube diameter or any of the other or any of the other mTOR pathway signaling proteins assessed ($P \geq 0.09$). The HS-PSC had a greater abundance and ratio of phosphorylated AKT Ser^{473} compared to LS-PSC ($P \leq 0.02$). There was a PP effect for the abundance of phosphorylated S6 Kinase and FOXO ($P = 0.02$), but PP did not affect myotube diameter, or any

of the other mTOR pathway signaling proteins ($P \geq 0.13$). The PPP-PSC media had a greater abundance of phosphorylated S6 Kinase and FOXO compared to PPN-PSC ($P = 0.02$).

DISCUSSION

Porcine Satellite Cell Proliferation

Improving the efficiency of pork production is a multi-faceted task that includes digestive function, immunity, and tissue deposition. The current study focuses on the potential of porcine plasma supplementation to directly stimulate skeletal muscle development through satellite cell stimulation in the early postnatal period. The PSC utilized were isolated from piglets within 24 h of birth, thus constituting the largest and most active satellite cell population during the post-natal period (Renault et al., 2000). Satellite cells are responsible for replenishing their own population and terminally differentiating into muscle fibers to contribute the DNA template needed for protein synthesis (Bentzinger et al., 2012). Satellite cell activity is modulated through the transition of transcriptional signals, that begins with elevated Pax7 expression levels in quiescent satellite cells and progresses through the expression of the myogenic regulator factors as the satellite cells begin to proliferate and commit to terminal differentiation (Zammit et al., 2006; Biressi and Rando, 2010). Li et al. (2011) categorized i*n vitro* proliferative satellite cells into three sub-classes of cells that express Pax7, Myf-5, and co-express Pax7 and Myf-5. Cells that solely express Pax7 are activated and are less proliferative than cells that co-express Pax7 and Myf-5, which are the most proliferative of the three populations of myogenic cells. As Pax7 expression subsides, the rate of proliferation is lessened, and cells that solely expressing Myf-5 are committed to myogenic differentiation (Zammit et al., 2006). Therefore, these markers can be utilized to identify the effects of treatment on PSC proliferation.

To date, little literature exists examining the effect of PP on *in vitro* cell proliferation. Tran et al. (2014) supplemented spray-dried porcine plasma to porcine jejunal epithelial cell lines to assess proliferation and observed that all levels of spray-dried porcine plasma resulted in greater proliferation compared to control cells. As described in chapter 3, porcine plasma stimulated proliferation rate of d-60 of gestation porcine fetal myoblasts. In the current study, PP treatment resulted in a proliferation rate that was decreased 43% and 27% compared to HS and LS, respectively. Additionally, proliferation rate of PP-PSC decreased 53% from 24 h to 96 h, but proliferation rate of LS and HS treatments were similar at 24 h and 96 h. The PP- and LS-PSC had 15% and 11% fewer cells that were Pax7/Myf-5+ compared to the HS treatment, respectively. Additionally, PP- and LS-PSC had 16% and 11% more Myf-5+ PSC compared to HS-PSC, respectively. Therefore, treatment of proliferative PSC with PP resulted in PSC that were less proliferative. Myogenic regulatory factor categorization data indicated PP expedited the transition of proliferative PSC from Pax7+ to Myf-5+ expression, which is a profile that is favorable for terminal differentiation.

Effect of Porcine Plasma on Porcine Satellite Cell Differentiation

The ultimate fate of myogenic precursor cells is to undergo terminal differentiation, and provide the DNA template needed for protein synthesis of existing muscle fibers (Moss and Leblond, 1971; Biressi et al., 2007). Data from the proliferation assay suggests PSC exposed to PP are pushed toward differentiation; however, there are not any studies that have evaluated myogenic differentiation in response to PP. Our current knowledge of PP is it is a composite material that contains high levels of amino acids and elevated concentrations of IGF-1 (Coffey and Cromwell, 1995; de Rodas et al., 1995). The protein IGF-1 has been implicated in promoting myogenic differentiation and protein synthesis through an autophosphorylation cascade mTOR

pathway signaling (Engert et al., 1996; Schiaffino and Mammucari, 2011). Insulin growth like factor-1 also decreased the extent of muscle atrophy through phosphorylation of FOXO and downregulation of the ubiquitin ligases MAFbx and MURF-1 (Stitt et al., 2004); however, proteasome inhibition is associated with reduced myoblast fusion (Gardrat et al., 1997). Ubiquitin ligases MAFbx and MURF-1 degrade myogenic regulatory factors to provide the appropriate expression of myogenic regulatory factors to promote myogenic differentiation, as well as, serve as the mechanism to clear oxidized proteins accumulated during the myogenic differentiation (Bell et al., 2016).

As an alternative to IGF-1 stimulation, previous research indicated that supplementation of methionine and leucine to myogenic cells resulted in an increase in the phosphorylation of S6 kinase at the Thr^{389} phosphorylation site, independently of mTOR and AKT (Tesseraud et al., 2003). As described in chapter 3, supplementation of PP to fetal myoblasts resulted in a reduced differentiation capacity; however, in the current study, PPP-PSC had a 33% greater differentiation capacity compared to PPN-PSC. Additionally, PP stimulated the PSC differentiation 13% more in the presence of LS media compared to HS media. The supplementation of PP resulted in an increase in a 31% and 35% increase in total and phosphorylated S6 Kinase, respectively. Despite a 60% and 54% decrease in the abundance of total AKT and mTOR, respectively, the increase in S6 Kinase was mediated by 58% and 36% increases in Thr^{308} phosphorylated AKT and phosphorylated mTOR, respectively. Additionally, PPP-PSC had a 33% increase in the abundance of MAFbx compared to PPN-PSC. Elevated levels of MAFbx are needed for the degradation of paired box transcription factors-3 and -7, thus promoting the expression of myogenic differentiation factors (Gardrat et al., 1997). Therefore, PP contains components that stimulate differentiation capacity, through upregulation of MAFbx,

to promote progression of the myogenic program and stimulation of S6 Kinase phosphorylation to promote translation.

Effect of Porcine Plasma on Protein Synthesis

In addition to its role in satellite cell differentiation, IGF-1 also plays an integral role in protein synthesis. Supplementation of IGF-1 *in vitro* stimulated increased average myotube diameter, and a greater abundances of phosphorylated AKT, phosphorylated S6 kinase, and a decreased abundance of total 4EBP-1 in murine cell lines (Rommel et al., 2001). In chapter 3, PP supplementation to fetal myoblasts resulted in a reduced myotube diameter; however after 72-h of exposure, PPP-PSC had a 14% increase in myotube diameter compared to PPN-PSC. Contrary to IGF-1 supplementation studies, PSC supplemented with PP had 29% less total AKT and 57% less Ser^{473} phosphorylated AKT compared to PPN-PSC. The PPP-PSC experienced a 31% increase in abundance of phosphorylated 4E-BP, which resulted in a 48% increase in the ratio of phosphorylated 4E-BP compared to PPN-PSC, which indicates the increased myotube diameter was a result of releasing the inhibitory effects of 4E-BP, thus allowing protein synthesis to proceed.

Because there was no linear increase in mTOR signaling protein phosphorylation, additional acute exposure studies were conducted to determine if the window of total pathway activation was missed at 72 h. Han et al. (2008) supplemented IGF-1 to PSC from 6 month old pigs for 15 to 180 min. Authors observed that 100 ng/mL recombinant IGF-1 stimulated the production of the phosphorylated forms of AKT, and mTOR at all four time points, illustrating that IGF-1 supplementation begins to impact protein metabolism very rapidly (Han et al., 2008). In the current study, treatment supplementation for 180 min did not result in increased myotube diameter, which is expected because 180 min was not enough time for effects on myotube

diameter to be seen. At 180 min, the additional growth factors of the HS treatment stimulated 53% more Ser^{473} phosphorylated AKT, which resulted in a 40% increase in the ratio of Ser^{473} phosphorylated AKT compared to LS treatments. Interestingly, PPP reduced Ser^{473} phosphorylated AKT by 47% in the presence of HS media, and increased phosphorylation of the same protein by 55% in the presence of LS media. These results suggest the full benefits of PP will be experience in a nutrient poor environment. Additionally, porcine plasma resulted in a 39% increase phosphorylated S6 Kinase and a 21% increase in phosphorylated FOXO; however once again, experimental conditions did not stimulate a linear increase in activation of the mTOR pathway. Therefore, these data indicate 180 min is still too long to demonstrate the effect of treatment on mTOR pathway or PP stimulation of increased myotube diameter occurs in a mTOR independent fashion. Possibly, amino acids have been shown to promote myogenic differentiation and protein synthesis in an AKT dependent and independent manner (Schiaffino and Mammucari, 2011; Kimball et al., 1999; Kimball and Jefferson, 2002). The stimulation of 4E-BP phosphorylation can be stimulated by leucine and low sulfur amino acids (Fox et al., 1998; Sikalidis et al., 2013). In its' hypo-phosphorylated form 4E-BP binds to S6 Kinase repressing initiation of translation, and phosphorylation of 4E-BP triggers its' release from S6 Kinase relieving the repression of 4E-BP on translation (Fox et al., 1998; Hidalgo et al., 2012; Sikalidis et al., 2013).

Table 4.1. The proliferation rate and nuclear area of porcine satellite cells (**PSC**) from the longissimus muscle of piglets within 24 h of parturition[1]

					P-value[2]		
Size	HS	LS	PP	SEM	Time × Trt	Time	Trt
Proliferation rate[3], %							
24 h	58.5	46.3	20.7	1.1	0.05	< 0.01	< 0.01
48 h	56.1	36.9	15.4				
72 h	59.6	38.3	11.7				
96 h	56.6	42.1	9.7				
Nuclear area[4], μm^2							
24 h	146.5	149.9	158.6	20.1	< 0.01	< 0.01	0.06
48 h	152.4	174.5	207.1				
72 h	162.4	194.1	272.7				
96 h	165.2	189.8	304.9				
Pax7+[5], %							
24 h	2.4	3.5	6.4	0.8	0.02	< 0.01	0.46
48 h	1.6	3.1	1.4				
72 h	0.6	0.3	0.4				
96 h	0.1	0.9	0.3				
Myf5+[6], %							
24 h	10.3	15.0	19.8	3.2	0.09	< 0.01	< 0.01
48 h	9.5	26.9	29.7				
72 h	14.9	25.5	37.8				
96 h	15.3	24.7	28.0				
Pax7+ and Myf5+[7], %							
24 h	85.2	76.9	72.2	3.0	0.12	< 0.01	0.03
48 h	84.3	71.1	68.1				
72 h	81.9	69.6	61.2				
96 h	83.1	72.7	71.5				

[1]Porcine fetal myoblasts from the SM, ME, and LG male fetuses maintained in 10% fetal bovine serum, 2% porcine serum in DMEM supplemented with 100 U penicillan/mL, 100 μg of strepmycin/mL, and 20 μg of gentamicin/mL. Parallel cultures were exposed to 5 μM bromodeoxyuridine (**BrdU**) and immunostained daily.

[2]Trt = treatment effect.

[3]The number of bromodeoxyuridine (**BrdU**) positive PFM divided by the total number of PFM present within representative photomicrographs

[4]Represents the average nuclear area of PFM

[5]Represents the percentage of all PFM that were only Pax7+

[6]Represents the percentage of all PFM that were only Myf-5+

[7]Represents the percentage of all PFM that co-expressed Pax7 and Myf-5

Table 4.2. Effect of serum type, and porcine plasma supplementation on the relative abundance of proteins downstream of the PI3-K signaling pathway in differentiating porcine satellite cells.

Serum	HS		LS		SEM	PP× Serum	Serum	PP
PP	PPN	PPP	PPN	PPP				
Differentiation capacity[3], %	30.7	38.5	24.1	43.3	2.48	< 0.01	0.58	< 0.01
mTOR pathway signaling[4]								
AKT								
Total, AU[5,]	1.23	0.47	0.69	0.29	0.24	0.35	0.07	< 0.01
Phosphorylated[6], AU	1.22	0.52	1.06	0.32	0.20	0.92	0.40	< 0.01
Ratio phosphorylated, AU	135	117	154	178	33.0	0.36	0.09	0.88
Phosphorylated[7], AU	0.77	0.79	0.57	0.53	0.14	0.78	0.06	0.93
Ratio phosphorylated, AU	158	402	177	398	92.9	0.78	0.86	< 0.01
mTOR								
Total, AU	0.93	0.45	0.57	0.22	0.17	0.65	0.05	0.01
Phosphorylated[8], AU	0.95	0.74	0.77	0.48	0.17	0.78	0.15	0.11
Ratio phosphorylated, AU	201	307	163	26	59.3	0.95	0.35	0.03
S6 Kinase								
Total, AU	1.09	1.68	0.84	1.11	0.20	0.39	0.04	0.03
Phosphorylated[9], AU	0.80	1.17	0.86	1.36	0.19	0.72	0.51	0.04
Ratio phosphorylated, AU	117	122	153	184	32.5	0.64	0.09	0.53
4E-BP								
Total, AU	2.41	4.12	1.11	0.83	1.24	0.44	0.08	0.57
Phosphorylated[10], AU	1.26	2.11	0.73	0.75	0.58	0.48	0.12	0.47
Ratio phosphorylated, AU	97	122	94	110	17.4	0.81	0.68	0.25
FOXO								
Total, AU	1.11	0.53	0.57	0.32	0.27	0.50	0.14	0.11
Phosphorylated[11], AU	1.79	1.62	1.29	0.83	0.51	0.79	0.23	0.55
Ratio phosphorylated, AU	272	589	302	779	209.8	0.71	0.61	0.08
MAFbx	0.99	1.14	0.28	0.76	0.10	0.13	< 0.01	< 0.01
MURF1	1.03	1.22	0.64	0.89	0.18	0.88	0.06	0.24

[1]Differentiating porcine satellite cells were treated with a high serum media containing 10% fetal bovine serum, 2% porcine serum in DMEM supplemented with 100 U penicillan/mL, 100 µg of strepmycin/mL, and 20 µg of gentamicin/mL (**HS**), or a low serum media containing 2% porcine serum in DMEM supplemented with 100 U penicillan/mL, 100 µg of strepmycin/mL, and 20 µg of gentamicin/mL (**LS**). The HS and LS media was supplemented with 10% (wt/vol) porcine plasma (**PPP**), or 0% (wt/vol) porcine plasma (**PPN**).

[2]PP = Porcine plasma effect.

[3]Percentage of all PFM that have incorporated into multinucleated sarcomeric myosin positive myotubes.

[4]AKT = protein kinase B, mTOR = mammalian target of rapamycin, S6 Kinase = p70 S6 kinase, 4E-BP = eukaryotic translation initiation factor 4E binding protein, FOXO = forkhead box O1, MAFbx = muscle atrophy F-box, and MURF-1 = muscle ring finger-1.

[5]AU = Arbitrary Unit

[6]AKT phosphorylated at Ser^{473}

[7]AKT phosphorylated at Thr^{308}

[8]mTOR phosphorylated at Ser^{2448}

[9]S6 Kinase phosphorylated at Thr^{389}

[10]4E-BP phosphorylated at $Thr^{37/46}$

[11]FOXO phosphorylated at Ser^{319}

Table 4.3. Effect of acute exposure of serum type, and porcine plasma supplementation on the relative abundance of proteins downstream of the PI3-K signaling pathway in differentiated porcine satellite cells.

Serum	HS		LS		SEM	PP× Serum	Serum	PP
PP	PPN	PPP	PPN	PPP				
Myotube diameter, %	27.9	28.1	28.4	28.2	0.43	0.63	0.48	0.96
mTOR pathway signaling[4]								
AKT								
Total, AU[5,]	0.97	1.36	1.00	0.86	0.16	0.14	0.19	0.49
Phosphorylated[6], AU	1.75	1.19	0.43	0.95	0.11	< 0.01	< 0.01	0.87
Ratio phosphorylated, AU	213	89	43	139	20.7	< 0.01	0.02	0.53
Phosphorylated[7], AU	2.12	2.29	1.70	2.23	0.64	0.78	0.72	0.60
Ratio phosphorylated, AU	253	169	182	264	51.1	0.14	0.82	0.99
mTOR								
Total, AU	1.30	1.38	1.25	1.22	0.14	0.67	0.46	0.87
Phosphorylated[8], AU	1.42	1.60	1.11	1.54	0.23	0.61	0.46	0.23
Ratio phosphorylated, AU	114	127	98	131	17.5	0.58	0.73	0.24
S6 Kinase								
Total, AU	0.75	1.04	0.52	0.71	0.17	0.77	0.13	0.18
Phosphorylated[9], AU	0.73	1.24	0.57	0.88	0.13	0.47	0.09	0.02
Ratio phosphorylated, AU	153	151	145	143	37.5	0.99	0.84	0.96
4E-BP								
Total, AU	1.07	1.40	1.61	1.20	0.13	0.02	0.19	0.75
Phosphorylated[10], AU	1.19	1.34	1.20	1.45	0.22	0.80	0.77	0.31
Ratio phosphorylated, AU	124	110	85	134	14.6	0.06	0.60	0.25
FOXO								
Total, AU	1.51	1.64	1.39	1.13	0.35	0.53	0.34	0.84
Phosphorylated[11], AU	0.81	1.05	0.78	0.96	0.08	0.66	0.44	0.02
Ratio phosphorylated, AU	84	93	79	104	13.2	0.46	0.73	0.13
MAFbx	1.90	1.46	1.29	2.01	0.47	0.25	0.95	0.77
MURF1	1.17	1.36	1.44	1.39	0.20	0.57	0.49	0.74

[1]Differentiated porcine satellite cells were treated with a high serum media containing 10% fetal bovine serum, 2% porcine serum in DMEM supplemented with 100 U penicillan/mL, 100 µg of strepmycin/mL, and 20 µg of gentamicin/mL (**HS**), or a low serum media containing 2% porcine serum in DMEM supplemented with 100 U penicillan/mL, 100 µg of strepmycin/mL, and 20 µg of gentamicin/mL (**LS**). The HS and LS media was supplemented with 10% (wt/vol) porcine plasma (**PPP**), or 0% (wt/vol) porcine plasma (**PPN**) for 180 min.

[2]PP = Porcine plasma effect.

[3]Average diameter of multinucleated myotubes from 10 representative photomicrographs.

[4]AKT = protein kinase B, mTOR = mammalian target of rapamycin, S6 Kinase = p70 S6 kinase, 4E-BP = eukaryotic translation initiation factor 4E binding protein, FOXO = forkhead box O1, MAFbx = muscle atrophy F-box, and MURF-1 = muscle ring finger-1.

[5]AU = Arbitrary Unit

[6]AKT phosphorylated at Ser^{473}

[7]AKT phosphorylated at Thr^{308}

[8]mTOR phosphorylated at Ser^{2448}

[9]S6 Kinase phosphorylated at Thr^{389}

[10]4E-BP phosphorylated at $Thr^{37/46}$

[11]FOXO phosphorylated at Ser^{319}

Table 4.4. Effect of acute exposure of serum type, and porcine plasma supplementation on the relative abundance of proteins downstream of the PI3-K signaling pathway in differentiated porcine satellite cells.

Serum	HS		LS		SEM	PP× Serum	Serum	PP
PP	PPN	PPP	PPN	PPP				
Myotube diameter, %	29.9	35.8	36.0	40.6	1.74	0.63	< 0.01	< 0.01
mTOR pathway signaling[4]								
AKT								
Total, AU[5,]	1.37	0.98	1.06	0.75	0.14	0.74	0.04	0.01
Phosphorylated[6], AU	1.55	0.65	0.95	0.41	0.12	0.13	< 0.01	< 0.01
Ratio Phosphorylated, AU	178	158	115	99	30.1	0.92	< 0.01	0.38
Phosphorylated[7], AU	1.59	2.23	1.08	1.00	0.33	0.24	0.01	0.35
Ratio Phosphorylated, AU	313	421	230	281	103.1	0.70	0.14	0.29
mTOR								
Total, AU	1.08	0.88	1.17	0.99	0.21	0.97	0.61	0.34
Phosphorylated[8], AU	1.10	1.04	0.77	0.76	0.15	0.88	0.06	0.80
Ratio Phosphorylated, AU	186	197	115	132	38.2	0.92	0.03	0.62
S6 Kinase								
Total, AU	1.13	1.39	1.12	0.97	0.19	0.32	0.28	0.77
Phosphorylated[9], AU	1.45	1.20	1.06	2.11	0.27	0.01	0.29	0.11
Ratio Phosphorylated, AU	166	169	130	250	45.5	0.66	0.62	0.20
4E-BP								
Total, AU	1.41	1.03	1.44	1.02	0.28	0.95	0.96	0.14
Phosphorylated[10], AU	1.04	2.04	1.31	1.34	0.25	0.02	0.27	0.02
Ratio Phosphorylated, AU	161	280	142	210	44.2	0.45	0.20	0.01
FOXO								
Total, AU	1.14	0.88	0.88	1.02	0.14	0.09	0.59	0.60
Phosphorylated[11], AU	1.55	1.55	1.43	0.86	0.42	0.49	0.34	0.49
Ratio Phosphorylated, AU	152	347	274	171	61.5	0.03	0.67	0.47
MAFbx	1.14	1.13	1.00	1.19	0.18	0.59	0.84	0.63
MURF1	0.99	1.23	1.09	1.05	0.21	0.49	0.84	0.63

[1]Differentiated porcine satellite cells were treated with a high serum media containing 10% fetal bovine serum, 2% porcine serum in DMEM supplemented with 1× antibiotic/mL and 1× gentamicin/mL (**HS**), or a low serum media containing 2% porcine serum in DMEM supplemented with 100 U penicillan/mL, 100 µg of strepmycin/mL, and 20 µg of gentamicin/mL (**LS**). The HS and LS media was supplemented with 10% (wt/vol) porcine plasma (**PPP**), or 0% (wt/vol) porcine plasma (**PPN**) for 72 h.

[2]PP = Porcine plasma effect.

[3]Average diameter of multinucleated myotubes from 10 representative photomicrographs.

[4]AKT = protein kinase B, mTOR = mammalian target of rapamycin, S6 Kinase = p70 S6 kinase, 4E-BP = eukaryotic translation initiation factor 4E binding protein, FOXO = forkhead box O1, MAFbx = muscle atrophy F-box, and MURF-1 = muscle ring finger-1.

[5]AU = Arbitrary Unit

[6]AKT phosphorylated at Ser^{473}

[7]AKT phosphorylated at Thr^{308}

[8]mTOR phosphorylated at Ser^{2448}

[9]S6 Kinase phosphorylated at Thr^{389}

[10]4E-BP phosphorylated at $Thr^{37/46}$

[11]FOXO phosphorylated at Ser^{319}

REFERENCES

Allen, R. E., R. A. Merkel, and R. B. Young. 1979. Cellular aspects of muscle growth: myogenic cell proliferation. J. Anim. Sci. 49:115-127.

Bell, R. A., M. Al-Khalaf, and L. A. Megeney. 2016. The beneficial role of proteolysis in skeletal muscle growth and stress adaptation. Skelet. Mus. 6:16. doi:10.1186/s13395-016-0086-6

Bentzinger, C. F., Y. X. Wang, and M. A. Rudnicki. 2012. Building muscle: molecular regulation of myogenesis. Cold Spring Harb. Perspect. Biol. 4. doi:10.1101/cshperspect.a008342

Biressi, S., and T. A. Rando. 2010. Heterogeneity in the muscle satellite cell population. Semin. Cell Dev. Biol. 21:845-854. doi:10.1016/j.semcdb.2010.09.003

Biressi, S., E. Tagliafico, G. Lamorte, S. Monteverde, E. Tenedini, E. Roncaglia, S. Ferrari, S. Ferrari, M. G. Cusella-De Angelis, S. Tajbakhsh, and G. Cossu. 2007. Intrinsic phenotypic diversity of embryonic and fetal myoblasts is revealed by genome-wide gene expression analysis on purified cells. Dev. Biol. 304:633-651. doi:10.1016/j.ydbio.2007.01.016

Coffey, R. D., and G. L. Cromwell. 1995. The impact of environment and antimicrobial agents on the growth response of early-weaned pigs to spray-dried porcine plasma. J. Anim. Sci. 73:2532-2539.

de Rodas, B. Z., K. S. Sohn, C. V. Maxwell, and L. J. Spicer. 1995. Plasma protein for pigs weaned at 19 to 24 days of age: effect on performance and plasma insulin-like growth factor I, growth hormone, insulin, and glucose concentrations. J. Anim. Sci. 73:3657-3665.

Dodson, M. V., E. L. Dodson, M. A. Martin, B. A. Brannon, D. C. Mathison, and McFarland. 1987. Optimization of bovine satellite cell-derived myotube formation in vitro. Tissue. Cell. 19:159-166.

Dolfi, S. C., L. L. Chan, J. Qiu, P. M. Tedeschi, J. R. Bertino, K. M. Hirshfield, Z. N. Oltvai, and A. Vazquez. 2013. The metabolic demands of cancer cells are coupled to their size and protein synthesis rates. Cancer Metab. 1:20. doi:10.1186/2049-3002-1-20

Engert, J. C., E. B. Berglund, and N. Rosenthal. 1996. Proliferation precedes differentiation in IGF-I-stimulated myogenesis. J. Cell Biol. 135:431-440.

Everts, H., M. J. A. Nabuurs, R. Margry, A. J. van Dijk, and A. C. Beynen. 2001. Growth performance of weanling pigs fed spray-dried animal plasma: a review. Livest. Prod. Sci. 68:263-274.

Fox, H. L., P. T. Pham, S. R. Kimball, L. S. Jefferson, and C. J. Lynch. 1998. Amino acid effects on translational repressor 4E-BP1 are mediated primarily by L-leucine in isolated adipocytes. Am. J. Physiol. 275:C1232-1238.

Gardrat, F., V. Montel, J. Raymond, and J. L. Azanza. 1997. Proteasome and myogenesis. Mol. Biol. Rep. 24:77-81.

Han, B., J. Tong, M. J. Zhu, C. Ma, and M. Du. 2008. Insulin-like growth factor-1 (IGF-1) and leucine activate pig myogenic satellite cells through mammalian target of rapamycin (mTOR) pathway. Mol. Reprod. Dev. 75:810-817. doi:10.1002/mrd.20832

Hidalgo, M., R. Le Bouffant, V. Bello, N. Buisson, P. Cormier, M. Beaudry, and T. Darribere. 2012. The translational repressor 4E-BP mediates hypoxia-induced defects in myotome cells. J. Cell Sci. 125:3989-4000. doi:10.1242/jcs.097998

Hinterberger, T. J., and K. F. Barald. 1990. Fusion between myoblasts and adult muscle-fibers promotes remodeling of fibers into myotubes *in vitro*. Development. 109:139-148.

Kimball, S. R., and L. S. Jefferson. 2002. Control of protein synthesis by amino acid availability. Curr. Opin. Clin. Nutr. Metab. Care. 5:63-67.

Kimball, S. R., L. M. Shantz, R. L. Horetsky, and L. S. Jefferson. 1999. Leucine regulates translation of specific mRNAs in L6 myoblasts through mTOR-mediated changes in availability of eIF4E and phosphorylation of ribosomal protein S6. J. Biol. Chem. 274:11647-11652.

Li, J., J. M. Gonzalez, D. K. Walker, M. J. Hersom, A. D. Ealy, and S. E. Johnson. 2011. Evidence of heterogeneity within bovine satellite cells isolated from young and adult animals. J. Anim. Sci. 89:1751-1757. doi:10.2527/jas.2010-3568

Moss, F. P., and C. P. Leblond. 1971. Satellite cells as the source of nuclei in muscles of growing rats. Anatomical Records 170:421-435.

Pardee, A. B. 1989. G1 events and regulation of cell proliferation. Science. 246:603-608.

Renault, V., G. Piron-Hamelin, C. Forestier, S. DiDonna, S. Decary, F. Hentati, G. Saillant, G. S. Butler-Browne, and V. Mouly. 2000. Skeletal muscle regeneration and the mitotic clock. Exp. Gerontol. 35:711-719.

Rommel, C., S. C. Bodine, B. A. Clarke, R. Rossman, L. Nunez, T. N. Stitt, G. D. Yancopoulos, and D. J. Glass. 2001. Mediation of IGF-1-induced skeletal myotube hypertrophy by PI(3)K/Akt/mTOR and PI(3)K/Akt/GSK3 pathways. Nat. Cell Biol. 3:1009-1013. doi:10.1038/ncb1101-1009

Schiaffino, S., and C. Mammucari. 2011. Regulation of skeletal muscle growth by the IGF1-Akt/PKB pathway: insights from genetic models. Skelet. Mus. 1:4. doi:10.1186/2044-5040-1-4

Sikalidis, A. K., K. M. Mazor, M. J. Kang, H. Y. Liu, and M. H. Stipanuk. 2013. Total 4EBP1 is elevated in liver of rats in response to low sulfur amino acid intake. J. of Amino Acids 2013:864757-Article ID 864757.

Stitt, T. N., D. Drujan, B. A. Clarke, F. Panaro, Y. Timofeyva, W. O. Kline, M. Gonzalez, G. D. Yancopoulos, and D. J. Glass. 2004. The IGF-1/PI3K/Akt pathway prevents expression of muscle atrophy-induced ubiquitin ligases by inhibiting FOXO transcription factors. Mol. Cell 14:395-403.

Tesseraud, S., K. Bigot, and M. Taouis. 2003. Amino acid availability regulates S6K1 and protein synthesis in avian insulin-insensitive QM7 myoblasts. FEBS Lett. 540:176-180. doi:10.1016/s0014-5793(03)00260-6

Tran, H., J. W. Bundy, Y. S. Li, E. E. Carney-Hinkle, P. S. Miller, and T. E. Burkey. 2014. Effects of spray-dried porcine plasma on growth performance, immune response, total antioxidant capacity, and gut morphology of nursery pigs. J. Anim. Sci. 92:4494-4504. doi:10.2527/jas.2014-7620

Zammit, P. S., T. A. Partridge, and Z. Yablonka-Reuveni. 2006. The skeletal muscle satellite cell: the stem cell that came in from the cold. J. Histochem. Cytochem. 54:1177-1191. doi:10.1369/jhc.6R6995.2006

Chapter 5 - Conclusion

Swine production efficiency is a multi-faceted measure that takes into account production parameters from all production stages. One metric of swine production efficiency is the quantity of pork produced per individual pig or on a per sow basis. Previous studies indicate lighter birth weight piglets within litters gain less weight early in life and require additional days on feed compared to heavier birthweight piglets of the same litter (Gondret et al., 2006), and skeletal muscle of lighter birth weight piglets contain fewer muscle fibers (Wigmore and Stickland, 1983; Handel and Stickland, 1987). The aim of these series of studies was to thoroughly characterize intra-litter variation and examine if porcine plasma can affect myogenic progenitor cell proliferation, differentiation, and protein synthesis *in vitro*, to determine if this dietary additive can help improve the performance of light birth weight pigs.

Pre-natal myogenesis occurs in a bi-phasic manner where primary muscle fibers are formed first and serve as the scaffolding for second wave of secondary muscle fibers. In the pig primary muscle fibers develop from d-25 to 50 of gestation, and secondary muscle fibers are formed between d-50 and 90 of gestation (Wigmore and Stickland, 1983). The data observed in chapter 2 indicated divergent myogenic development between the smallest (**SM**), median (**ME**), and largest (**LG**) fetuses within litters. The SM and ME fetuses exhibited a delayed myogenic trajectory, which was indicated by reduced LM cross-sectional area (**CSA**) compared to LG fetuses at both d-60 and 95 of gestation. Interestingly, at d-60 of gestation LM CSA was influenced by primary fiber number, primary fiber CSA, and secondary fiber number; however, at d-95 of gestation the reduced LM CSA was primarily due to differences in hypertrophy of secondary muscle fibers. Additionally, delayed muscle fiber development of SM fetuses was accompanied with a reduced total number of myogenic progenitor cells compared to ME and LG

fetuses. It is hypothesized the reduced number of myogenic progenitor cells could be responsible for decreased skeletal muscle development observed early in life of light birth weight piglets. Therefore, porcine fetal myoblasts (**PFM**) were isolated to assess activity at d-95 and 60 of gestation in chapters 2 and 3, respectively.

Even though myogenic development was delayed for SM fetuses at both d-60 and 95 of gestation, fetal size affected PFM activity at d-60 but not at d-95 of gestation. At d-60 of gestation proliferation rate and myotube diameter of SM-PFM was greater than LG- and ME-PFM; however, LG-PFM had a greater differentiation capacity compared to ME- and SM-PFM and ME-PFM had a greater differentiation capacity compared to SM-PFM. This indicates that in a nutritionally equivalent environment SM-PFM at d-60 of gestation contain the ability to maintain a proliferative state longer and mediate a greater amount of muscle hypertrophy compared to LG-PFM. These data indicate SM-PFM contain compensatory activity at d-60 of gestation but, not at d-95 of gestation, suggesting d-60 of gestation serves as a potential developmental period where dietary or pharmacological interventions to improve placental efficiency may be able to preferentially promote myogenesis of SM fetuses.

Until the current investigation, research involving porcine plasma supplementation have focused on the overall gains, gut health, and immunity (Coffey and Cromwell, 1995; de Rodas et al., 1995; Everts et al., 2001; Tran et al., 2014). Porcine plasma supplementation during the nursery phase increases ADG and feed intake (Everts et al., 2001), and stimulates the proliferation of intestinal epithelial cells, promoting gut health and nutrient absorption (Tran et al., 2014). In the current studies, porcine plasma supplementation elicited direct effects on PFM and porcine satellite cell (**PSC**) growth and protein synthesis signaling. The current studies indicate a divergent response of myogenic progenitor cells based on the developmental stage,

where PFM were stimulated to proliferate and PSC were stimulated to differentiate and synthesize protein. Additionally, in chapter 3, the response to porcine plasma was dependent on fetal size, where PFM from SM and ME fetuses developed smaller myotubes when supplemented with porcine plasma, but porcine plasma supplementation to LG-PFM did not impact myotube diameter, suggesting LG-PFM are metabolically more similar to PSC than PFM from SM and ME fetuses. It is likely the combination of amino acids and insulin like growth factor-1 (**IGF-1**) in porcine plasma is capable of promoting skeletal muscle growth through myoblast proliferation *in utero* and muscle fiber hypertrophy of neonatal pigs in a satellite cell mediated fashion. Further determination of the effects of individual amino acids, IGF-1, and combinations of individual components on myoblast and satellite cell activity will assist in elucidating the biological mechanism elicited through porcine plasma supplementation.

REFERENCES

Coffey, R. D., and G. L. Cromwell. 1995. The impact of environment and antimicrobial agents on the growth response of early-weaned pigs to spray-dried porcine plasma. J. Anim. Sci. 73:2532-2539.

de Rodas, B. Z., K. S. Sohn, C. V. Maxwell, and L. J. Spicer. 1995. Plasma protein for pigs weaned at 19 to 24 days of age: effect on performance and plasma insulin-like growth factor I, growth hormone, insulin, and glucose concentrations. J. Anim. Sci. 73:3657-3665.

Everts, H., M. J. A. Nabuurs, R. Margry, A. J. van Dijk, and A. C. Beynen. 2001. Growth performance of weanling pigs fed spray-dried animal plasma: a review. Livest. Prod. Sci. 68:263-274.

Gondret, F., L. Lefaucheur, H. Juin, I. Louveau, and B. Lebret. 2006. Low birth weight is associated with enlarged muscle fiber area and impaired meat tenderness of the longissimus muscle in pigs. J. Anim. Sci. 84:93-103.

Handel, S. E., and N. C. Stickland. 1987. Muscle Cellularity and Birth-Weight. Anim. Prod. 44:311-317.

Tran, H., J. W. Bundy, Y. S. Li, E. E. Carney-Hinkle, P. S. Miller, and T. E. Burkey. 2014. Effects of spray-dried porcine plasma on growth performance, immune response, total antioxidant capacity, and gut morphology of nursery pigs. J. Anim. Sci. 92:4494-4504. doi:10.2527/jas.2014-7620

Wigmore, P. M., and N. C. Stickland. 1983. Muscle development in large and small pig fetuses. J. Anat. 137 (Pt 2):235-245.